# DESIGN AND PERFORMANCE OF THE GEORGIA TECH AQUATIC CENTER PHOTOVOLTAIC SYSTEM



Aerial Photo of the Georgia Tech Aquatic Center

**A. Rohatgi, M. Begovic, R. Long,**
**M. Ropp and A. Pregelj**

## FINAL REPORT

**U. S. Department of Energy**
**Subcontract #DE-FC36-94GO10019**



**VOLUME II**

## DISCLAIMER

## Table of Contents

# Table of Figures

## Table of Charts

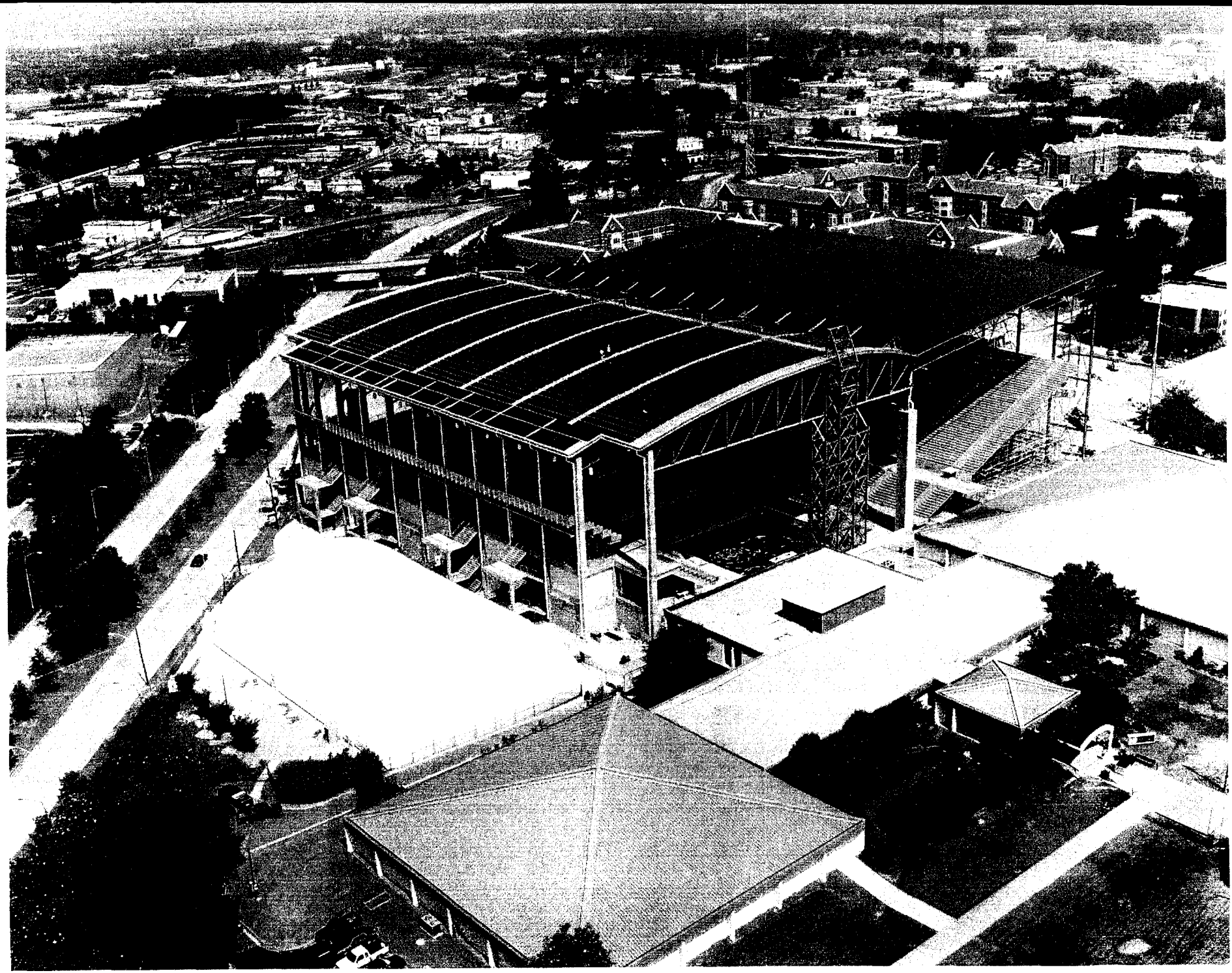

*Chapter 0*

# EXECUTIVE SUMMARY

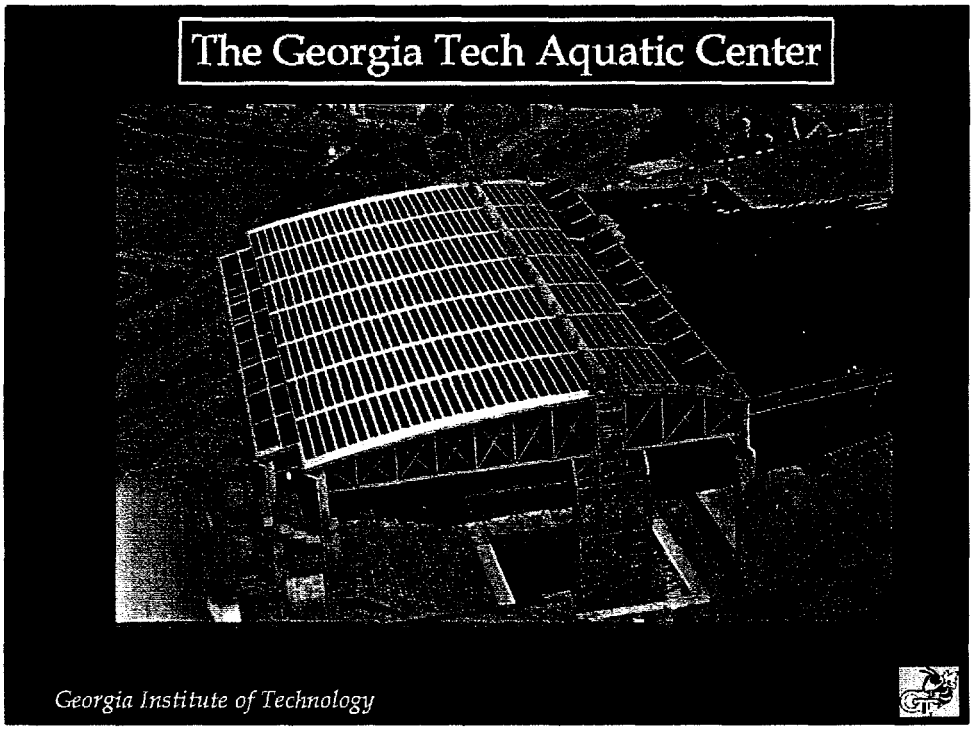


World's largest roof-mounted PV system on a single structure

- PV modules: 120W Solarex multicrystalline Si
- Array size: 2856 modules
- Array configuration: 12 series modules x 238 parallel module strings
- Nominal array voltage: 410.4 V
- Nominal array current: 833 A
- Rated power output: 342 kW
- Utility connection: PCU feeds an isolation transformer, which backfeeds an AC breaker. Reverse sequence and imbalance protection are also provided.

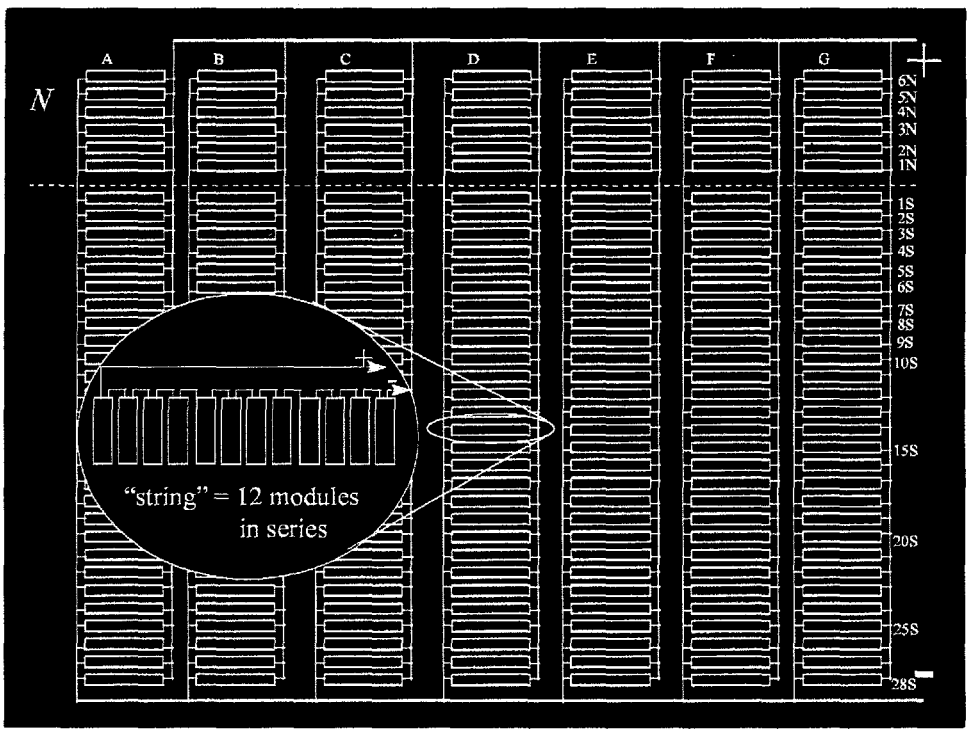


Schematic of Aquatic Center roof PV array configuration.

- Twelve modules are connected in series to form a "series string" to provide the desired voltage to the system, and then 238 of these series strings are connected in parallel to achive the desired power.
- The dotted line through the array is the crest of the roof curvature. Series strings shown above that line face north; all others face south.
- Note the convention for identifying individual strings of modules; the string shown in the "blowup" in the figure is string D-14S.

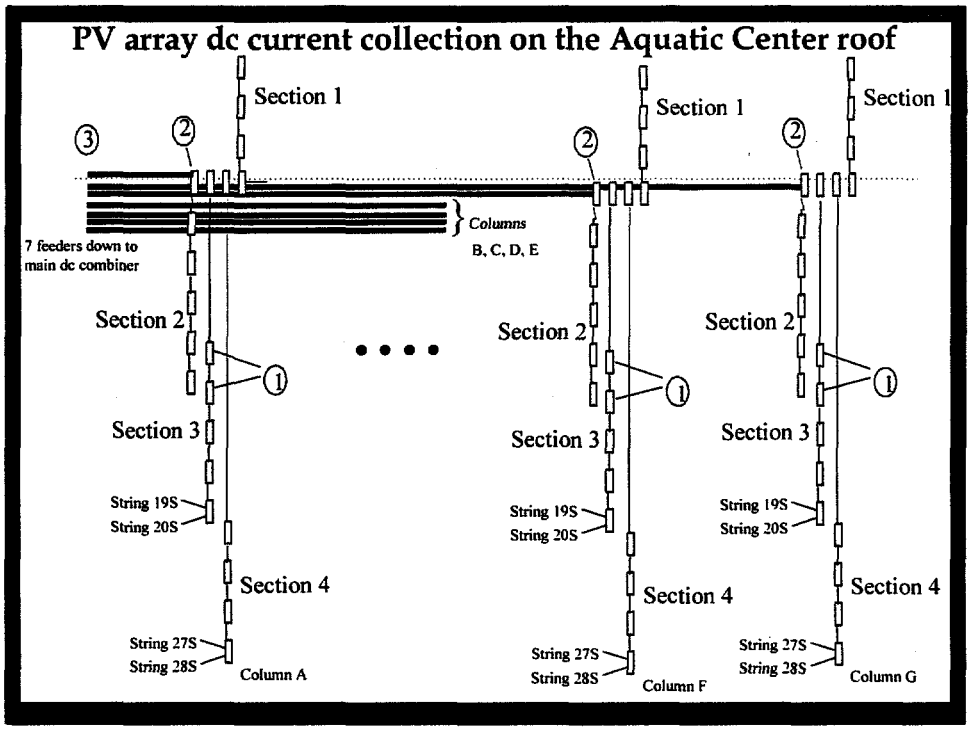


DC-side current collection scheme

① Combiner boxes

② Rooftop disconnect switches

③ Collection circuits and feeders

Note the further subdivision of the array into "sections". In each column, each of the four rooftop disconnect switches controls one section.

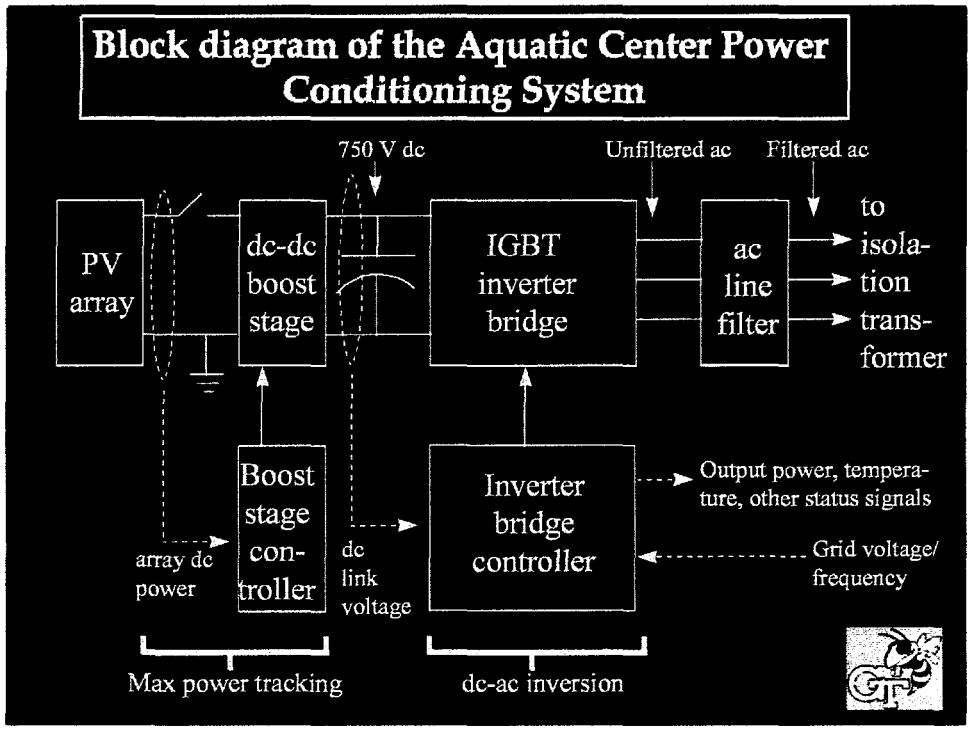


Aquatic Center Power Conditioning System

- The DC-DC boost stage steps the array voltage up to 750 $V_{DC.}$
- The capacitor between the DC-DC boost stage and the inverter is the "DC link".
- The IGBT full bridge inverter that performs the DC/AC conversion uses six 1200 V, 1200 A IGBTs, switching at 6 kHz.
- The AC line filter removes unwanted harmonics from the bridge output, which gives an output current waveform with less than 5% THD at full load.

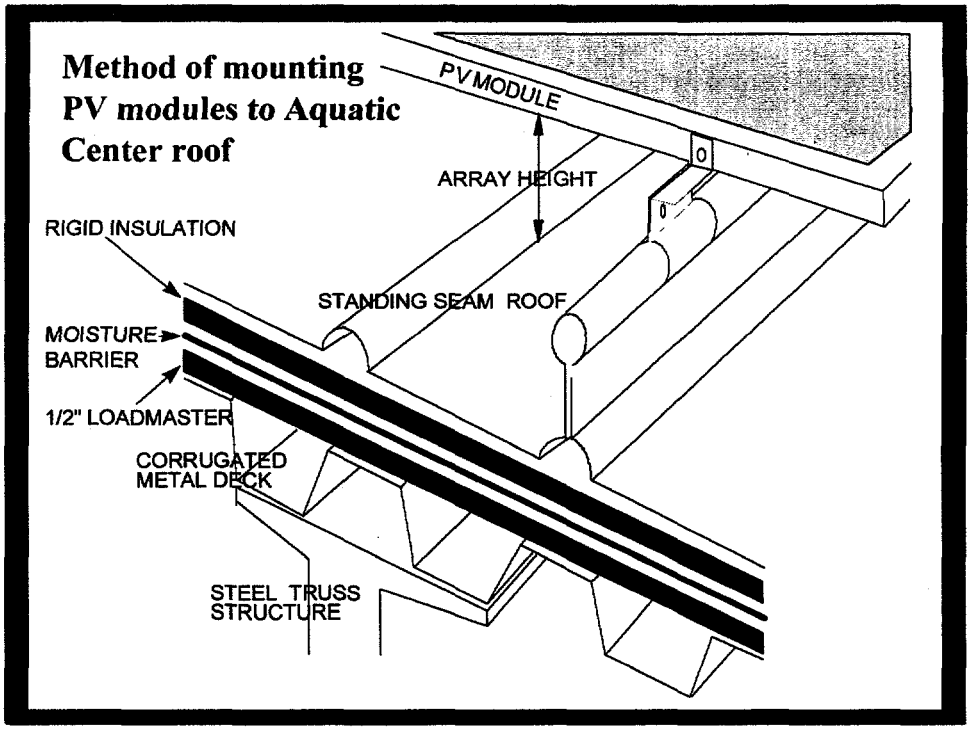


Module mounting scheme

- The array is mounted to the roof using clamps that clamp directly to the aluminium standing seams, which results in an effective array standoff height of 3.5 inches. There is also a two-foot-wide aisle between columns of series strings.
- The string combiner boxes and the conduit containing the conductors for each collection circuit are placed in these aisles.

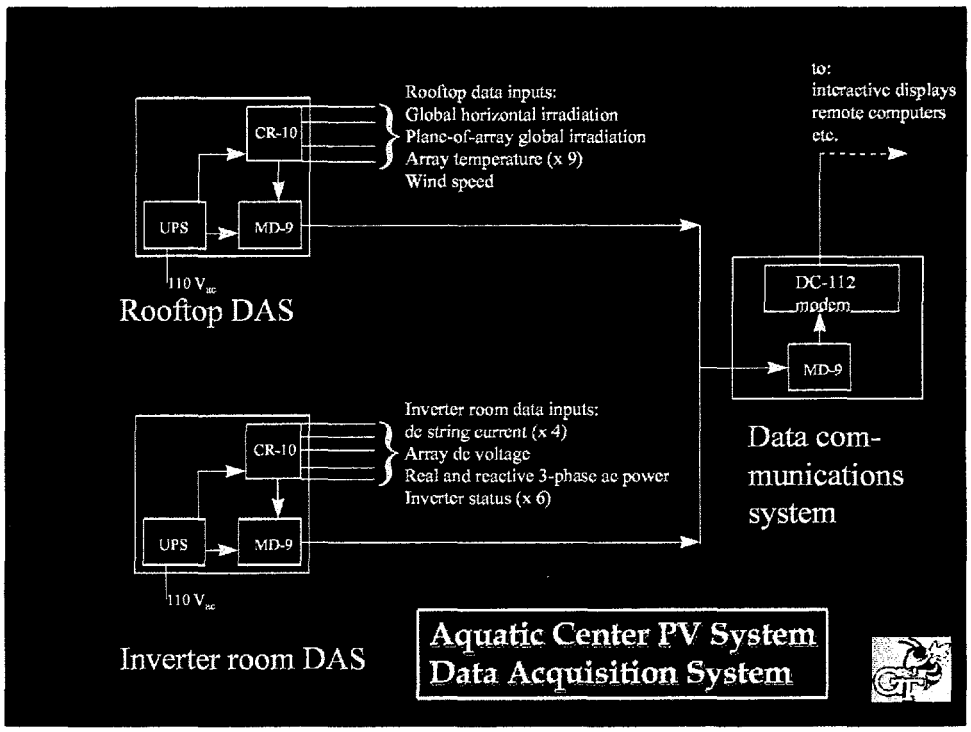


The Aquatic Center PV System Data Acquisition System

- The Rooftop DAS collects the meteorological parameters.
- The Inverter room DAS collects system performance data.
- The Data Communications System (including all three MD-9 multidrop interfaces) provides access to the DAS data from remote computers.

The DAS allows accurate determination of the array's performance and enables thorough research of the system. All data is sampled every 10 seconds, and averages are stored every 10 minutes for all the measured variables.

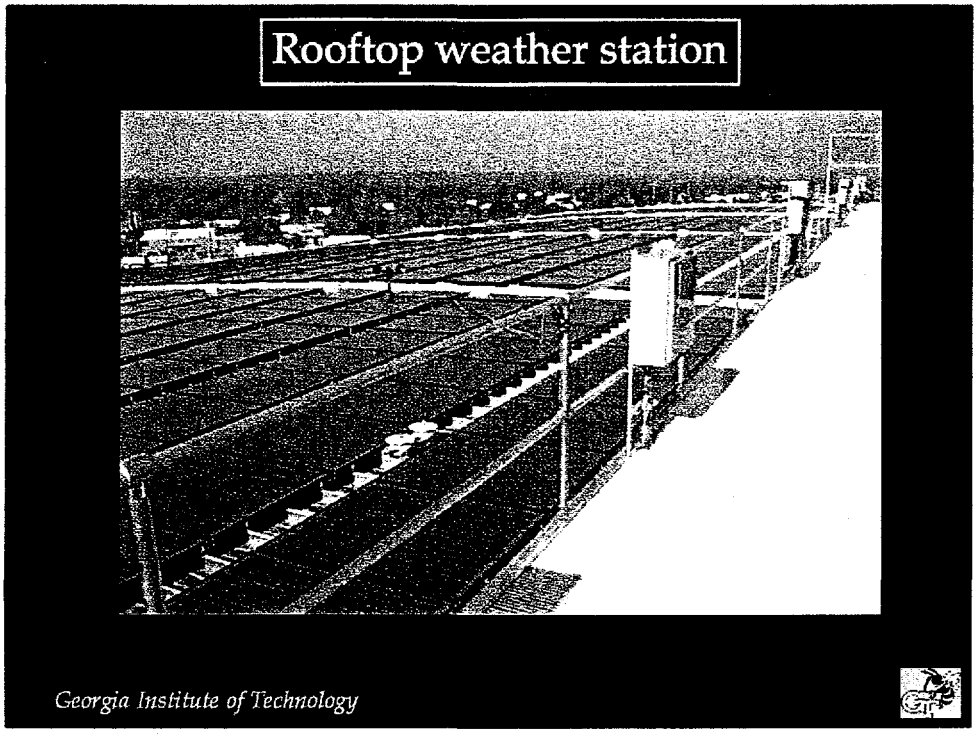


The Rooftop Weather System

This unit of DAS monitors four meteorological parameters:

- Global horizontal irradiation
- Plane-of-array irradiation
- Ambient temperature
- Wind speed

All data are collected by a CR-10 datalogger mounted in a Hoffman electrical enclosure situated roughly in the center of the catwalk of the roof. The CR-10 is connected to the communication system of the DAS by an MD-9 interface, which is also located in the Hoffman box.

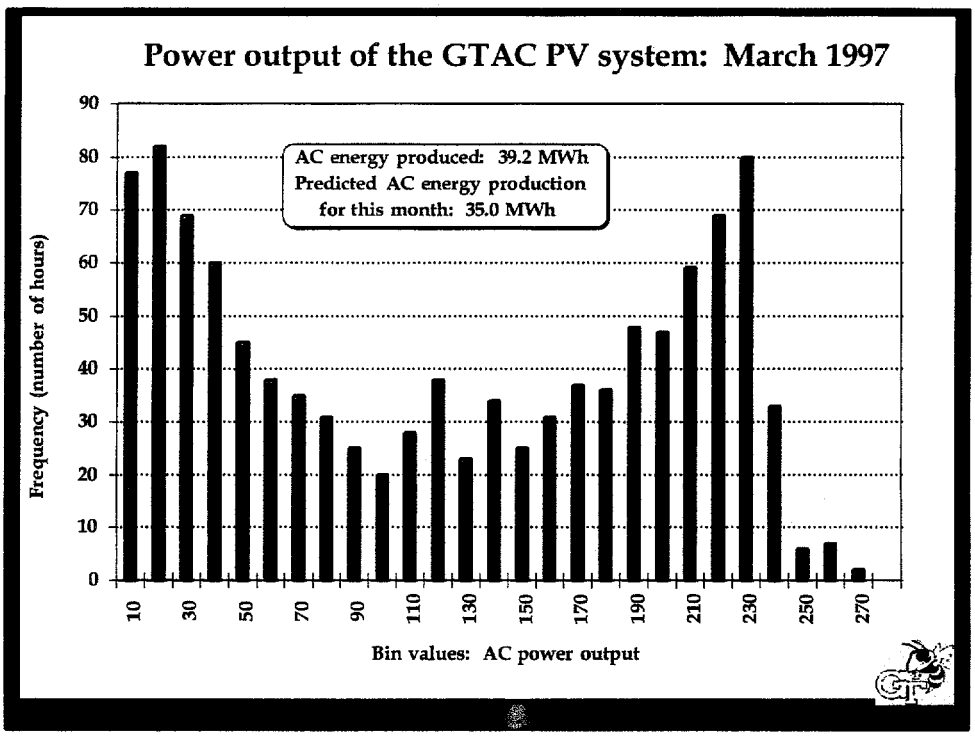


Histogram of the AC power output, March 1997.

- The average daily flux this month is considerably greater than that predicted by PVFORM/TMY modeling. As a result of that and moderate temperatures the AC power production is quite strong.
- The 39.2 MWh of total AC energy production for March exceeds the predicted value of 35.0 MWh, with peak values exceeding 260 kW.

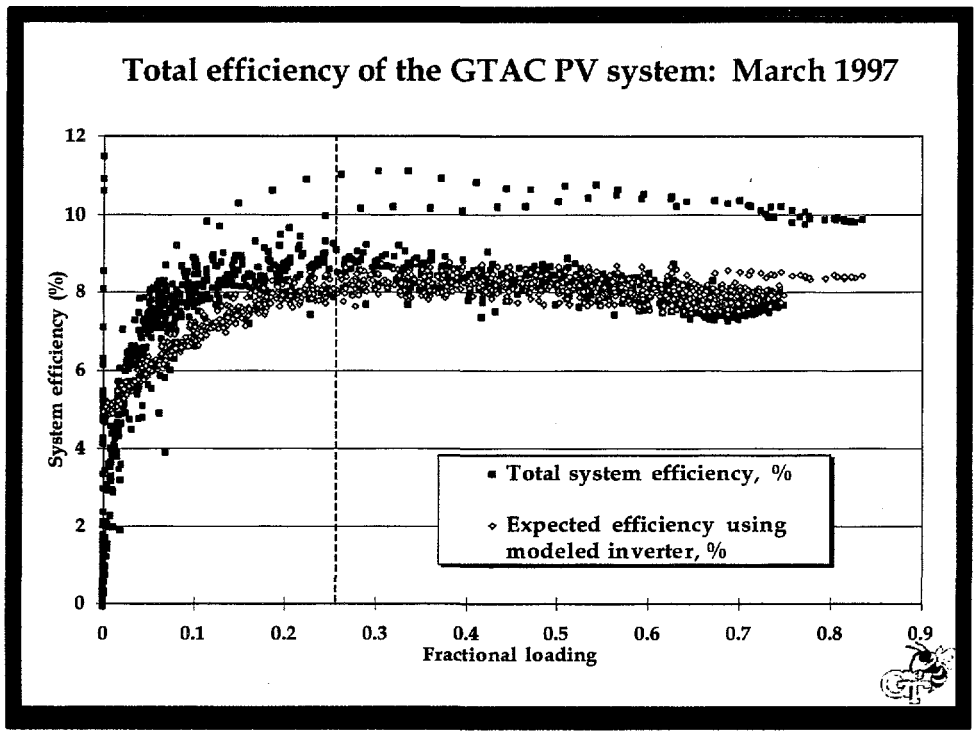


Total efficiency of the GTAC PV System, March 1997

- Expected and measured system efficiences agree extremely well, with the given mismatch parameter value.
- If the measured inverter efficiency is used, the measured system efficiency is slightly lower than the expected system efficiency. By lowering the $K_{dust}$ factor from 10% to 4%, which is the measured value, the match is better for the measured inverter but worse for the modeled inverter.
- We are continuing to experiment on the system to "tune" the parameter values in our model.

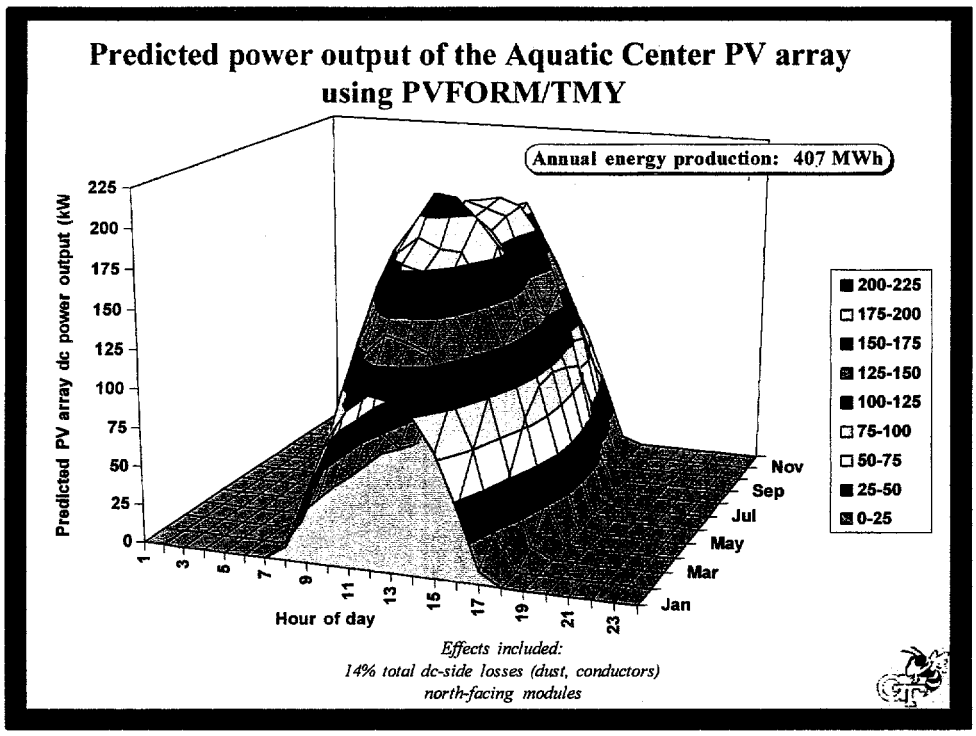


Predicted power output of the GTAC PV array using PVFORM

- Predicted maximum power production ~ 290 kW
- Peak power month: May
- This 3-D plot shows an "average" day for each month of the year.

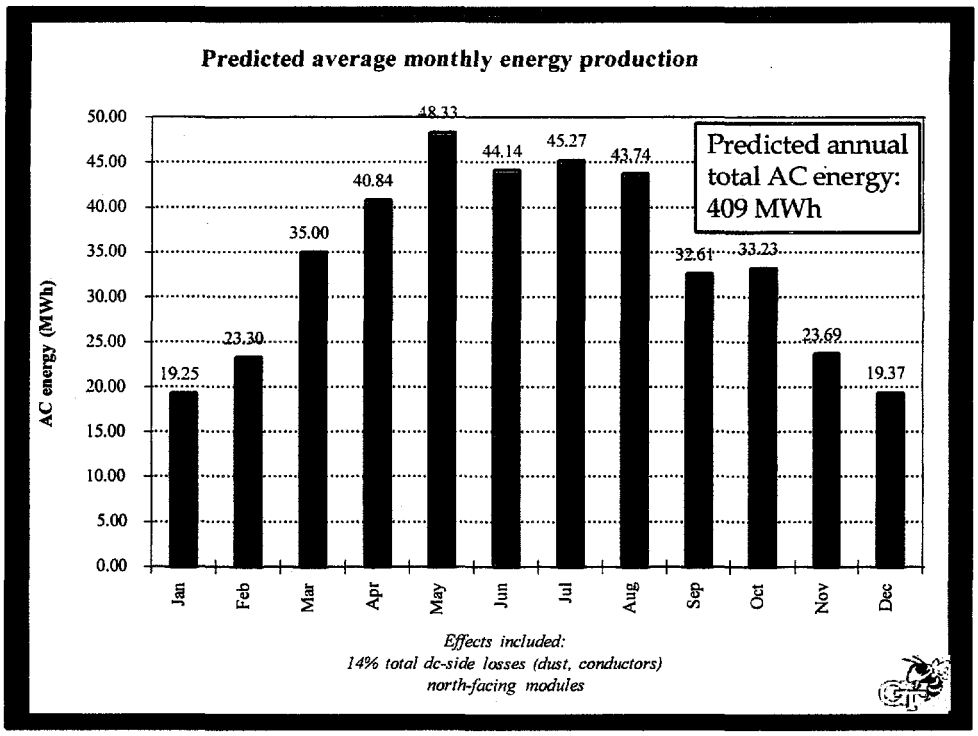


Predicted average monthly energy production

- Maximum energy production occurs in May because irradiances are approaching summer levels but temperatures are still moderate. Also, skies are usually clear during May.
- Total annual energy production, including the effects of variable sunlight, temperature, dust, DC-side losses, module mismatch and roof curvature is predicted to 409 MWh.

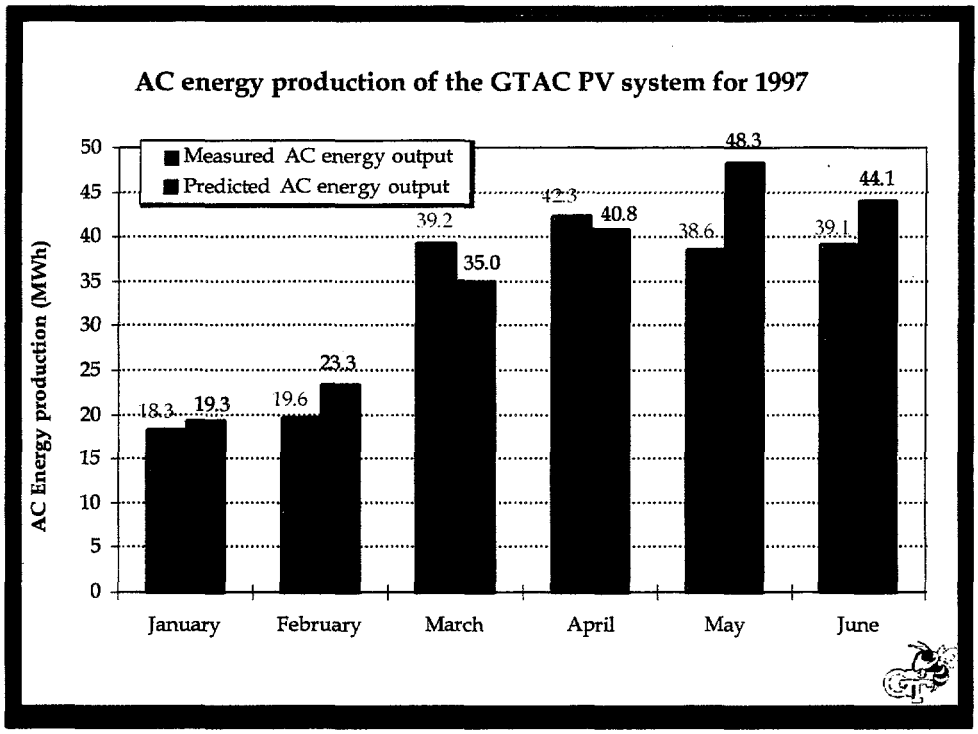


AC energy production of the GTAC PV system for 1997

- Actual AC energy production of the GTAC PV sytem compared with the predicted values (TMY/PVFORM). Data are for the first half of 1997.
- Total energy produced: 197.1 MWh
- Predicted for same period: 210.8 MWh
- Actual prediction is 94% of predicted production.

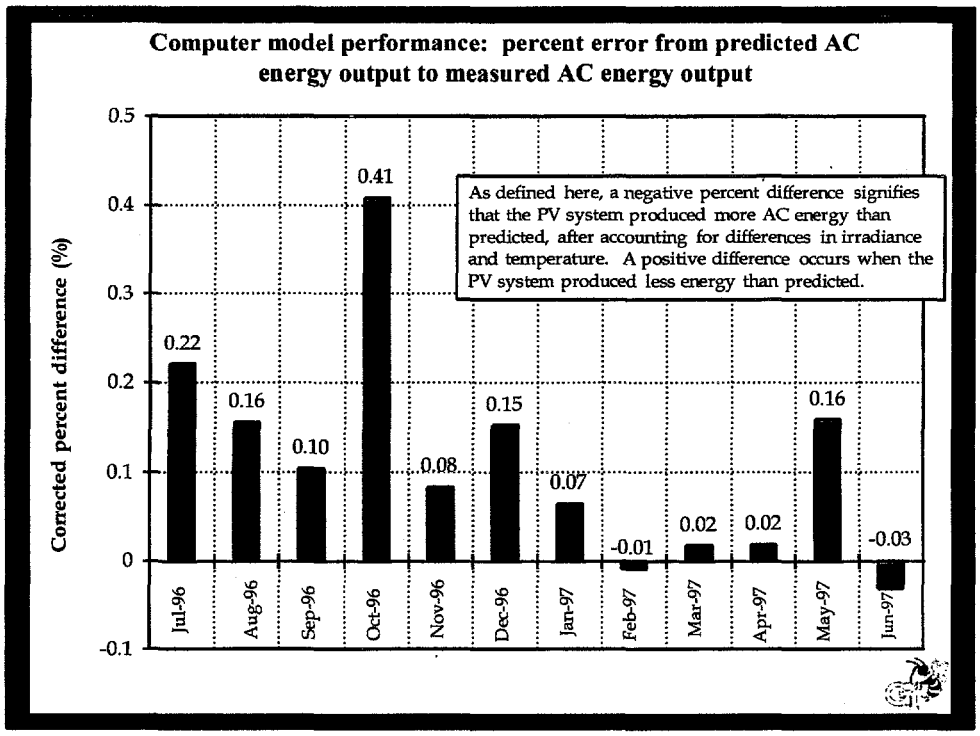


Computer model performance for 1997

- Sensor recalibration occured in March, 1997. Data from before that time reflect sensor error.
- Since March, system performance has agreed very well with predicted performance.
- Error in May 1997 is due to unexpected down time.

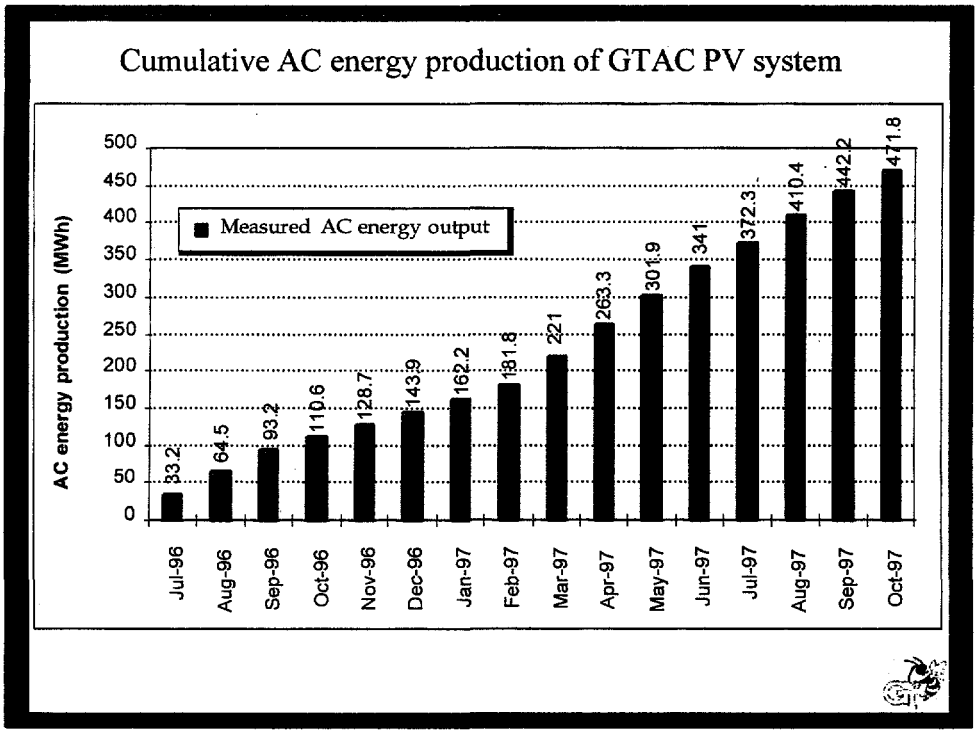


Cumulative AC energy production of GTAC PV system

- The slightly uneven growth rate is impacted by seasonal weather variations and occasional effects of scheduled and unscheduled maintenance. However, it complies reasonably well with performance predictions.

## PV Systems research at GT

❶ Monitoring of GTAC PV system
- ① Verification of PV systems models and design procedures
- ② Parameter estimation and measurement
- ③ Monthly reports available on the WWWeb (public education and awareness)

❷ PV system power electronics
- ① Islanding prevention
- ② Module-integrated maximum power point tracking

*Georgia Institute of Technology*

*Chapter 1*

# THE AQUATIC CENTER PV SYSTEM: DESIGN AND CONSTRUCTION

# 1. The Aquatic Center PV System: Design and Construction

## *1.1 Introduction*

A building-integrated DC PV array has been constructed on the Georgia Tech campus. The array is mounted on the roof of the Georgia Tech Aquatic Center (GTAC), site of the aquatic events during the 1996 Paralympic and Olympic Games in Atlanta. At the time of its construction, it was the world's largest roof-mounted photovoltaic array, comprised of 2,856 modules and rated at 342 kW. This section describes the electrical and physical layout of the PV system, and the associated data acquisition system (DAS) which monitors the performance of the system and collects measurements of several important meteorological parameters.

## *1.2 Electrical Design of the PV System*

### 1.2.1 The PV Modules

The electrical design of the PV system begins with the PV modules themselves. The modules used in this installation are Solarex MSX-120 modules. Each module contains 72 100cm$^2$ multicrystalline silicon solar cells connected in series. The performance specifications of this module are given in Table 1-1. These modules have a low-iron tempered glass front encapsulation, which also provides structural rigidity (i.e. the "structural front" design) and a Tedlar vapor barrier on the back, surrounded by a bronze-anodized extruded aluminum frame.

### 1.2.2 Array Layout

The modules are connected in the traditional DC-array configuration: twelve modules are connected in series to form a "series string" to provide the desired voltage for the system, and then 238 of these series strings are connected in parallel to achieve the desired power. This configuration is shown in Figure 1-1, and the resulting array parameters are given in Table 1-2. Interconnection of the modules in this array was simplified by the plug-in pin-and-socket type connectors provided by Solarex. The pin-type connector from each module is the negative terminal; the socket is the positive.

The National Electric Code (NEC) states that photovoltaic systems cannot produce DC voltages in excess of 600V. Therefore, it is important to choose the number of modules in series such that the maximum voltage produced by the array will not exceed this limit. Underwriters' Laboratories (UL) recommend using the lowest known ambient temperature at the site with the known module voltage derating coefficient and the rated open-circuit voltage $V_{oc}$ in calculating this maximum voltage.

**Table 1-1. Solarex MSX-120 Module Parameters**

| Parameter | Value |
|---|---|
| Modules used | Solarex MSX-120 (24V configuration) |
| Module area | 1.1118 $m^2$ = 11.97 $ft^2$ |
| $V_{OC}$ | 42.6 V |
| $I_{SC}$ | 3.8 A |
| $V_{mp}$ | 34.2 V |
| $I_{mp}$ | 3.5 A |
| $P_{mp}$ | 120 W |
| Fill factor | 0.7394 |
| Module efficiency | 10.8% |
| $K_{voc}$ | -0.146 V/°C |
| $K_{\eta}$ | -0.38 %/°C |
| NOCT | 45°C |
| Test conditions | 1 kW/$m^2$ irradiance with AM 1.5 spectrum, $T_{module}$ = 25 °C |

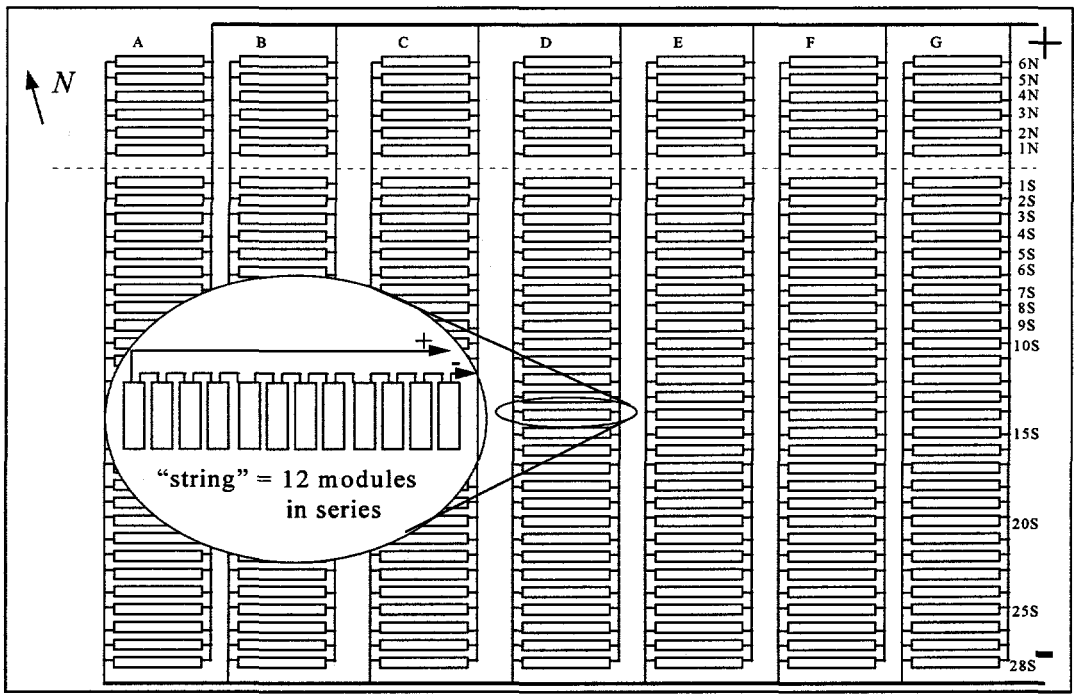


**Figure 1-1. Schematic of Aquatic Center roof PV array configuration. The dotted line through the array is the crest of the roof curvature and the location of the access catwalk. Series strings shown above that line face north; all others face south. Note also that the convention which will be used in identifying individual strings of modules is presented in this figure; for example, the string shown in the "blowup" in the figure is string D-14S. The array is treated as a matrix; each letter denotes a "column" while the numbers + N or S denote "rows".**

### 1.2.3 DC-side Current Collection

The DC-side current collection scheme is shown in Figure 1-2. Note that all the components in Figure 1-2 are part of the "+"-side of the array shown in Figure 1-1. The "-" leg, or return leg, is actually connected to ground.

**Table 1-2. Array Parameters**

| Parameter | Value |
|---|---|
| Array power rating | 341280 kWp |
| Array configuration | 12(s) x 238 (p) = 2856 modules<br>504 modules on north-facing roof slope<br>2352 modules on south-facing roof slope |
| Nominal array voltage | 410.4 V |
| Nominal array current | 833 A |
| Array area | 3162.1 $m^2$ = 34,037 $ft^2$ |
| Measured average array tilt: south-facing | 6.4° up from horizontal |
| Measured average array tilt: north-facing | 5.9° up from horizontal |
| Measured array azimuth | 12° west of south |

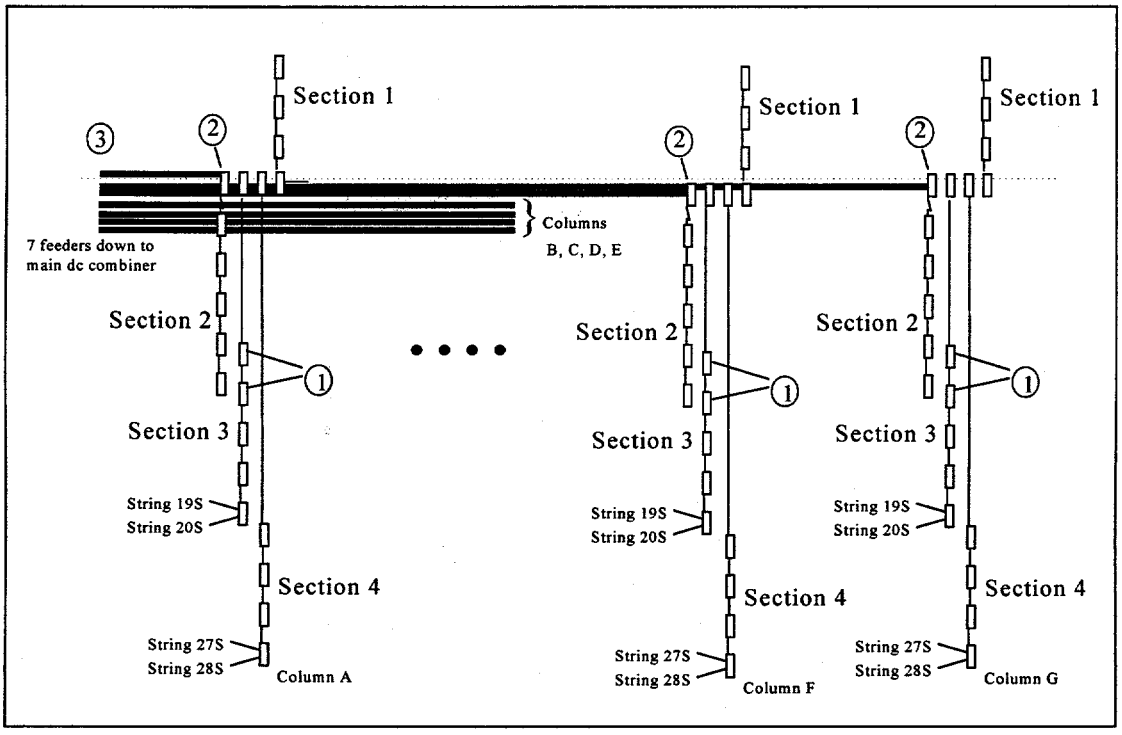


**Figure 1-2. DC-side current collection scheme showing combiner boxes (①), rooftop disconnect switches (②), collection circuits and feeders (③). Note also the further subdivision of the array into "sections"; this, like the "matrix" notation in Figure 1-1, is simply a standardization of notation for various parts of the array. In each column, each of the four rooftop disconnect switches ② controls one "section".**

### 1.2.3.1 Series String Combiners

The boxes labeled ① are string combiner boxes; each of these combines the output of two series strings. The combiner boxes used in this installation are Ascension Technology source circuit protectors. Fuse protection is provided for each series string connected to the box. The source circuit protectors contain the blocking diodes necessary in the DC array design configuration; each box contains one blocking diode per series string. These prevent shadowed or damaged series strings from operating in a region of the I-V curve in which they absorb power. A surge suppressor is provided in the combiner box to prevent transients from getting to or from the series strings. The combiner boxes are series-connected up to the current limit of the device, for a maximum of five boxes in series. Thus, in each column, there are four "collection circuits" as shown in Figure 1-2. All conductors used on the roof are run through conduit, and the cables themselves are Type RHH/THHN, with insulation rated at 90° F. Type RHH/THHN cables are rated for use in humid or moist environments, and most can tolerate direct sun exposure. The boxes also include a ground lug to which is connected a bare copper wire for grounding the frames of the PV modules. Without this ground, it would be possible for the metal module frames to float above ground potential if a short should develop within the module which connected the cells to the frame. This failure mechanism is frequently seen; therefore, in this array, every single module frame is grounded to a ground lug in a combiner box.

### 1.2.3.2 Rooftop Disconnect Switches

The boxes labeled ② are the rooftop disconnect switches mounted on the catwalk. These contain three-pole DC disconnect switches and give the ability to isolate any of the four collection circuits in each column. These switches are wired such that, when the switch is thrown, the fuse is isolated, but the grounded negative leg of the circuit is not broken, thus maintaining ground continuity. A bar of copper with size chosen to match the conductor ampacity is inserted into the fuse bracket of the first pole. A jumper wire, again sized to match

the conductors, is inserted between the first and third poles, and a fuse is inserted into the fuse bracket of the third pole, thus completing the circuit. This fuse is intended to protect against faults on the array itself. The second (middle) pole of the switch is not used. The box itself is connected to the system ground.

Each column in the array is separated into four sections, each with its own disconnect switch as shown in Figure 1-2. The arrangement of switches and connections is as shown in Figure 1-2; a person standing in front of the switch boxes would see, from left to right, disconnect switches for sections 1, 4, 3, 2 in that order. The two boxes on the left are smaller because their ampacities need not be as high since fewer series strings are connected to them.

#### *1.2.3.3 Power Transport to the Inverter Room*

Just downstream from the disconnect switches, the four collection circuits are combined to form a main DC feeder. At point ③, there are seven of these feeders, one for each column. The feeders run through conduit down from the roof, where they go underground and run the length of the building back to the inverter room.

### 1.2.4 The Main DC Collection Switchboards

In the inverter room, the layout of which is diagrammed in Figure 1-3, there are two main DC collection switchboards. These switchboards, made by Siemens Energy and Automation Division, are near the corner of the inverter room in large grey cabinets. The seven lines from the roof first enter a switchboard (the "first DC switchboard") with a separate circuit breaker for each feeder (seven circuit breakers). These breakers protect against faults between point ③ in Figure 1-2 and the first DC switchboard. The seven feeders, after passing through the seven breakers, are joined on a common bus into one main feeder. This main DC bus is in turn connected through another circuit breaker, the main DC circuit breaker, to the power conditioning system (PCS). This breaker protects against faults between the DC collection switchboard and the PCS. This main breaker is wired in a slightly unusual way to ensure proper operation. It is a standard three-phase AC breaker. To ensure that it will trip under the proper conditions, all three poles must be energized; therefore, the positive leg of the DC bus passes through one pole and is doubled back through a second pole. The negative leg passes through the third pole. Note that the main breaker does break the negative leg of the DC circuit. The ground leads coming down from the roof pass through the DC switchboard cabinets directly to the ground bus of the power conditioning system (PCS) without passing through any switches. This is necessary to allow the PCS to properly detect ground faults on the system. It should be noted that two of the ground leads from the roof are connected to the ground rail of the main DC breaker cabinet. Another cable runs from this ground rail through the conduit to the system

ground in the DC isolation switch box on the PCS cabinet, thus grounding the DC switchbox chassis.

## 1.2.5 The Power Conditioning System (PCS)

### *1.2.5.1 Functional/Electrical Description of the PCS*

The PCS in this installation is a 315 kW unit supplied by Trace Technologies, Inc. (formerly Kenetech Windpower). A block diagram of the PCS is shown in Figure 1-4. The PCS is equipped with a "no-load-break" switch which isolates it from the array; this switch is shown in Figure 1-4 between the array and the boost stage. The term "no-load-break" means that the switch does not have the capability to interrupt the full array current, and therefore it cannot be opened while the DC-side line is energized. The array must be disconnected by opening the main DC breaker, all seven main feeder breakers, or all 28 of the rooftop disconnect switches before the no-load-break switch can be opened. A similar switch (not shown in Figure 1-4) is supplied on the AC side, to isolate the PCS from AC power. Both of these switches should be locked open before the inverter cabinet is opened. Normally, the switches should be locked in the closed ("1") position.

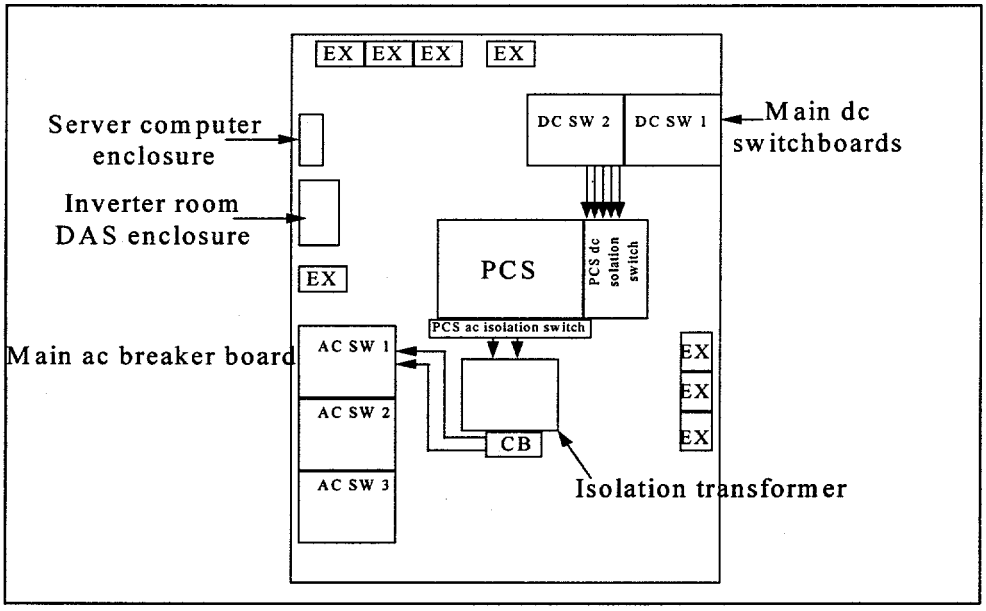


**Figure 1-3. Layout of the inverter room. EX stands for "existing"; these are other devices (lighting panels, breaker boxes etc.) which are not part of the PV system. The first DC breaker box containing the seven feeder breakers is labeled "DC SW 1"; the main DC breaker cabinet is "DC SW 2". The arrows between components indicate the power cable conduit runs.**

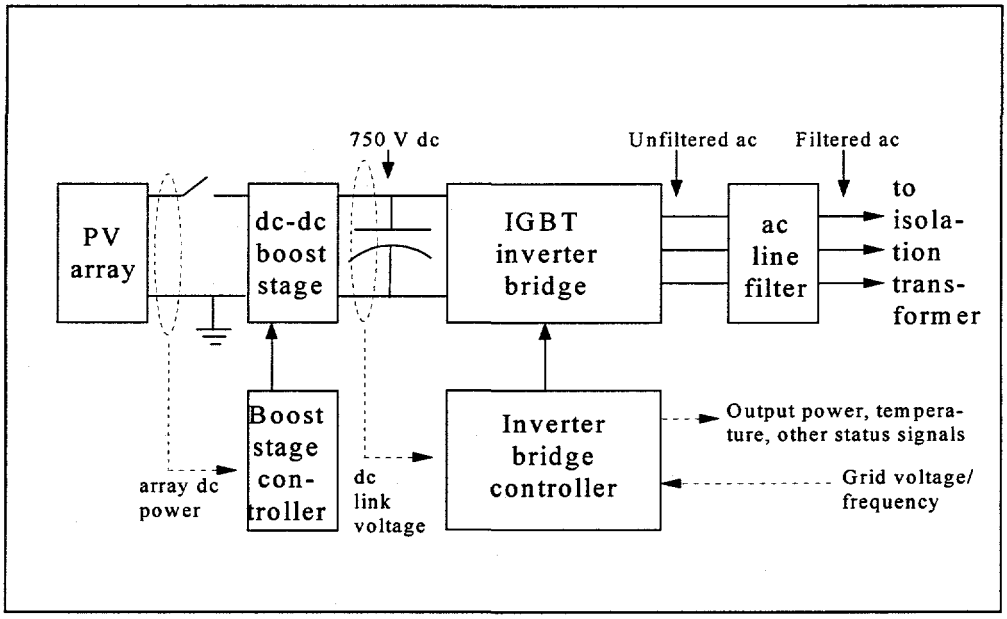


**Figure 1-4. Block diagram of the Aquatic Center PV system power conditioning system (PCS). The boost stage steps the (variable) array voltage up to 750 $V_{DC}$; the inverter bridge is an IGBT bridge circuit that performs the inversion. The capacitor between the DC-DC boost stage and the inverter bridge is the "DC link".**

The power switching stages of the PCS uses 1200V, 1200A insulated gate bipolar transistors (IGBTs) as the semiconductor switches, switching at 6 kHz. The converter topology contains twelve IGBTs divided into two sets. One set forms a DC-DC "boost"-type converter, with the switches acting in parallel; the other is a six-switch, three-phase inverter bridge. A pulse-width modulation (PWM) switching scheme is used in both the boost stage and the inverter bridge. In the boost stage, the control variable used to determine the PWM duty ratio is the array power output; the switching function is controlled so as to keep the array operating at its maximum power point. In the inverter bridge, by sinusoidal modulation of the duty ratio, an output waveform with a large fundamental-frequency component (at the frequency of the sinusoidal modulation) but with small low-order harmonic amplitudes is obtained, allowing for easy filtering to obtain the desired sinusoidal output current. The inverter bridge switching is also controlled in order to maintain the DC link voltage at 750 V. The bridge is self-commutated, allowing for a near-unity power factor. However, the line voltage waveform is used by the inverter controller as a template for the output current waveform (i.e. to modulate the IGBT duty ratios). The line filter just downstream from the inverter bridge removes unwanted harmonics from the bridge output, particularly harmonics at and above the switching frequency. Because of its size, the line filter is contained in a separate enclosure from the rest of the PCS. The manufacturer's specifications state that this configuration produces an output current waveform with less than 5% THD at full load.

It is important to note that the PWM output waveform of the inverter bridge is asymmetric about zero; that is, its maximum value is the voltage across the DC bus, and its minimum is zero, since the DC bus is not grounded at its center. Therefore, this output waveform has a DC component approximately equal to half the DC bus voltage. To prevent injection of this component into the grid, a three-phase isolation transformer is provided on the AC side between the bridge and the grid. This transformer is $\Delta$-Y connected, with the Y on the utility side. The center of the Y is grounded.

Table 1-3, taken from the manufacturer's literature, collects some of the performance specifications of the PCS. The efficiency quoted for the PCS is its efficiency under "full load" conditions; that is, when the PV array is producing power equal to the PCS's continuous rating (315 kW). The efficiency is not constant under all loading conditions, however, and Figure 1-5 shows a curve of the PCS efficiency vs. PV array power production.

**Table 1-3. Specifications of the Aquatic Center array PCS**

| Parameter | Value |
|---|---|
| Continuous rated DC (PV) power input | 315 kW |
| Maximum rated DC (PV) power input | 324 kW |
| Nominal DC-terminal voltage | 380V |
| Maximum DC-terminal voltage | 600V |
| Efficiency | 95% at full load |
| Output power factor | 1.00 |
| THD of AC output current | ≤ 5%, in compliance with IEEE-519 |
| Semiconductor switching device | IGBTs rated at 1200V, 600A |
| Switching speed | 6 kHz |

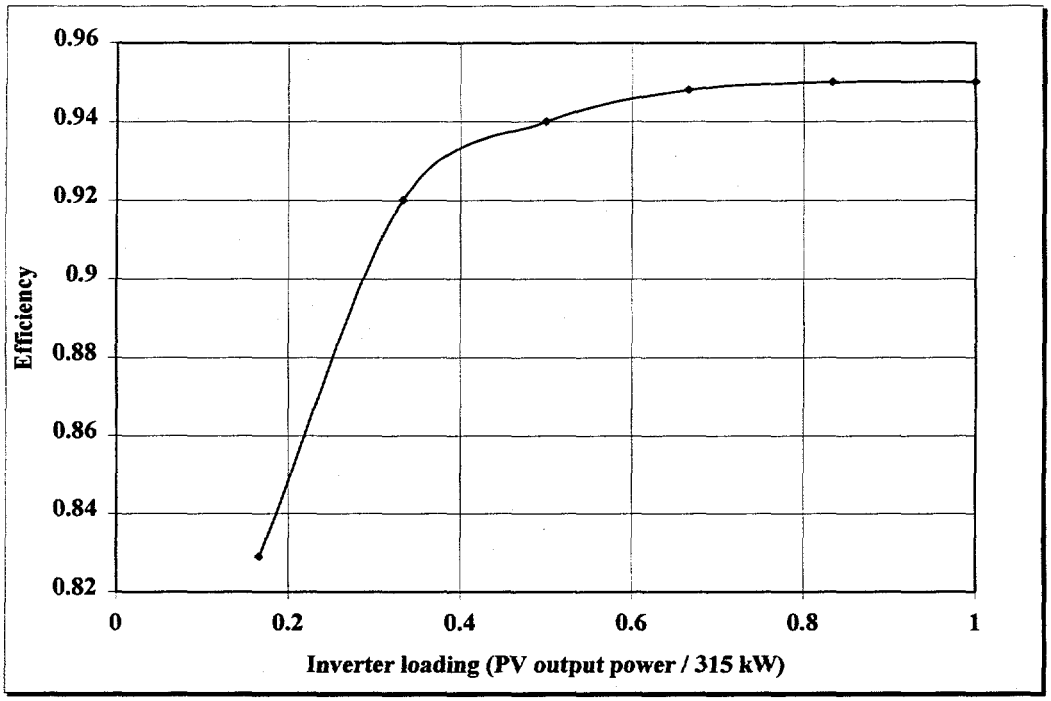


**Figure 1-5. Efficiency of Trace 315 kW PCS as a function of PV power input. x-axis values are in terms of "fractional loading", which is the input power to the PCS (in this case the PV array's power production) divided by the PCS's continuous rating.**

*1.2.5.2 Control Functions*

The PCS provides many control and protection functions for the system.

a) Maximum power point tracking: the PCS uses a "dithering" scheme in which the PV array's output current is changed in 5A increments and the resulting output power is calculated. If the power has increased since the last increment, the next 5A increment will have the same sign (i.e. be in the "same direction"); if the power has decreased, the sign will be reversed in subsequent increments. The inverter switching function is controlled to maintain the 750 $V_{DC}$ across the link capacitor. In this way, the PV array current is controlled such that it operates at or near its maximum power point at all times.

b) Self-protection: DC overvoltage and overcurrent and also overtemperature conditions are monitored by the PCS's control system. Device protection is accomplished in part by an "over-power" protection function: if the input power from the array attempts to go over 324 kW, the maximum power point tracking circuit acts as a limiter and prevents the array current from increasing, thus preventing the PV array output power from exceeding 324 kW.

c) Islanding protection: AC-side over/undervoltage and over/underfrequency monitors are included in the PCS's control system to enable detection of islanding. In addition, if the grid voltage decays to zero, the template for the inverter bridge output current also goes to zero, meaning that the inverter output current in turn will vanish.

d) DC-side ground-fault detection: the PCS is capable of shutting down the system in the event of a short to ground on the DC side. A current sensor is provided on the ground bus from the PCS to the actual earth ground. When large currents in the ground bus are detected, some type of ground fault exists and a command is generated to stop power production and disconnect the PV array. It is because this function is provided in the PCS that it is important for the array ground lines to pass directly from the roof to the PCS ground bus, with no other

ground path. If another ground path were provided, two conditions would exist: first, the PCS may not detect the ground fault because current flow would be divided between the multiple ground paths; and second, if the fault were detected, the PCS would be unable to interrupt it because the fault current could continue to flow through the other ground paths. The PV array would indefinitely feed the ground fault with essentially its short-circuit current, which would very likely lead to a fire.

e) Lightning protection: MOV surge arrestors are provided on both the AC and DC terminals for the purpose of preventing high-voltage lightning-induced transients from reaching the semiconductor switches.

f) Automatic normal start-up and shut-down: the PCS automatically begins conditioning power each morning when the array voltage exceeds 400V and remains above that level for five minutes. The extra time is inserted to prevent the system from "cycling", or starting and stopping repeatedly. Similarly, the system automatically "sleeps" at night, shutting down when the array power drops below 3kW and remains below that level for fifteen minutes. This long time interval is required to prevent the system from cycling during the passage of unusually dark clouds.

### 1.2.6 The Isolation Transformer

The AC output of the PCS is then fed into the main isolation transformer, which is 480 VΔ-480 VY connected. This transformer provides electrical isolation from the grid and also prevents passage of the DC component of the output of the inverter bridge into the grid. A circuit breaker is provided on one side of the cabinet.

## 1.2.7 The Main System Circuit Breaker

There are two main system circuit breakers. The first is a standard, three-phase AC breaker located on the system's AC switchboard. The second is a specific protection system made up of three different components. The first, called an 86 device, is a locking circuit breaker. This is the actual switch that disconnects the PV system from the building service entrance. This 86 device can be tripped by either of the other two components: a phase imbalance detector and a device called a "32 device".

The phase imbalance sensor monitors the current flows in the three phases coming from the PV system. In the event that an unbalance condition occurs, indicating any of a number of abnormal operating conditions, the phase imbalance sensor "trips" (opens) the 86 breaker, which locks open and disconnects the PV system from the grid.

The 32 device monitors the direction of power flow in the main isolation transformer. If the power flow attempts to reverse, flowing from the grid to the PV system, the 32 device trips the 86 breaker and disconnects the system. The threshold value of reverse power flow, above which the 32 device generates a trip, must be chosen carefully to avoid false trips due to the array going off-line at night. To avoid this problem, the designers of this installation realized that the core loss of the main isolation transformer will appear to the grid as a load when the PV system is off-line, and this is a normal condition in the case of nighttime PV system shutdown. Therefore, this core loss is used as the threshold value for reverse power flow. If the reverse power flow is at or below this threshold, no trip is generated. However, if reverse power flow exceeds this core loss, an abnormal condition exists, and the 86 device is tripped.

## 1.2.8 Lightning Protection

The array is protected against lightning strikes by two air terminals, one located on each main steel support structure at either end of the roof. These air terminals were designed by Lightning Arrestor of America, Inc. Each is designed to provide a radius of protection of approximately 250 feet. The air terminals are bonded directly to the steel support structure and are thus grounded via this structure. There is no other ground connection for these terminals. The installer reports testing the resistance from the air terminal to ground at "not more than 5 Ω", which is deemed sufficient for this application. One potential problem with this arrangement is that the aluminum roof skin is also electrically connected to the steel support structure and is thus in the ground path for the air terminals. In this way, the roof appears as a shunt-connected resistance between the two air terminal-to-ground paths, and in the event of a lightning stroke on either terminal, part of the current could travel through the roof structure to the other ground path. The resistance offered by the roof is unknown, however; it could well be much higher than the 5 Ω specified for the air-terminal-to-ground path, and in that case the current through the roof could be negligible.

## *1.3 Physical Design of the PV Array*

### 1.3.1 Module Mounting Scheme

The roof structure provides a convenient way to mount the PV array. In Figure 1-6, this structure, called a standing-seam design, is illustrated. The array is mounted to the roof using clamps that clamp directly to the aluminum standing seams, as shown in Figure 1-6. This mounting configuration results in an array-roof standoff height of 1.5 inches (the height of the clamps themselves) plus 2 inches (the height of the standing seams) equals 3.5 inches between the roof deck and the bottom edge of the PV module frames. The array is laid out on the roof essentially as illustrated in Figure 1-1. There is a two-foot-wide aisle between columns of series strings. This allows a space along which maintenance workers may reach all parts of the array. Also, the Ascension Technology string combiner boxes and the conduit containing the conductors for each collection circuit are placed in these aisles.

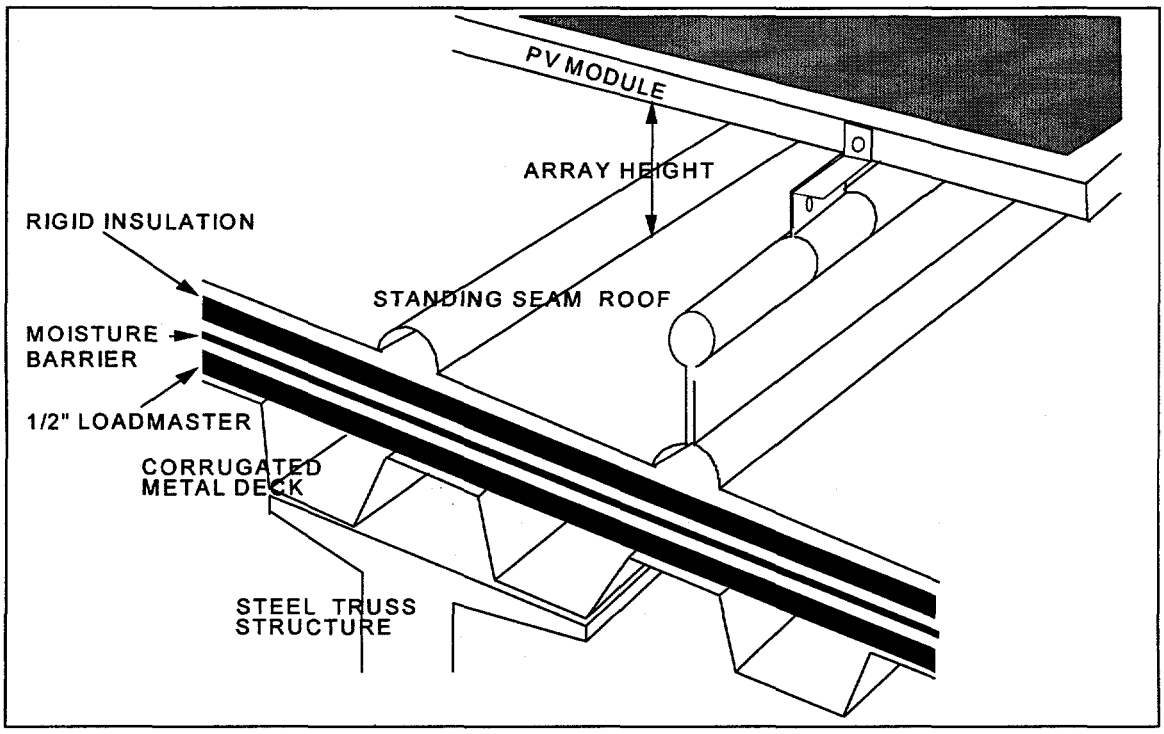


**Figure 1-6. Method used in mounting PV modules to the Aquatic Center roof.**

## 1.3.2 Module Orientation

Since the array is flush-mounted to the roof, its tilt is continuously changing with the roof curvature, and thus the orientations of all of the rows of modules are slightly different. The tilt angles of all rows of series strings were measured using a protractor with a self-leveling indicator needle. The results of this measurement are given in Table 1-4. (The row number-letter designations are taken from Figure 1-1.) Also, the azimuth angle of the entire array was measured using a magnetic compass. According to the magnetic declination chart supplied by the compass manufacturer, the magnetic declination correction required in Atlanta is, conveniently, 0°. For the south-facing modules, the measured azimuth angle was 12° west of south; for the north facing angles, it is 192° west of south, or 12° east of north.

**Table 1-4. Measured module tilts on the Aquatic Center roof.**

| Row designation (from Figure 3-1) | Measured tilt angle, ° up from horizontal |
|---|---|
| 6N | 9.75 |
| 5N | 8.0 |
| 4N | 6.5 |
| 3N | 5.0 |
| 2N | 3.75 |
| 1N (north side of catwalk) | 2.25 |
| 1S (south side of catwalk) | 0.0 |
| 2S | 0.0 |
| 3S | 1.0 |
| 4S | 1.0 |
| 5S | 2.0 |
| 6S | 2.5 |
| 7S | 2.5 |
| 8S | 3.0 |
| 9S | 3.0 |
| 10S | 4.5 |
| 11S | 5.0 |
| 12S | 5.5 |
| 13S | 6.0 |
| 14S | 6.0 |
| 15S | 6.5 |
| 16S | 7.25 |
| 17S | 7.0 |
| 18S | 9.0 |
| 19S | 9.25 |
| 20S | 9.25 |
| 21S | 10.0 |
| 22S | 10.0 |
| 23S | 11.0 |
| 24S | 11.0 |
| 25S | 11.0 |
| 26S | 11.5 |
| 27S | 12.5 |
| 28S | 13.0 |

## 1.4 The Data Acquisition System (DAS)

The Aquatic Center PV array is heavily instrumented for measurement of many performance and meteorological parameters, thus allowing for accurate determination of the array's performance and enabling thorough research of the system. This section describes the DAS, its function, and its operation. The DAS is divided into three functional parts: the rooftop DAS, the inverter room DAS, and the data communications system, as illustrated in Figure 1-7.

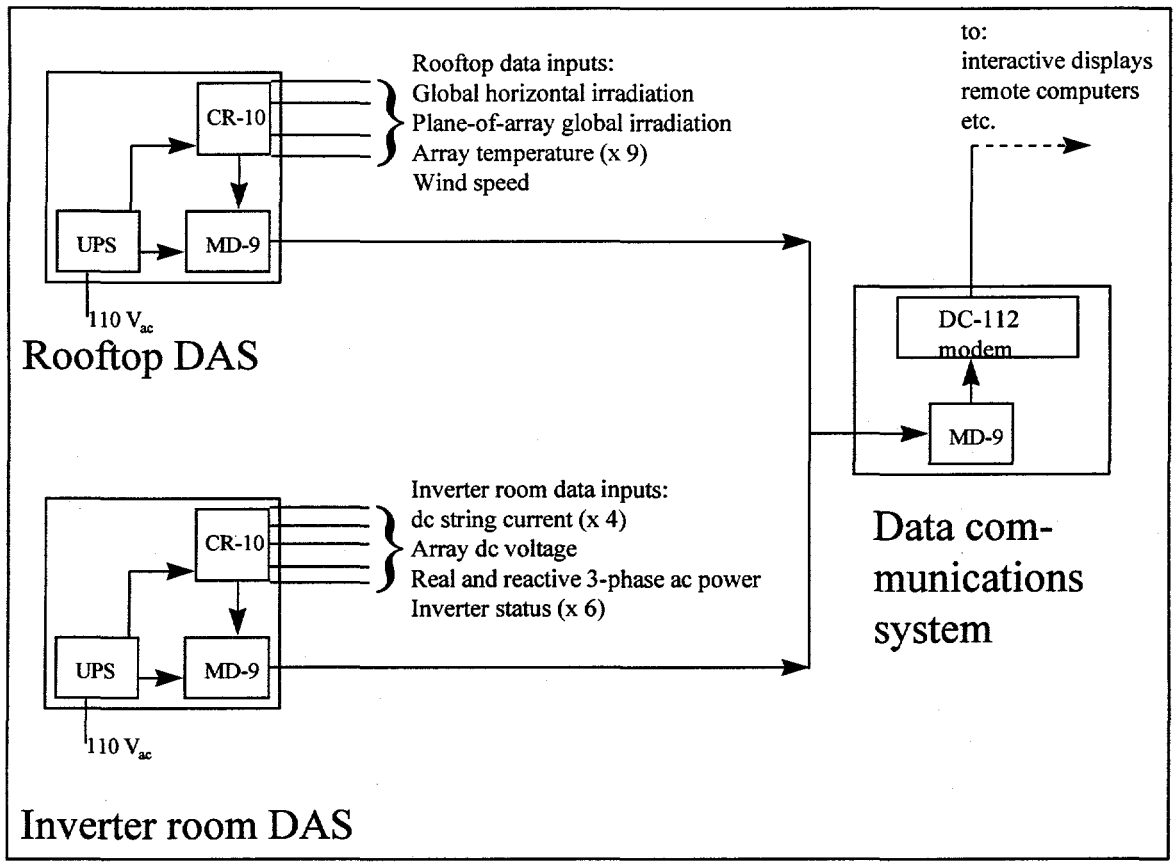


**Figure 1-7. The Aquatic Center array data acquisition system (DAS), showing its three functional units: the rooftop DAS, which collects the meteorological parameters, the inverter room DAS, which collects system performance data, and the data communications system (which includes all three MD-9's), which allows remote retrieval.**

## 1.4.1 Primary Components of the DAS

### *1.4.1.1 Campbell Scientific CR-10 Datalogger*

The datalogger is the heart of the DAS. It performs several vital functions:

a) It receives the raw data from the sensors or other outboard devices. This data can be in any of several forms, including analog voltage signals from thermocouples and pyranometers, digital signals such as the status indication from the inverter, and "pulse" type signals from anemometers.

b) It performs initial data manipulation, such as conversion of the electrical signals into measurement data with the proper units (scaling, etc.) and averaging of a set number of data points. This averaging is very commonly done in order to reduce the required amount of data storage space. The datalogger can also identify maxima and minima, or compute standard deviations.

c) It stores this manipulated data. The CR-10's long-term or "final" storage can hold over 29,000 processed values.

The rate at which the raw data from the various sensors is sampled, as well as the processing done before final storage, is set in the datalogger's program. This program is written on a PC using the PC-208 software provided by Campbell Scientific. PC-208 contains a subprogram called EDLOG which provides a programming language for setting up the instructions to be executed by the datalogger. In the Aquatic Center DAS, all data will be sampled every 10 seconds, and averages stored every 10 minutes for all the variables listed below. The PC-208 software also allows real-time monitoring and verification of the operation of the DAS. In addition, the program can generate tabular or graphical reports and check for missing or out-of-range data points.

#### *1.4.1.2 Campbell Scientific MD-9 Multidrop Interface*

The MD-9 interface "translates" serial-port data signals to or from a format that can be sent via coaxial cable. In this way, the MD-9's allow a coaxial "data bus" to be built which can connect all the data loggers to a single computer for long-term storage and remote access to this data. In the GTAC installation, use of coaxial cable facilitates the long cable runs necessary to connect the rooftop and inverter room DAS units. Ribbon (serial) cable is much more susceptible to electrical noise and is much less physically robust, and would also be difficult to pull through conduit.

### 1.4.2 Rooftop DAS

The rooftop DAS is, as its name implies, mounted on the roof with the PV array itself. This unit of the DAS monitors four meteorological parameters as given in Table 1-5. All data from all sensors is collected by a CR-10 datalogger mounted in a Hoffman electrical enclosure situated roughly in the center of the catwalk on the roof. The two pyranometers are also located atop this enclosure. The CR-10 is connected to the communication system of the DAS by an MD-9 interface, which is also located in the Hoffman box on the roof. The CR-10 is powered by an uninterruptible power supply (UPS), which is connected to a standard 110 $V_{AC}$ supply connected at the AC breaker board in the inverter room. The MD-9 is powered by the CR-10.

**Table 1-5. Meteorological parameters measured by rooftop DAS.**

| Parameter | Sensor |
|---|---|
| Global horizontal irradiation | horizontal pyranometer |
| Plane-of-array global irradiation | pyranometer at average array tilt |
| Ambient (air) temperature | shielded thermistor |
| Array temperature | six (6) module-mounted thermocouples |
| Wind speed | anemometer mounted 2 feet above roof surface |

### 1.4.3 Inverter Room DAS

The configuration of this system is essentially the same as the one on the rooftop, except that the Hoffman box in which it is contained is wall-mounted on the north wall of the inverter room. It monitors the system performance parameters shown in Table 1-6.

**Table 1-6. System performance parameters measured by inverter room DAS.**

| Parameter | Sensor |
|---|---|
| Inverter temperature | Thermocouple mounted on IGBT heat sink |
| Real AC power (3-phase, 480 $V_{AC}$) | Available directly from inverter; also monitored independently by DAS sensors |
| Reactive AC power (3-phase, 480 $V_{AC}$) | |
| DC string current (x 4) | Four Hall-effect current transformers |
| Total DC current | Available directly from inverter; also monitored independently by DAS sensors |
| Array DC voltage (inverter DC input voltage) | Available directly from the inverter; also monitored independently by DAS sensors |
| Inverter status (x 6) | Available directly from the inverter |

### 1.4.4 Data Communication System

The data communication system provides access to the DAS data from remote computers. Each DAS enclosure includes one MD-9 multidrop interface linking its datalogger to the coaxial cable "data bus". On the other end of this "bus" is another MD-9 which connects the coaxial network to a DC-112 Campbell Scientific modem which can be accessed by telephone from a remote computer running the PC-208 software from Campbell.

### 1.4.5 Interactive Tutorial Computers

During the Olympic Games, the DC-112 modem was not present in the system. Instead, a computer was installed in the electrical room. Besides serving a long-term data archiving function, this PC also acted as the data server for a computer located in a kiosk in a publicly-accessible area of the Aquatic Center. This computer provided an interactive tutorial on the system, its performance, and photovoltaics and energy in general, as well as information about the project sponsors and other related information. The program running on the tutorial computer is a Visual Basic program originally developed by the Southwest Technology Development Institute (SWTDI), the same organization that designed and installed the DAS.

*Chapter 2*

# CALCULATIONS AND COMPUTER MODELING USED IN THE DESIGN AND MONITORING OF THE GTAC PV SYSTEM

# 2. Calculations and Computer Modeling Used in the Design and Monitoring of the GTAC PV System

## *2.1 Introduction*

This chapter describes calculations and modeling used in the design and monitoring of the GTAC PV system. The software package PVFORM v. 3.3 was extensively utilized to simulate the system's performance. The inputs to PVFORM used to describe the system, and procedures required to adapt PVFORM for application to the GTAC system, are described. The system's expected behavior, including maximum power output, annual energy output, and maximum expected temperature, are then presented, and the use of this information in making informed design decisions is described. Since the orientation of the PV array is not optimized, the effect of the unoptimized array orientation on the GTAC system's performance is quantified. In addition, other calculations made in judging the system's performance are described.

## 2.2 Brief Review of PVFORM and Background Regarding Required Modifications

PVFORM v. 3.3 is a comprehensive photovoltaic system simulation software package prepared by Sandia National Laboratories. This program is generally accepted to be one of the most accurate and powerful PV system computer models available today [1,2]. The primary features of the package which make it such a useful analysis and design tool for PV systems are its two main submodels, the Perez anisotropic diffuse irradiance model and the Fuentes thermal model [3, 4, 6].

Two difficulties were experienced in applying PVFORM to the GTAC PV system. First, PVFORM assumes that the entire PV array is planar; that is, at the same tilt and azimuth angles. This assumption is implicit in the calculation of the plane-of-array irradiance, since the program only calculates the irradiance incident on a single tilt. PVFORM is therefore not capable of accurately modeling the sunlight on all sections of the curved Aquatic Center array in a single simulation.

The second difficulty arose when we attempted to obtain AC performance results. PVFORM attempts to allow this capability by including a power conditioning unit (PCS) submodel which uses a piecewise-defined function of the unit's efficiency as a function of the fractional loading, or the ratio of the array's DC power output to the unit's rated (full-load) power capacity [7]:

$$\eta_{PCU} = \eta_{PCU,rel}\left(\frac{\eta_{PCU,rated}}{0.91}\right) \qquad [2\text{-}1]$$

where

$$\eta_{PCU,rated} = \text{PCU efficiency at rated capacity}$$

$$\eta_{PCU,rel} = \begin{cases} 8.46F - 0.15, \ 0 \le F < 0.1; \\ 0.774 + 0.663F - 0.952F^2 \\ + 0.426F^3, \ F \ge 0.1 \end{cases}$$

$$F = \frac{\text{PV array output power}}{\text{PCU rated capacity}}$$

Figure 2-1 shows a comparison of the results of this model with actual fractional load efficiency curves for the PCS. The figure shows some disagreement between the PVFORM model and the actual curve. Our original approach to improving on this was to replace the above-described PCS model by a fifth-order polynomial fit to the actual PCS efficiency curve:

$$\eta_{inv} = 3.3089F^5 - 11.1375F^4 + 14.7141F^3 - 9.6373F^2 + 3.1981F + 0.5037 \qquad [2\text{-}2]$$

where F again is the PCS fractional loading. The plot of this polynomial corresponds almost exactly with the actual curve over the range $0.18 < F < 1$. However, we were unable to use PVFORM's internal PCS model due to the non-coplanar nature of our PV array. The approach adopted in this work will be described shortly.

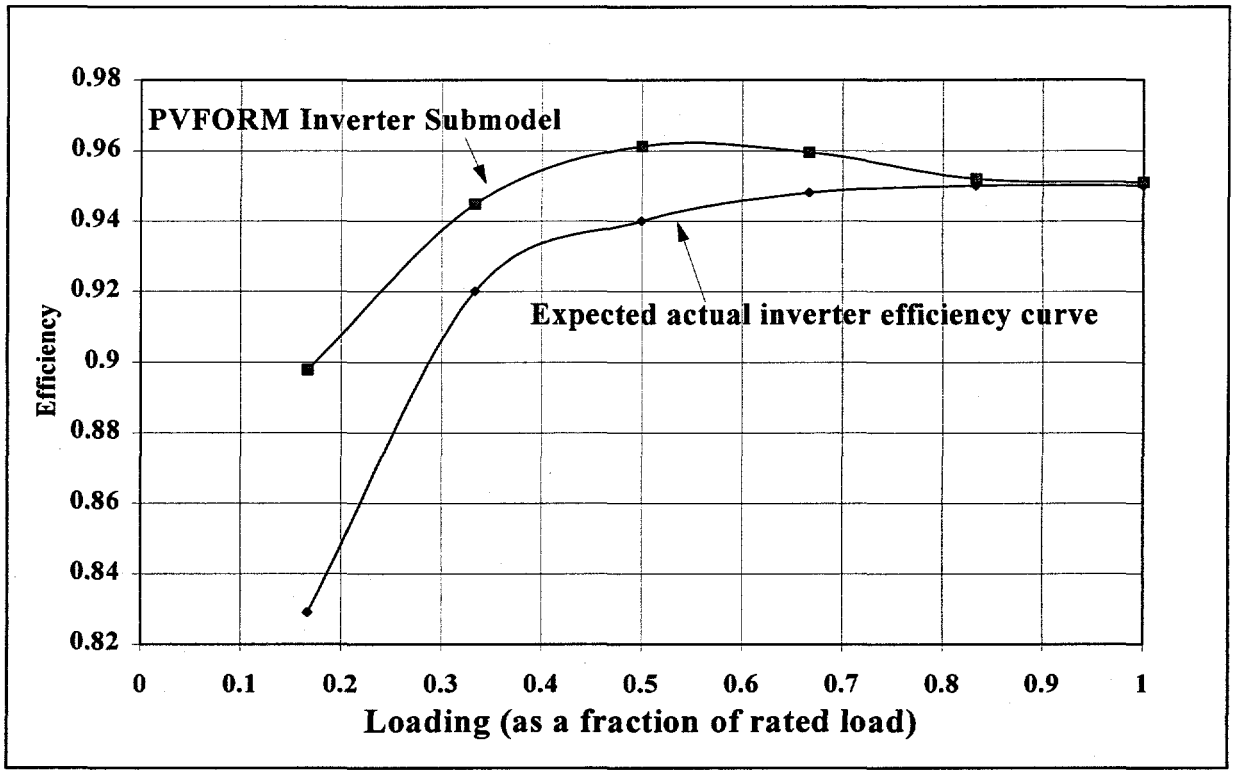


**Figure 2-1. PCU efficiency curve compared with PVFORM model.**

## 2.3 Determination of the PV Array's Expected Power Output and Application to Selecting an Appropriate PCS Power Capacity

PVFORM was useful in several stages of the design process for the GTAC PV system. One of the first applications which arose was the selection of an optimally-sized PCS for the system. Clearly, for economic reasons it is desirable to use the smallest-capacity PCS possible which can still handle the full power output of the array. The best candidate PCS for this system was rated at 315 kW; however, it had already been decided for other reasons that the rated array output power would be 342 kW. The PCS's maximum power point (MPP) tracking circuitry incorporates a self-protection mechanism against PCS damage due to overload: if PV power production exceeds the PCS's power-handling ability, the MPP tracker moves the array off of its MPP, reducing the array output power. For this reason, damage to the PCS was not a concern. However, if this condition could occur frequently under actual operating conditions, the result would be a waste of significant amounts of PV power. It is well known that the 342-kW nameplate rating of the array is determined under conditions which will never be duplicated in the field, so the array will probably never produce that much power, and therefore an exact knowledge of the maximum power which the array will produce under "real" conditions would facilitate PCS selection. PVFORM was used to obtain this information. However, before this could be done, a problem had to be circumvented. The Aquatic Center array is flush-mounted to the roof of the Center, which is curved, and a portion of the array is actually on the north-facing slope of the roof. Obviously, there would be considerable mismatch in the plane-of-array insolation across the array, but PVFORM contains no provisions for dealing with this case, and furthermore we have found no software package which integrates capabilities for handling noncoplanar arrays with those for determining the insolation on each section of the array. Certainly, such a package could be created by integrating PVFORM with a model such as that presented by Bishop [8], but the computation time involved in simulating an array like the one on the Aquatic Center would be extreme. To avoid these difficulties, we adopted a simpler approach.

On the south-facing side of the roof, the tilt angles of the modules vary from about 13° up from horizontal to 0° , with an average tilt of 6.4°; on the north-facing side, the variation is from about 2° to about 10° , with an average tilt of 5.9°. All series strings are coplanar; there is no insolation mismatch between series-connected modules. Since the sections of the array which are under differential illumination are connected in parallel, their operating voltages will be affected. However, it is well-known that the voltage of a PV module or array is only logarithmically dependent on the insolation, and therefore a relatively large difference in insolation is required to produce an appreciable change in voltage. Considering the north-facing and south-facing sides of the roof separately, we noted that the variations from the average tilt on each side are small, and thus, with the above-mentioned consideration about the relative insensitivity of voltage to insolation variations taken into account, the insolation over each side of the roof could be considered to be roughly uniform. Each side of the roof could then be modeled as a separate array with tilt equal to the average tilt on that side. However, a suitable method for combining the two subarrays was required. PVFORM will assume that each subarray operates at its maximum power point, thus ignoring their interaction (effectively "decoupling" them). Due to their parallel interconnection and voltage interaction this will not be strictly true; each subarray will slightly pull the other off of its MPP. If it could be shown that the insolation difference between the two parallel-connected subarrays is sufficiently small, the power output of the subarrays computed independently by PVFORM and that actually produced under parallel interconnection would be almost the same, and the total array power output could then be computed by simply summing the power and energy outputs of the two subarrays. First, PVFORM was employed to quantify the difference in insolation between the two subarrays. It was found that the maximum insolation mismatch occurred during a time at which there was 645 $W/m^2$ of insolation on the south-facing side. If the mismatch was defined as

$$G_{mismatch} = G_{South} - G_{North} \qquad [2\text{-}3]$$

then $G_{mismatch}$ at the time described above was 165 $W/m^2$. Then, a software package called IVCURVE was employed to determine the amount of voltage mismatch between the two subarrays while operating at their maximum power points. IVCURVE computes the array I-V

curve given the insolation, module temperature, and the module electrical parameters. It also can calculate the current and power produced by the array if given the operating voltage, so the maximum power point can be located by iteration, substituting in voltage values until the maximum in power is located. Under the conditions described above, it was found that $V_{MP}$ for the south-facing side was about 363V and that for the north side was 10V lower. This represents just under a 3% difference in voltage. To predict what the "real" operating voltage would be under this condition, we note that the south-facing subarray accounts for 82% of the total array area and should therefore operate closer to its decoupled voltage than the north-facing side will. Thus, we linearly scale the difference between the two operating voltages and predict that the real, coupled operating voltage will be about 361V. Plugging this operating voltage into IVCURVE and computing the PV power produced by the two subarrays, we find that the difference in the predicted power output between the decoupled subarrays and the parallel-interconnected subarrays would be only about -0.1%. This is a negligible error, particularly when compared with other known errors such as that introduced by the assumption of 100% efficient maximum power point tracking, which can be nearly 5% [2]. Therefore, the approach of modeling the Aquatic Center array as two independent subarrays and then adding their power outputs is justified and will result in negligible error.

Using this approach, the array's power output over the course of a year was calculated. Table 2-1 lists the input parameters to PVFORM for the two subarrays, and Figure 2-2 shows a histogram of the array DC power output based on the Typical Meteorological Year (TMY) for Atlanta. Note that the maximum array power output, which occurs on April 1 of the TMY, is 279.7 kW, which is well below the PCS's rated capacity. Therefore, we can conclude that the 315 kW PCS is sufficient for this installation and that its self-protection against overload will not result in a significant loss of power.

**Table 2-1. Listing of PVFORM parameters used in the two-array model of the Aquatic Center PV array.**

| Parameter | Subarray 1: south side | Subarray 2: north side |
|---|---|---|
| Site latitude | 33.7 °N | |
| Array tilt angle (° up from horizontal) | 6.4 | 5.9 |
| Array azimuth angle (° E of S, S = 0°) | 348 | 168 |
| Tracking flag | 1 (fixed tilt, no tracking) | |
| Array area ($m^2$) | 2614.7 | 560.3 |
| Mismatch and line losses (fraction) | 0.04 | |
| Ground albedo (fraction) | 0.20 | |
| Average array height (m) | 9.14[1] | |
| INOCT (°C) | 50.5 | |
| INOCT corresponds to a standoff height of (in / cm) | 3.5 / 8.9 | |
| Reference temperature (°C) | 25 | |
| Reference efficiency (fraction) | 0.1077 | |
| Efficiency reduction coefficient (change/°C) | 0.0037[2] | |

[1] The average array height is used in calculating the average wind velocity over the array. The value given here corresponds to a free-stream height; that is, the wind velocity is constant. Below this height, the wind speed is a function of height because of friction effects between the moving air stream and the ground. The height from the ground of the lowest portion of the Aquatic Center array is about 30.5m, which is clearly greater than 9.14m and is thus in the free stream.

[2] This value is specified by the module manufacturer.

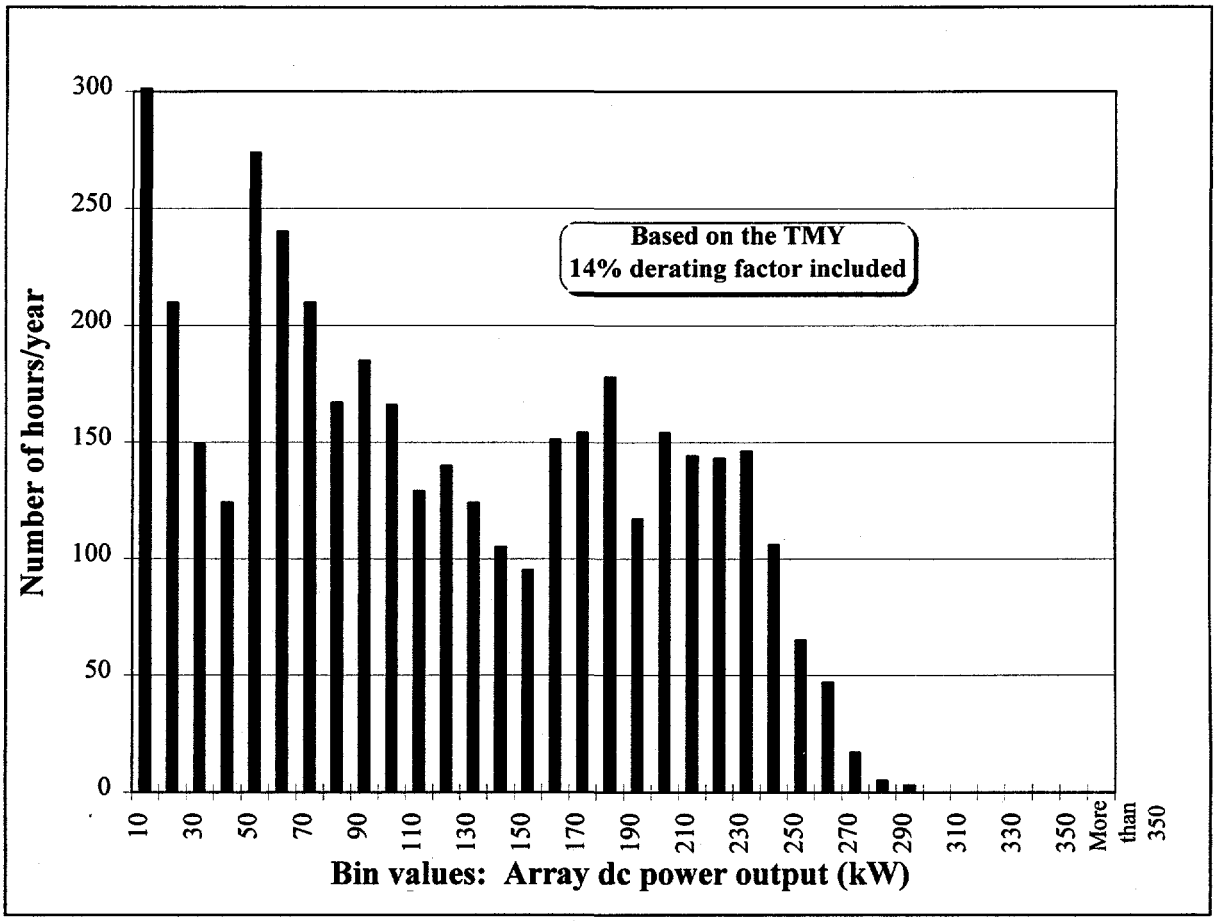


**Figure 2-2. Histogram of the Aquatic Center array's DC power output. The y-axis shows the number of hours that the array produced an amount of power between the x-axis bin value and the next-lowest bin value.**

Using the DC power histogram, we also calculated an "effective PCS efficiency" using the expression

$$\eta_{inv,eff} = \frac{\sum_{j=1}^{N_b} \{N(F_j) \cdot P_j \cdot \eta_{inv,j}(F_j)\}}{\sum_{j=1}^{N_b} N(F_j) \cdot P_j} \qquad [2\text{-}4]$$

where $\eta_{inv,j}(F_j)$ is the PCS efficiency at fractional load $F_j$ (determined from the actual curve), $N(F_j)$ is the number of hours during the year that the PV power production results in fractional loading $F_j$, $P_j$ is the power production corresponding to bin j, and $N_b$ is the number of bins (discrete values of F considered), as demonstrated in Figure 2-3. An important feature of this expression which should be noted is that the effective PCS efficiency depends not only on the PCS efficiency itself but also on the power production of the array, and therefore this parameter can also be used as a measure of how well the PCS is matched to the PV array by comparing the effective PCS efficiency to the full-load PCS efficiency. Using this expression and the information in Figure 2-3, the PCS's effective efficiency for this installation is found to be approximately 90.5%. This compares favorably with the PCS's full-load efficiency of 95%, supporting the choice of this PCS for this PV array. The effective PCS efficiency also provides an easy way to determine the system's AC output. Note that, as mentioned previously, our modeling procedure renders PVFORM's internal PCS submodel unusable, because it is the sum of the subarray powers which needs to be fed into the PCS submodel. This effective PCS efficiency can be used in lieu of writing software to compute the solution of the fifth-order polynomial given above for each DC output data point given by PVFORM. Using the 90.5% effective PCS efficiency, PVFORM predicts that the annual AC energy production of the PV system will be 409 MWh.

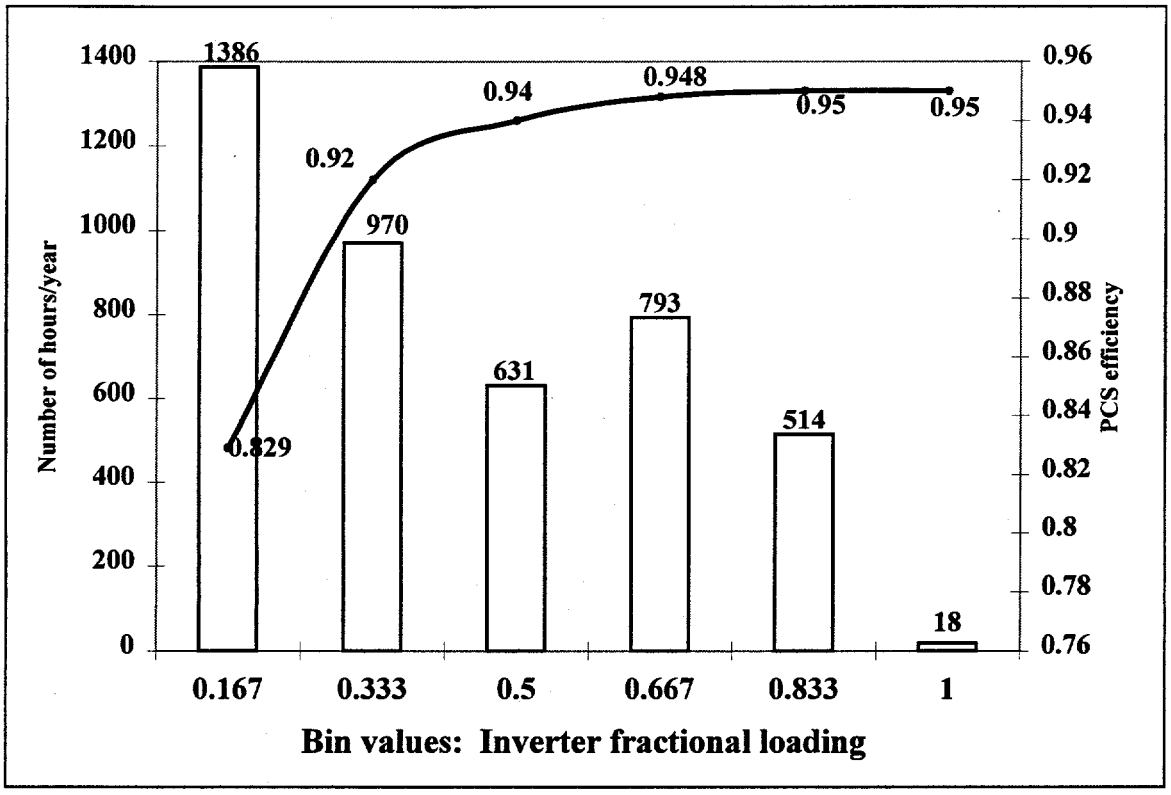


**Figure 2-3. Comparison between the array DC power output histogram and the PCU's efficiency curve. The right-side axis is for the bar chart, showing the number of hours/year that the PV array's power output falls into the given bin value. The left-side axis is for the PCU efficiency curve.**

## *2.4 A Word About Proper Selection of PVFORM Modeling Parameters for the Aquatic Center Array*

### 2.4.1 Sensitivity of Simulation Results to Values of INOCT, Average Array Height, and Ground Albedo

Three of the parameters required by PVFORM, average array height, ground albedo, and INOCT, introduce some uncertainty into the simulation results. The actual height of the Aquatic Center array from the ground ranges from about 30-38 m, but the maximum value of this parameter allowed by PVFORM is 10 m [3]. The ground albedo is not precisely known, but can be assumed to fall in the range of 15-30%. [3, 15] (The 20% value was chosen because this is standard practice in PV systems modeling.) Finally, the method of computing the INOCT is not exact and involves empirically-determined values based on modules other than those in use in this installation [3,6]. As a measure of the sensitivity of the PVFORM results to changes in these parameters, the percent change in annual DC energy production of the array was modeled for six sets of conditions, varying the array height and INOCT. Table 2-2 presents these results, and shows the insensitivity of the results to fairly large variations in these two parameters. Note that the result is more sensitive to changes in the INOCT than in the average array height. A similar set of comparisons was made to examine the effect of varying the ground albedo, but changing the ground albedo from 20% to 100%, which represents the largest possible change, resulted in a change of only +0.14% in the array's DC energy production. This small change is to be expected: because the tilt angle of the array is so low, very little light reflected from the ground will strike the array at an angle which would allow for coupling into the module.

**Table 2-2. Sensitivity of PVFORM calculation results to variations in INOCT and array height from the ground. Results are based on simulations done on the coplanar array used in the optimization studies in Section 5.6.**

| Array Height | INOCT = 46°C | INOCT = 51 | INOCT = 56 |
|---|---|---|---|
| 2.0 | 0.32% | -0.78% | -1.87% |
| 10.0 | 0.97% | -- | -0.97% |

## 2.4.2 Investigation of Wind Speed Effects

The maximum value allowed by PVFORM for average array height is only 10 m, as mentioned earlier. The array height is used in figuring the wind speed over the array, which is a fairly strong function of the array height [6]:

$$V_{wind}(z) = V_{wind}(z_{ref}) \times (\frac{z}{z_{ref}})^{p} \qquad [2\text{-}5]$$

The reference height $z_{ref}$ = 30 ft = 9.14 m is the standard anemometer height at a TMY measuring station, and $V_{wind}(z_{ref})$ is the measured windspeed at $z_{ref}$ (read from the database). The value of the parameter p used by PVFORM is that usually used for open countryside, which is 1/5. This wind speed strongly affects the convective heat transfer coefficient from the front surface of the module [15]:

$$h = 0.028 \frac{\rho^{0.8} c_p^{0.6} k^{0.4}}{\mu^{0.2} L^{0.2}} V_{wind}^{0.8} \qquad [2\text{-}6]$$

where $\rho$, $\mu$ and $c_p$ are the density, viscosity and specific heat of the fluid (air), k is the thermal conductivity of the module, and L is the "characteristic length" of the flow past the body, assumed by PVFORM to be 0.5 m which is a typical hydraulic diameter for a PV module (but incorrect for our PV modules, which would have L values considerably larger than this). This convection parameter in turn strongly affects the module temperature calculated by PVFORM, and thus has a significant effect on the modeling results. Equation 2-5 describes a wind velocity profile as a function of height from the ground. The wind velocity at zero height is zero, as required by frictional effects. This equation is valid for heights up to the reference height $z_{ref}$; above this height it is assumed that surface effects become negligible and the wind speed is a constant, no longer a function of height. This constant value is called the free-stream wind velocity and is equal to $V(z_{ref})$. Since our average array height is much greater than $z_{ref}$, we can

assume the free-stream velocity to be valid over our array. Therefore, we should use 9.14 m as our average array height in Aquatic Center array simulations.

As an aside, recall that the exponent p in Equation 2-5 was set to 1/5, which is the typical value used for open countryside. Clearly, the Aquatic Center is not in the open country, and the value of p suggested for urban areas is 1/3 [6]. However, since we are in the free-stream region of the air flow over the ground, this parameter does not matter because the argument of this exponent is equal to 1. If we did wish to change the value of p, we could edit and recompile the FORTRAN source code.

We should also note that our array is constructed on a curved roof surface which, again based on elementary fluid mechanics, will result in an increased wind speed over the array and thus slightly greater power production [16]. This error is partially offset by the fact that the assumption of a 0.5 m hydraulic diameter is based on module dimensions of 0.3 x 1.2 m, which is obviously incorrect for our modules (1.1 x 1.1 m) [14]. A larger hydraulic diameter will tend to reduce the array power production, as can be seen from Equation 2-6. These two effects combined should result in simulation results that are not more than 3-4% below actual values (an extreme case, based on a doubling of both the wind velocity {as happens with flow past a cylinder [16]} and the hydraulic diameter).

### 2.4.3 Modeling of Fixed DC-side Losses

A fractional power loss due to module-module mismatch is required as an input to PVFORM. Since we are not using the built-in PCS model, we can set this value to zero and simply multiply the DC powers calculated by PVFORM by a fixed derating factor in subsequent post-processing of the data. This is the approach adopted here. The primary reason is that PVFORM allows a maximum mismatch loss of only 8%, but it is common practice to derate the system's power output by 10% to account for dust, soiling and shadowing of the array, and this value alone is too large to input to PVFORM. Therefore, strictly for purposes of clarity and reduction of user error, we have combined all of the DC-side fixed losses into a single parameter which is considered in post-processing.

Values for two of the DC-side loss mechanisms, conductor loss and module-module mismatch, were determined based on values suggested by the system designers and component manufacturers. Each of these mechanisms accounts for a 2% power loss. The fourth DC-side loss which must be considered in this installation is power loss due to the array curvature. When using the procedure outlined above, separating the array into two subarrays, this fourth parameter may be set equal to zero as this loss has been accounted for in the two-subarray modeling scheme. However, for other calculations such as diagnostic calculations, it would be useful to have a value for the fractional power loss due to this parameter. We can find one by comparing the PVFORM-predicted annual energy output of the system for the two-subarray model with that of a single array with all modules at the average tilt of the south-facing side. Rerunning the simulation with this array configuration, we find the predicted annual energy output to be 415 MWh; comparison with the two-subarray prediction of 409 MWh leads to the selection of an annual curvature mismatch loss of 1.4%. However, it should be noted that this is an annually-averaged value. Kcurv will actually be a function of time. It must also be noted that these DC-side loss mechanisms operate in parallel, and therefore the total derating factor is found by multiplying them, not by adding them. This subject will be discussed in Section 5.8.

## 2.5 Maximum Voltage vs. PCS DC Input Rated Voltage

The 315kW PCS has a maximum DC open-circuit input voltage of 600V, as do the DC-side conductors and switchgear. Therefore, care must be taken to ensure that the series-parallel configuration of the array is such that the array voltage will not exceed 600 V. Since the array has a negative voltage temperature coefficient, and temperatures lower than the STC-specified 25°C could be encountered in the field, PVFORM was used to model the temperature of the cells for an entire year, using the TMY as input. The output was then scanned for the lowest cell temperature which occurred during daylight hours. This temperature was -7.3°C. The maximum voltage produced by the array was calculated using the equation

$$V_{\max} = \left[V_{OC} + (K_{Voc})(\Delta T_{\max})\right] \times N \qquad [2\text{-}7]$$

where N is the number of series modules (12), $\Delta T_{max}$= ($T_{min}$ - 25°C), $V_{OC}$ is the open-circuit voltage (42.6V), and $K_{Voc}$ is the voltage derating coefficient per module given by the manufacturer (-0.146 V/°C). Substituting the values for this system, $V_{max}$ is found to be 568 V. It is important to note that when this low temperature occurs there will be very little usable sunlight, so the actual voltage will be lower than 568 V. Therefore, based on PVFORM modeling, we conclude that the array design is acceptable and will not produce voltages in excess of the 600 $V_{DC}$ rating of the DC-side equipment.

It should also be noted that Underwriters' Laboratories (UL) standards dictate that the lowest expected ambient temperature at the site should be used in determining the maximum array voltage [9]. In order to determine this temperature, all 30 years of the NSRDB-SAMSON database on CD-ROM were scanned for the minimum temperature during that time period in Atlanta, which was -22.2°C (occurring on January 21, 1985). Substituting this value into Equation 2-7 gave

$$\Delta T = -47.2^{o}C$$
$$V_{max} = 594V$$

This is still below the 600 $V_{DC}$ limit, again supporting the suitability of the array design.

## 2.6 Investigation of the Effects of Standoff Height

One of the novel features of this PV installation is that the array is mounted to the roof directly using clamps connected to the standing seams. The standing seam height is about 2.5 inches, and the mounting clamps hold the modules about 1 inch above the standing seams, resulting in an array-roof standoff height of about 3.5 inches. From a photovoltaic standpoint, the standoff height is important because it affects the ventilation behind the array and thus the array temperature. PVFORM was utilized to quantify this effect. The standoff height is reflected in PVFORM in the choice of INOCT, where INOCT is the Installed NOCT (Nominal Operating Cell Temperature) and is calculated using the manufacturer's specified NOCT and a set of empirically-determined rules [3,6]. We used INOCT values of 56°C, 50°C, and 48°C, which correspond to standoff heights of 2", 4" and 6" respectively, to examine the effect of standoff height on the array's performance. We also assessed an additional "penalty" of +4 °C [3,6] because the underlying standing-seam roof is "channelized", meaning that the standing seams will partially restrict airflow behind the array and increase INOCT. To investigate the importance of the standoff height, we examined the array annual AC energy production and the maximum temperature attained by the array as a function of standoff height (Figure 2-4). As expected, the model calculations reveal that as the array-roof standoff height increases, the maximum cell temperature attained during the year decreases and as a result the annual energy production of the array increases.

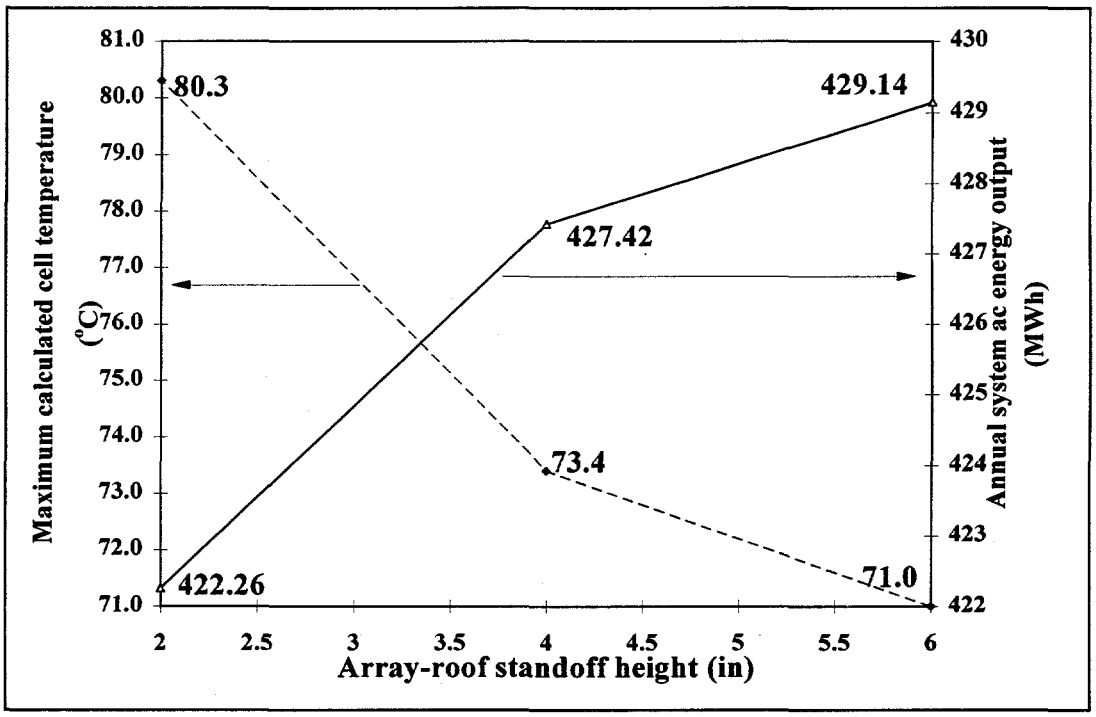


**Figure 2-4. Maximum cell temperature attained during a typical year in Atlanta vs. array-roof standoff height, compared with the annual PV energy production vs. array-roof standoff height.**

As was mentioned previously, the annual DC energy output variation as a function of standoff height is fairly small. Notice, however, that the maximum temperatures attained by the cells in the array are quite high, approaching 77°C for the 3.5" array-roof distance. This calculation is justified and important because it allows for design within tighter tolerances, since the maximum temperature which will be attained by the array will be known. Cable temperature ratings (90°C for this system) and other factors affected by operating temperatures beneath the array, which will always be below the array temperature (assuming that ampacities are properly selected), can be adjusted for greater economy without jeopardizing reliability.

## 2.7 Investigation of the Optimum Orientation of the PV Array

The orientation of the Aquatic Center PV array is not optimized. The tilt and azimuth of the array were determined by the shape of the roof, which in turn was selected according to architectural and aesthetic considerations. We undertook the task of quantifying the performance penalty incurred by this unoptimized orientation using PVFORM. For this exercise, the array was modeled as being coplanar because the computational intensity involved in accounting for the variable tilt in such a large number of PVFORM simulations would have become extreme. The baseline for these comparisons was thus a coplanar array at the average tilt of the south-facing side (6.4°), whose annual AC energy production as computed by PVFORM is about 415 MWh. A matrix of 84 PVFORM simulations covering tilt angles from 0° (horizontal) to 60° up from horizontal and azimuth angles of 20° east of south to 90° west of south at 10° increments was constructed. From this matrix, two sets of data were extracted and plotted: the total annual AC energy production as a function of array orientation, and the array's AC energy production during the peak hours of 12-7 pm, June through September, as a function of array orientation ("peak-shaving energy production").

Figure 2-5, which is a 3-D plot of the array's annual energy production as a function of array orientation, shows that the optimum array orientation for maximum annual energy production is a tilt of about 30° with a due-south azimuth. To increase the accuracy of this figure, we ran further simulations at increments of 2° and found that 30° is the optimum to within 2°. Notice that the optimum tilt is slightly less than the site latitude (33.7°N). This is to be expected, since the optimum tilt for maximum annual energy production is roughly equal to the site latitude, but high-humidity locations can have slightly lower optimum tilts because high humidity will increase the diffuse component [10], and this component decreases with increasing tilt because more diffuse light hits the back of the array at higher tilts [4]. However, Figure 2-5 also demonstrates that the sensitivity of the system performance to such small deviations is fairly small (performance penalties of only about 1% or less). The model calculations show that the

annual energy output could be increased from about 415 MWh/year to about 462 MWh/year (an 11% increase) by changing the tilt angle to 30° from its installed orientation (6.4°). Recall that the 415 MWh/year baseline figure was computed for a coplanar array. If the comparison is instead made to the curved array as represented by our two-subarray model, thus adding the effect of the roof curvature, we find that the output could have been increased by almost 14%, from 407 MWh to 462 MWh, by placing the entire array at the same (optimized) tilt.

Since peak shaving is an important potential application of PV systems, we also investigated the "peak-shaving effectiveness" of our system. To optimize the array for peak shaving, conventional wisdom would state that the array should be oriented by the position of the sun at the peak demand time on the local utility's system. For the Georgia Power Company, the peak demand occurs at about 3-4pm during the four summer months of June-September. According to the simple set of equations for determining solar position found in [10,11] or the solar geometry charts found in [10], the "rule of thumb" optimum array orientation should be approximately 43° tilt and about 82° azimuth west of south to achieve maximum peak shaving at the peak demand time (3-4pm). To look for the peak shaving optimum, we examined the array's energy production during "peak hours", defined by Georgia Power as noon-7pm during the four summer months, as a function of array orientation. The results of our simulations are shown in Figure 2-6, which shows that the peak shaving optimum is approximately 30° tilt and 70° W of S azimuth. As before, we increased the resolution of our matrix near this point and found that the optimum is actually 35° tilt and 75° W of S azimuth. These results demonstrate that applying the rule of thumb in Atlanta yields values that are slightly high, although again the sensitivity of the system performance to small deviations from the optimum orientation is small.

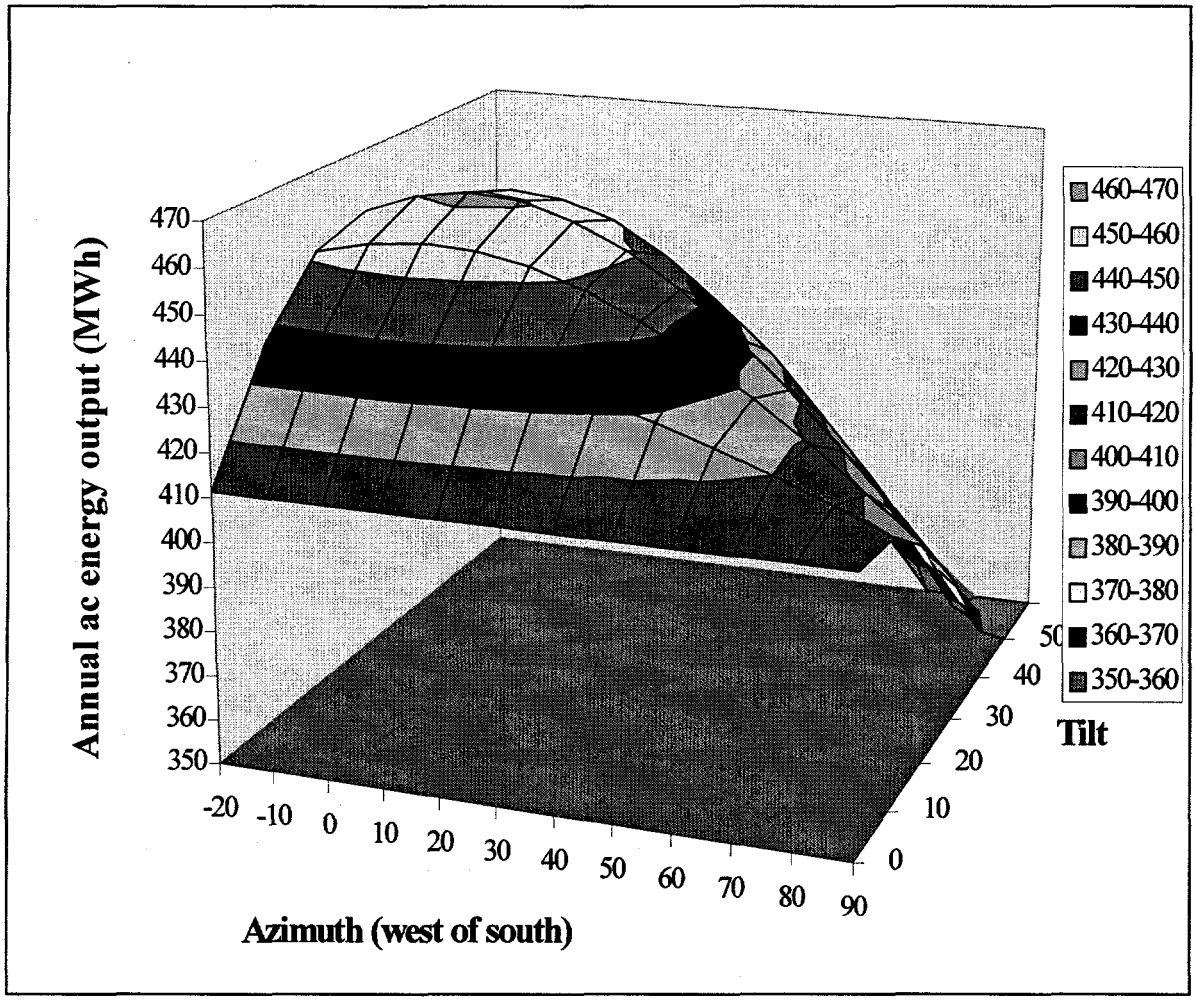


**Figure 2-5. Annual AC energy output of the Aquatic Center array as a function of array orientation.**

The small discrepancy between predicted optimum tilts can be explained as before: as the tilt angle is increased, more and more diffuse irradiation is lost because it strikes the back of the array. In the case of the azimuth, the disagreement arises because the peak demand time falls relatively late in the day, at a time when less solar energy is available, and orienting the array for maximum production at that time sacrifices energy production at earlier times in the window, when more insolation is available. Too great an azimuth results in an excessive loss of this midday solar energy and an eventual reduction of peak shaving capability, with the peak window as defined here (noon-7pm).. The model calculations (Figure 2-6) show that the annual electricity generation of the Aquatic Center array during the peak window could be increased from about 109.1 MWh/year to 123.6 MWh/year, an increase of 13%, by moving the orientation to 35° tilt and 75° azimuth west of south.

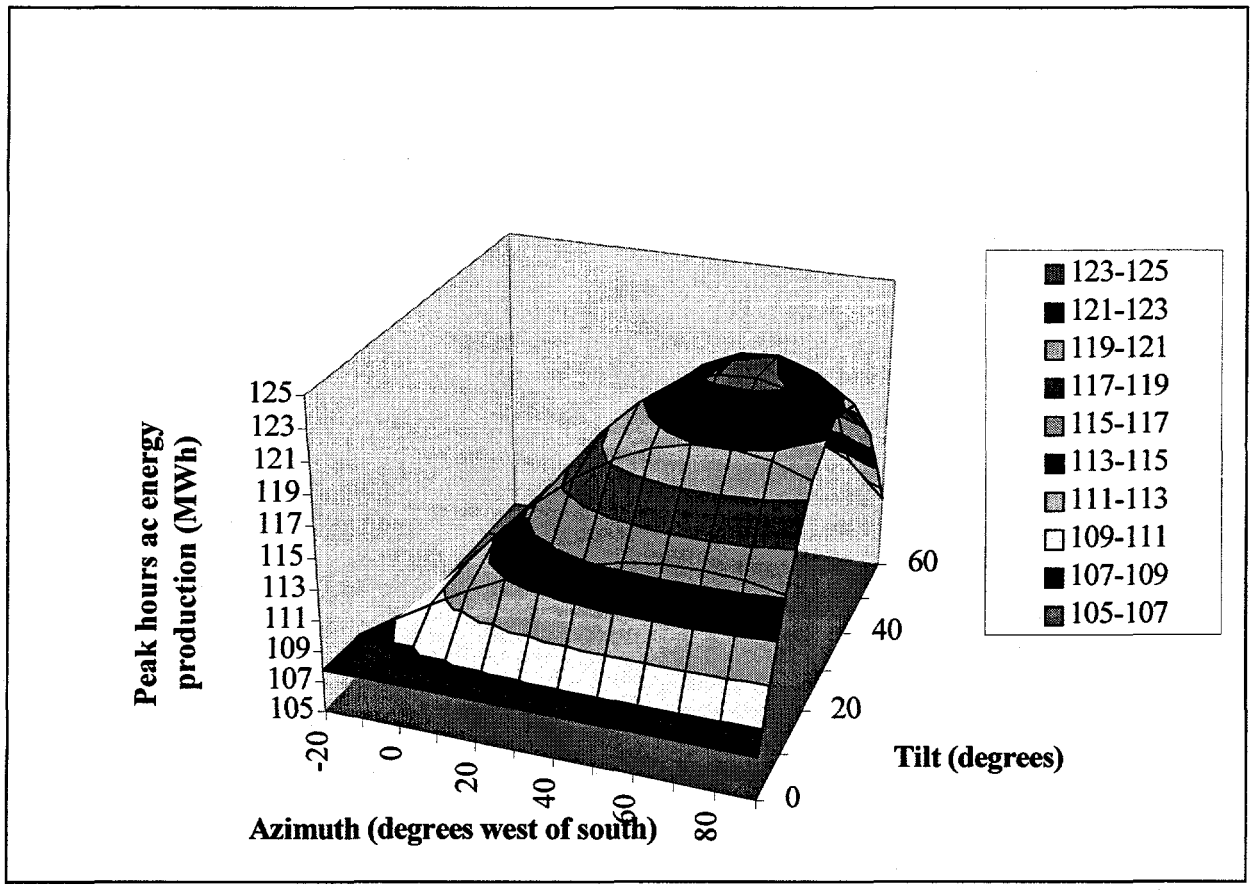


**Figure 2-6. Peak hours (noon-7pm, June-Sept) energy production of the Aquatic Center array vs. array orientation.**

## 2.8 Use of Modeling in System Monitoring

The Aquatic Center PV system is equipped with an extensive monitoring and data acquisition system (DAS) which allows researchers to closely observe the performance of the system and compare this performance with expected values. The DAS also collects meteorological data for comparison purposes. In early July, 1996, just before the start of the Summer Olympics, observers at Georgia Tech's University Center of Excellence in Photovoltaics noted that the power output of the system recorded by the DAS was much lower than had been predicted by the modeling described here. Where power outputs of 220-240 kW were expected, only 180-190 kW of PV electric power was actually being produced. The meteorological measurements and readings of the module temperatures were used to calculate the expected system output according to the simple system model

$$P_{dc} = G_{poa} A_{array} \eta_{PV} \qquad [2\text{-}8]$$

where

$$\eta_{PV} = \eta_{rated} \cdot (1 - K_{dust})(1 - K_{curv})(1 - K_{mism})(1 - K_{dcloss})[1 - (T_{module} - T_{STC})K_{\eta}] \qquad [2\text{-}9]$$

with $\eta_{rated}$ = the modules' rated efficiency (10.77%), $K_{dust}$ = 10% is the derating factor due to soiling, $K_{curv}$ = 1.4% is the power loss caused by the roof curvature, $K_{mism}$ = 2% is the derating factor due to module-module intrinsic parameter mismatch, $K_{DCloss}$ = 2% is the derating factor due to losses in DC-side conductors and equipment, $T_{module}$ is the measured module temperature, $T_{STC}$ is the standard test condition temperature (25°C), and $K_{\eta}$ is the modules' efficiency temperature coefficient. Each of these terms must be individually calculated and then all terms multiplied in order to get the derated system efficiency, since the effects operate in series. It is incorrect to add the derating factors; for example, using the values of the fixed DC losses above, we would calculate their product to be 82.7%, meaning that they have decreased the system efficiency by 17.2%. This is different than the 18.2% we would predict by adding the parameters. Admittedly, the difference is small, but technically the addition approach is

incorrect. In applying this procedure to the Aquatic Center system in July of 1996, the expected DC-side system efficiencies were around 7.5%; actual DC-side system efficiencies were as low as 5%. This made it clear that there was a problem with the system, and subsequent on-site investigation revealed the nature of the problem: one-seventh of the array was producing no power. It turned out that the roof had received a direct lightning strike in early July, and this strike blew fuses and surge arrestors in one entire section of the array. Fortunately, the problem was detected in time to allow for repairs before the Olympics. However, without the forewarning provided by the lack of consistency with performance expectations obtained from both simple and detailed models, the situation might have been very different, and the opportunity to showcase the system before a worldwide audience could have been lost.

## 2.9 Conclusions

The use of modeling in design considerations for the PV array on the Georgia Tech Aquatic Center has been described. The primary model used, PVFORM v. 3.3, was thoroughly reviewed. Calculations of the predicted PV array power output showed that it could be expected to remain below 315 kW, and thus the 315 kW PCS was adequate. PVFORM's cell temperature submodel was used to obtain the lowest cell temperature attained by the array, with which it was shown that the maximum array voltage would not exceed the 600 V DC-side limit and thus the array design was acceptable. The effects of varying the array standoff height on array energy output were quantified and shown to be consistent with expectations. Finally, the effect of the array's non-optimal orientation, which was fixed by aesthetic considerations, was examined. We have demonstrated that the array's annual energy production is reduced by 11% and that its peak shaving capability is reduced by 13% due to the unoptimized orientation, when compared with a coplanar array. If the effect of the roof curvature is taken into account, the reduction in annual energy production becomes almost 14%, and the reduction in peak-shaving capability would similarly increase.

## 2.10 References


[1] S. Rahman and B. H. Chowdhury, "Simulation of Photovoltaic Power Systems and Their Performance Prediction", IEEE Transactions on Energy Conversion 3(3), p. 440-446, 1988.

[2] R. Perez, J. Doty, B. Bailey, and R. Stewart, "Experimental Evaluation of a Photovoltaic Simulation Program", Solar Energy 52(4), p. 359-365, April 1994.

[3] D. F. Menicucci and J. P. Fernandez, User's Manual for PVFORM: Photovoltaic System Simulation Program for Stand-Alone and Grid-Interactive Applications, Sandia National Laboratories publication SAND85-0376, October 1989.

[4] R. Perez, R. Seals, P. Ineichen, R. Stewart, and D. Menicucci, "A New Simplified Version of the Perez Diffuse Irradiance Model for Tilted Surfaces", Solar Energy 39(3), p. 221-231, 1987.

[5] P. Ineichen, R. Perez, and R. Seals, "The Importance of Correct Albedo Determination for Adequately Modeling Energy Received by Tilted Surfaces", Solar Energy 39(4), p. 301-305, 1987.

[6] M. K. Fuentes, "A Simplifies Thermal Model for Flat-Plate Photovoltaic Arrays", Sandia National Laboratories publication SAND85-0330, May 1987.

[7] D. F. Menicucci, "Photovoltaic Array Performance Simulation Models", Solar Cells 18, p. 383-392, 1986.

[8] J. W. Bishop, "Computer Simulation of the Effects of Electrical mismatch in Photovoltaic Interconnection Circuits", Solar Cells 25(1), p. 73-89, October 1988.

[9] J. C. Wiles, Photovoltaic Power Systems and the National Electric Code: Suggested Practices, Photovoltaic Design Assistance Center, Sandia National Laboratories, March 1995.

[10] M. Buresch, Photovoltaic Power Systems, by McGraw-Hill, 1981.

[11] S. R. Wenham, M. A. Green, and M. E. Watt, Applied Photovoltaics, Centre for Photovoltaic Devices and Systems, University of New South Wales, Australia, 1994.

[12] R. Hulstrom (ed.), Solar Resources, MIT Press, 1989.

[13] Values suggested by system integrator Mr. Dan Nall of Roger Preston Associates.

[14] Module specifications from Solarex MSX-120 spec sheet provided by the manufacturer.

[15] F. D. Incropera and D. P. DeWitt, Fundamentals of Heat and Mass Transfer, 3rd ed., pub. John Wiley and Sons 1990.

[16] B. R. Munson, D. F. Young, and T. H. Okiishi, Fundamentals of Fluid Mechanics, 2nd ed., pub. John Wiley and Sons 1994.

*Appendix A*

# REPORTS ON THE PERFORMANCE OF THE GEORGIA TECH AQUATIC CENTER PV ARRAYY

# *REPORT ON THE PERFORMANCE OF THE GEORGIA TECH AQUATIC CENTER PV ARRAY: JULY, 1996*

**Table 1. Summary of the performance of the Georgia Tech Aquatic Center PV Array, July 1996.**

| | |
|---|---|
| Typical PV array DC voltage: | 340-370V |
| Energy produced (AC): | 33.2 MWh |
| Maximum module temperature recorded: | 75.3°C = 167.5 °F |
| Maximum AC power recorded: | 221.3 kW |
| System operational hours: | 379.5 |
| System down time (hours)[a]: | 23.8 |

[a] The system down time includes all hours during which the PV system was turned off. Hours during which the PV system was not producing power due to darkness are not included.

Figures 1 and 2 give the distributions of the insolation on the array and the AC power produced by the system. Figure 1 also shows the insolation distribution predicted by our modeling and the measured and predicted average daily insolation.

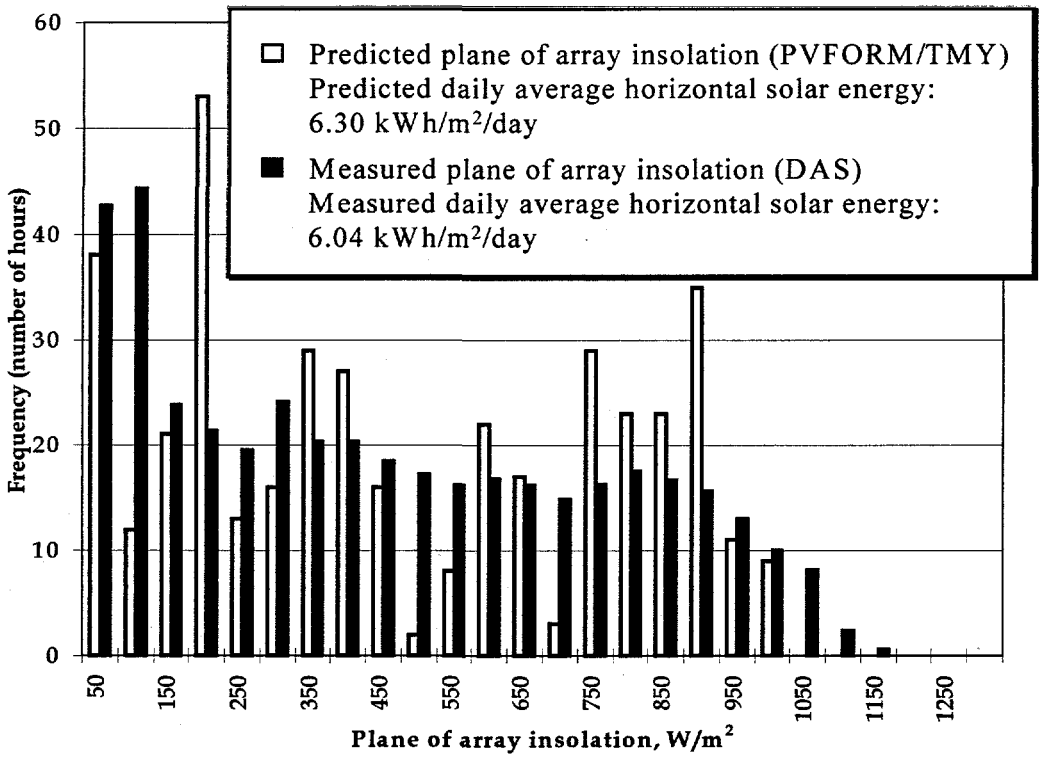


**Figure 1. Histogram of the plane of array insolation on the Aquatic Center PV array, July 1996. The insolation distribution predicted by the TMY and PVFORM is included for comparison.**

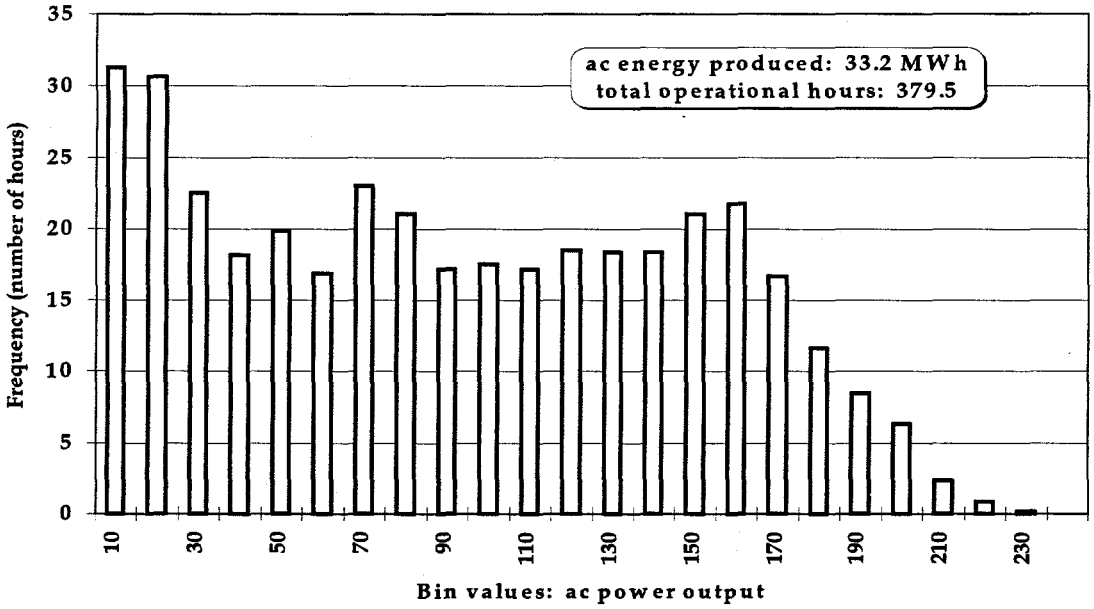


**Figure 2. Histogram of the AC power output of the Aquatic Center PV system, July 1996. Total energy for the month is given also.**

Figure 3 shows the system's measured and predicted apparent efficiencies. Note that there are two distinct branches of the measured curve. During the first part of July, it was noted by UCEP researchers that the system's apparent efficiency was on the lower branch and was much lower than the expected apparent efficiency. Investigation of the array revealed that one of the seven source circuits in the PV array was inoperative due to blown fuses, apparently the result of a direct lightning hit to the roof. After replacement of the fuses, the system's apparent efficiency moved to the upper branch of the measured curve, more closely matching the expected apparent efficiency. For the modeled system AC efficiency, the following model was employed:

$$\eta_{PV,AC} = \eta_{rated}\eta_{inv}\left(1-K_{dust}\right)\left(1-K_{curv}\right)\left(1-K_{mismatch}\right)\left(1-K_{DCloss}\right)\left[1-K_T\left(T_{PV}-T_{STC}\right)\right]$$

where

$\eta_{rated}$ = the rated efficiency of the PV modules = 10.77%

$\eta_{inv}$ = either the measured value (AC power out ÷ DC power out) or the modeled value (from a fifth-order polyfit to the manufacturer's power-efficiency curve) of the inverter's efficiency

$K_{dust}$ = the percentage of power loss due to dust/soiling on modules = 10%

$K_{curv}$ = the power loss due to the roof curvature = 4.2%

$K_{mismatch}$ = the power loss due to module parameter mismatch = 2%

$K_{DCloss}$ = the power loss due to DC-side $I^2R$-type losses = 2%

$K_T$ = the modules' thermal derating coefficient = 0.0037 %/°C

$T_{PV}$ = the module temperature (measured)

$T_{STC}$ = the Standard Test Condition temperature = 25°C

Note that this equation gives what we are referring to as the system's "apparent" efficiency, which is not the actual system efficiency. The source of this problem is the fact that the PV array is curved, with a portion of it facing north. Recall that efficiency is defined in terms of power as (power out) / (power in). When we compute the measured efficiency of the Aquatic Center PV system, we are using an irradiation measurement

made using a pyranometer which is tilted at the average tilt of the south-facing side. This is then multiplied by the total array area (north and south sides) to obtain the total radiant power incident on the array. However, this does not account for the fact that not all of the radiant power is actually intercepted by the array, because part of the array is at a different tilt than the pyranometer. Therefore, the system efficiency we are calculating from these measurements using (power out) / (power in) is actually lower than the true system efficiency; the power out will be the true power output of the system, but the power in does not account for the roof curvature and is thus artificially high. This is the origin of the term "apparent" efficiency. To correct the efficiency which our model above will predict so that it accounts for this effect, we have included the $(1-K_{curv})$ term, which is intended to convert our predicted efficiency to a predicted "apparent" efficiency.

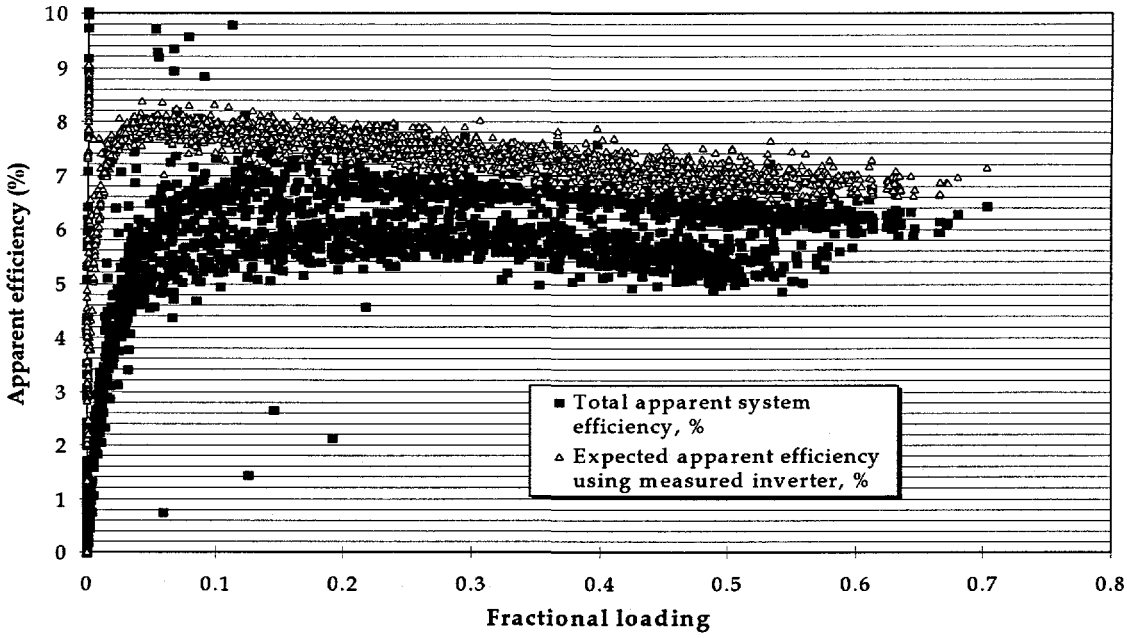


**Figure 3. The apparent efficiency of the Aquatic Center PV system. The hollow triangles are the apparent efficiencies predicted by the model given below, and the filled squares are the measured values.**

# *REPORT ON THE PERFORMANCE OF THE GEORGIA TECH AQUATIC CENTER PV ARRAY: AUGUST, 1996*

**Table 1. Summary of the performance of the Georgia Tech Aquatic Center PV Array, August 1996.**

| | |
|---|---|
| Typical PV array DC voltage: | 320-385V |
| Energy produced (AC): | 31.3 MWh |
| Maximum module temperature recorded: | 75.5°C = 170.0 °F |
| Maximum AC power recorded: | 208.4 kW |
| System operational hours: | 365.5 |
| System down time (hours)[a]: | 2 |

[a] The system down time includes all hours during which the PV system was turned off. Hours during which the PV system was not producing power due to darkness are not included.

The accompanying figures illustrate the performance of the Aquatic Center PV array for August, 1996. The histogram of plane of array insolation for the month (Figure 1) shows that the insolation over the course of the month is lower than that predicted by our computer models but is still fairly good, with maximum values of nearly 1000 W/m$^2$ (one sun). The AC energy production, however, is significantly lower than predicted by our modeling for August (43.7 MWh). Figure 2 shows a histogram of the system's actual AC power output for the month.

We have also plotted the system's measured total efficiency and compared it with two different theoretically-predicted efficiencies, one using a fifth-order polynomial model of the inverter's efficiency curve (Figure 3), the other using an inverter efficiency calculated from measured AC and DC power data from the system (Figure 4). In both plots, a vertical dashed line is drawn at a fractional loading value of 20% because neither the measured data nor the model is accurate for $F < 0.20$.

For the modeled system efficiency, the following model was employed:

$$\eta_{PV,AC} = \eta_{rated}\eta_{inv}\left(1-K_{dust}\right)\left(1-K_{curv}\right)\left(1-K_{mismatch}\right)\left(1-K_{DCloss}\right)\left[1-K_T\left(T_{PV}-T_{STC}\right)\right]$$

where

$\eta_{rated}$ = the rated efficiency of the PV modules = 10.77%

$\eta_{inv}$ = either the measured value (AC power out ÷ DC power out) or the modeled value (from a fifth-order polyfit to the manufacturer's power-efficiency curve) of the inverter's efficiency

$K_{dust}$ = the percentage of power loss due to dust/soiling on modules = 10%

$K_{curv}$ = the power loss due to the roof curvature = 4.2%

$K_{mismatch}$ = the power loss due to module parameter mismatch = 2%

$K_{DCloss}$ = the power loss due to DC-side $I^2R$-type losses = 2%

$K_T$ = the modules' thermal derating coefficient = 0.0037 %/°C

$T_{PV}$ = the module temperature (measured)

$T_{STC}$ = the Standard Test Condition temperature = 25°C

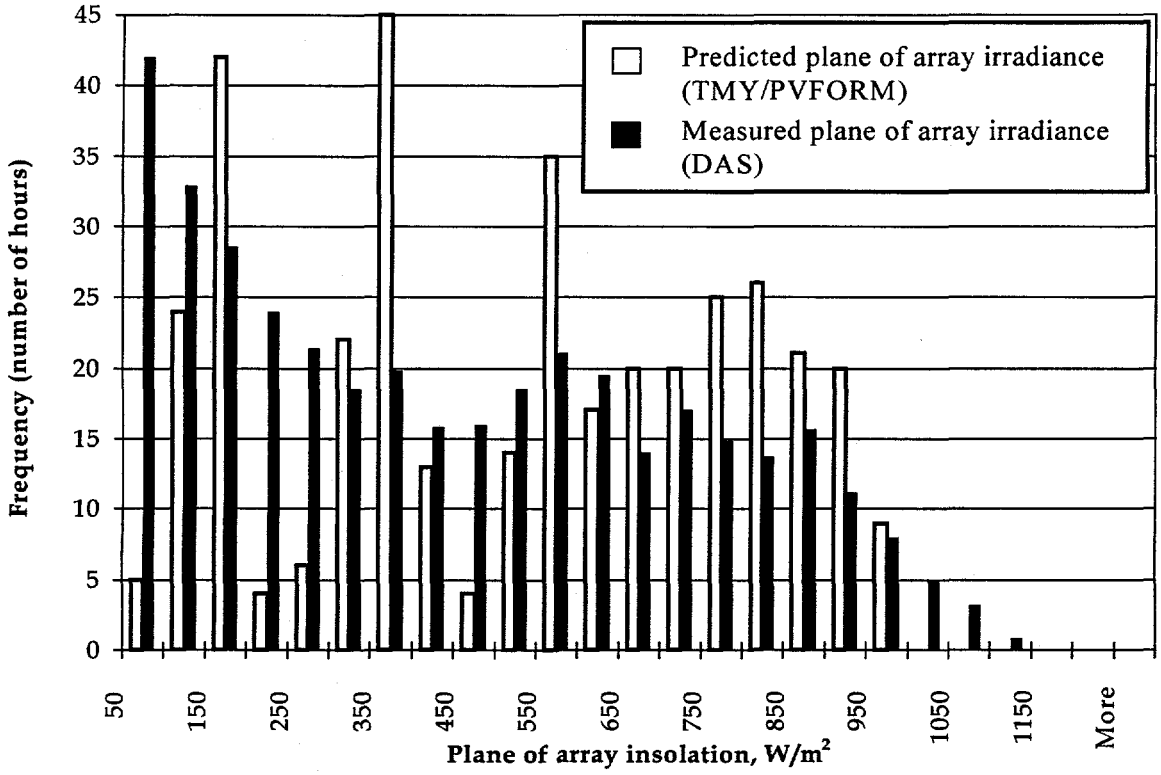


**Figure 1. Histogram of the predicted and measured plane of array insolation on the Aquatic Center PV array, August 1996.**

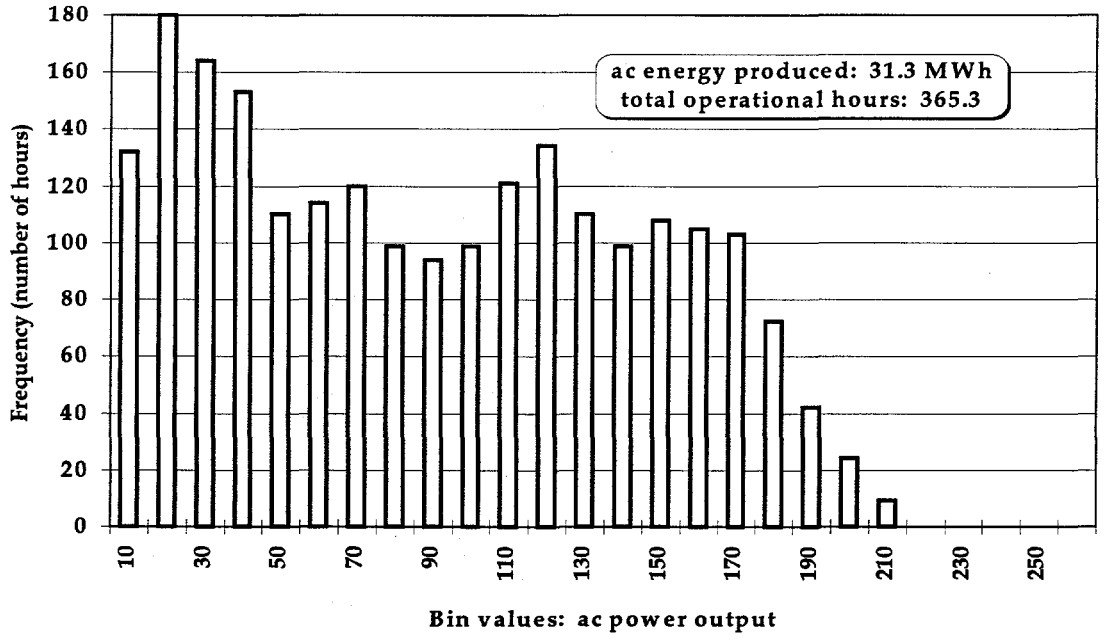


**Figure 2. Histogram of the AC power output of the Aquatic Center PV system, August 1996. Total energy for the month is given also.**

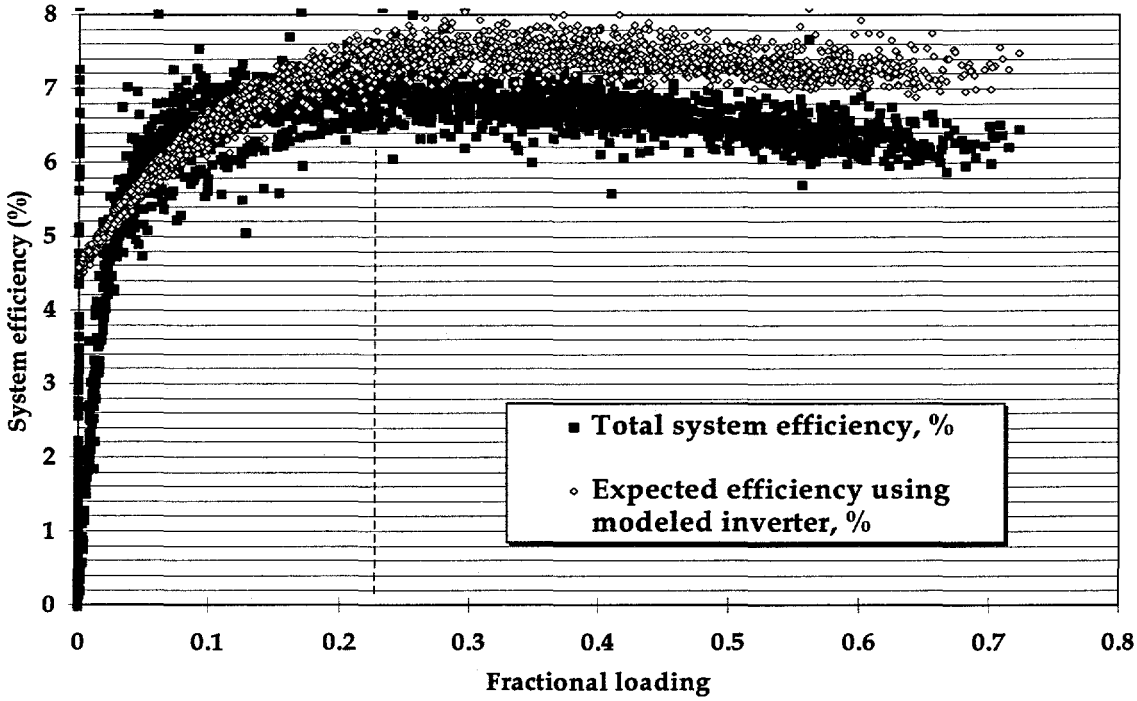


**Figure 3. Aquatic Center PV system total efficiency measurement compared with expected system efficiency value calculated using the modeled inverter efficiency, August 1996.**

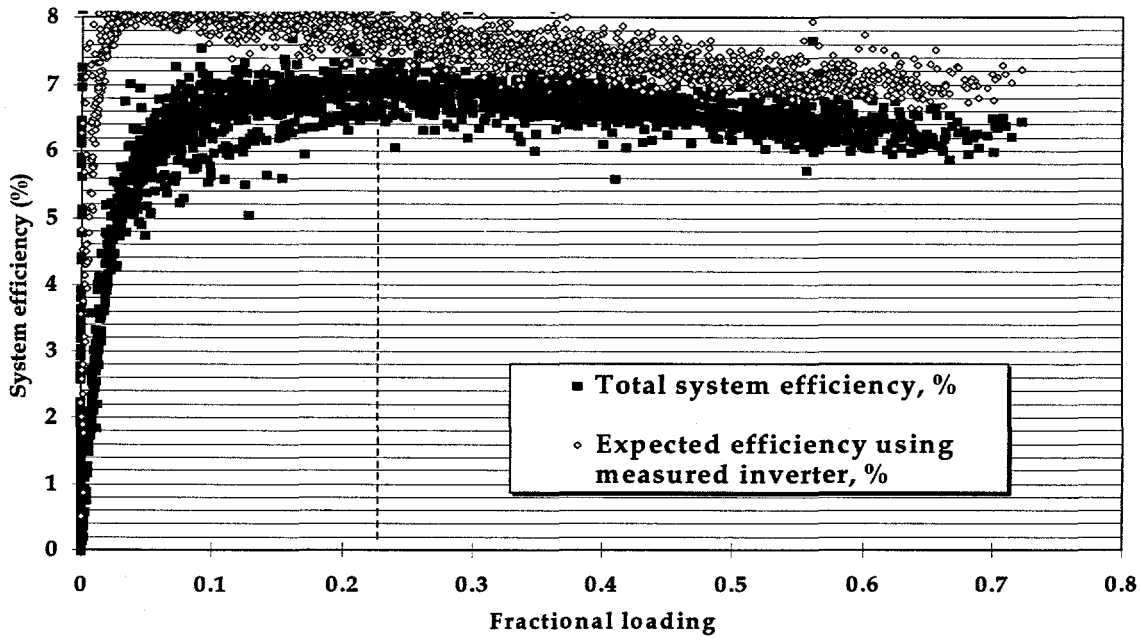


**Figure 4. Aquatic Center PV system total efficiency measurement compared with expected system efficiency value calculated using the measured inverter efficiency, August 1996.**

We see a marked difference (about 0.75% absolute) between the predicted and measured system efficiencies during August. The reasons for this are not yet clearly understood. It is known that one small section of the PV array was disconnected during most of the month for servicing, but this factor has been accounted for in the measured system efficiency. The temperatures during the month were higher than normal, but this factor has been accounted for in the calculated system efficiency. All periods during which the inverter was in standby mode during daylight hours coincide with the passage of strong storms which reduced the system's power output to below the inverter's low-power cutoff, which means that the system's AC power and the incident insolation will show the same trend during these times and the measured system efficiency should not be affected. Therefore, none of these factors is responsible. Strangely, the predicted and measured system efficiencies during subsequent months are in much better agreement. This puzzle remains unsolved.

Figure 5 shows a comparison between the modeled and measured inverter efficiency curves. The figure shows the inverter's efficiency to be slightly lower than expected for $F > 0.5$. This could be the case, but there are two other possible explanations as well: 1) sensor drift, leading to inaccurate measurements; 2) a need to adjust the model.

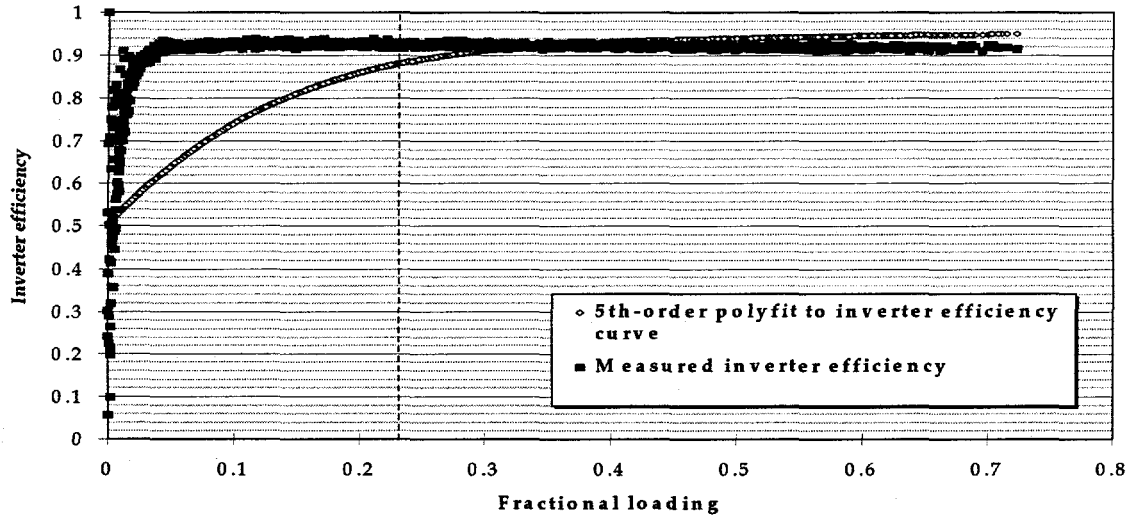


**Figure 5. Comparison between modeled and measured efficiency curves.**

## *REPORT ON THE PERFORMANCE OF THE GEORGIA TECH AQUATIC CENTER PV ARRAY: SEPTEMBER, 1996*

**Table 1. Summary of the performance of the Georgia Tech Aquatic Center PV Array, September 1996.**

| | |
|---|---|
| Typical PV array DC voltage: | 330-400V |
| Energy produced (AC): | 28.7 MWh |
| Maximum module temperature recorded: | 69.0°C = 156.2 °F |
| Maximum AC power recorded: | 231.7 kW |
| System operational hours: | 333.3 |
| System down time (hours)[a]: | 0.33 |

[a] The system down time includes all hours during which the PV system was turned off. Hours during which the PV system was not producing power due to darkness are not included.

The accompanying figures illustrate the performance of the Aquatic Center PV array for September, 1996. The histogram of plane of array insolation for the month (Figure 1) shows that the average daily energy flux for this month is essentially the same as that predicted by PVFORM/TMY modeling, but its distribution is considerably different. As in all other months during which the system has been monitored in this way, the predictions are more optimistic than the measured data. Nonetheless, the AC power production is quite strong, as shown in Figure 2, with peak values exceeding 230 kW, and the 28.7 MWh of AC energy production for September compares quite favorably with the predicted value of 32.6 MWh.

We have also plotted the system's measured total efficiency and compared it with the theoretically-predicted efficiencies using a fifth-order polynomial model of the inverter's efficiency curve (Figure 3) and an inverter efficiency calculated from measured

AC and DC power data from the system (Figure 4). The models and measurements are valid for fractional loading $F \geq 0.20$. For the modeled system efficiency, the following model was employed:

$$\eta_{PV,AC} = \eta_{rated}\eta_{inv}\left(1 - K_{dust}\right)\left(1 - K_{curv}\right)\left(1 - K_{mismatch}\right)\left(1 - K_{dcloss}\right)\left[1 - K_T\left(T_{PV} - T_{STC}\right)\right]$$

where

$\eta_{rated}$ = the rated efficiency of the PV modules = 10.77%

$\eta_{inv}$ = either the measured value (AC power out ÷ DC power out) or the modeled value (from a fifth-order polyfit to the manufacturer's power-efficiency curve) of the inverter's efficiency

$K_{dust}$ = the percentage of power loss due to dust/soiling on modules = 10%

$K_{curv}$ = the power loss due to the roof curvature = 4.2%

$K_{mismatch}$ = the power loss due to module parameter mismatch = 2%

$K_{DCloss}$ = the power loss due to DC-side $I^2R$-type losses = 2%

$K_T$ = the modules' thermal derating coefficient = 0.0037 %/°C

$T_{PV}$ = the module temperature (measured)

$T_{STC}$ = the Standard Test Condition temperature = 25°C

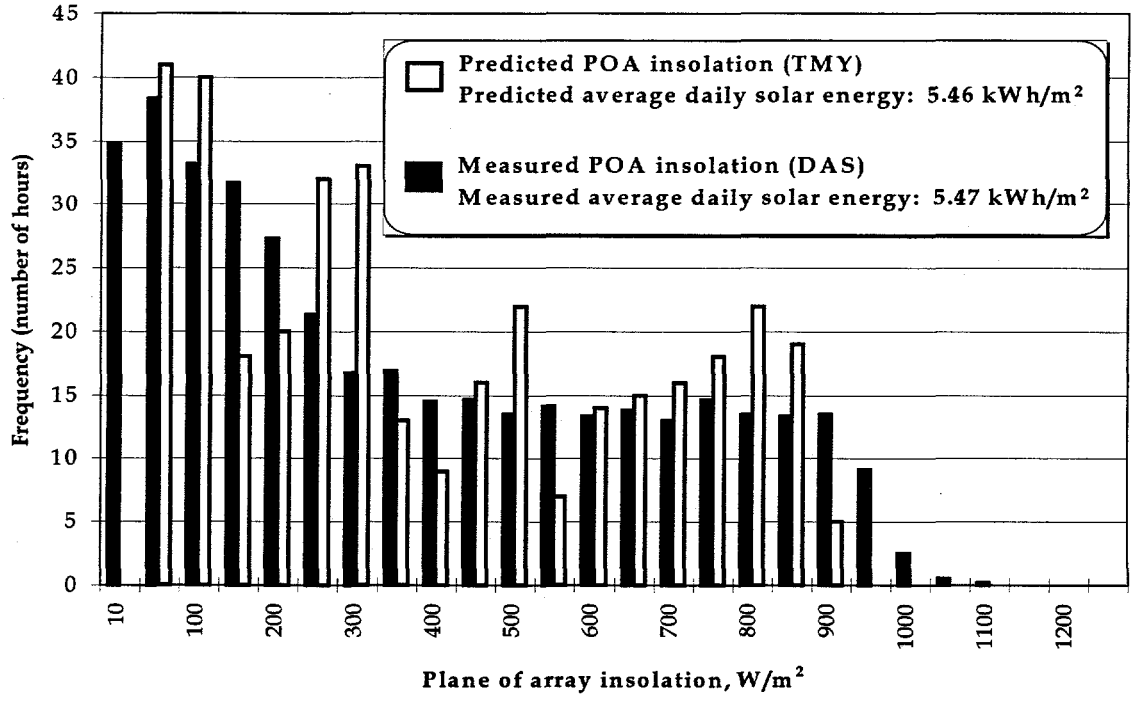


**Figure 1. Histogram of the plane of array insolation on the Aquatic Center PV array, September 1996.**

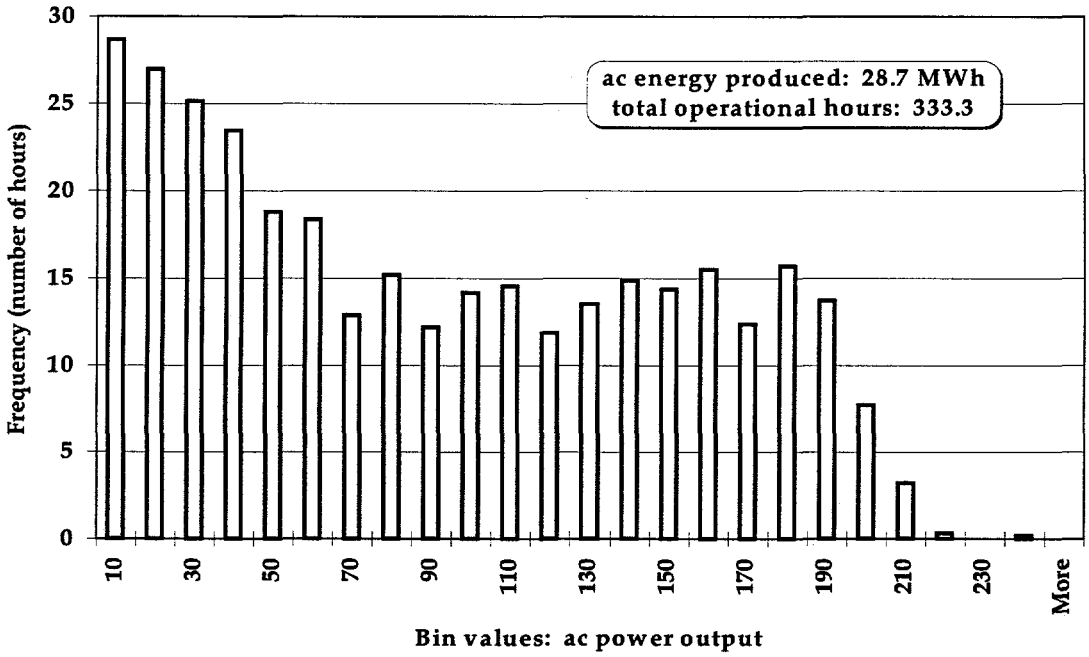


**Figure 2. Histogram of the AC power output of the Aquatic Center PV system, September 1996. Total energy for the month is given also.**

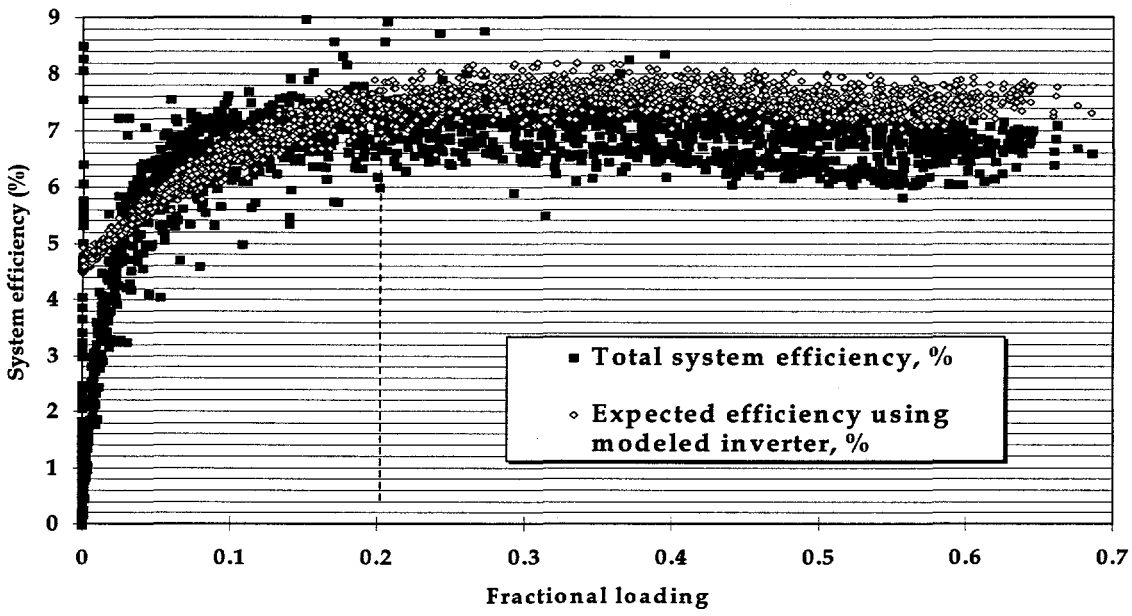


**Figure 3. Aquatic Center PV system total efficiency measurement compared with expected system efficiency value calculated using the modeled inverter efficiency, September 1996.**

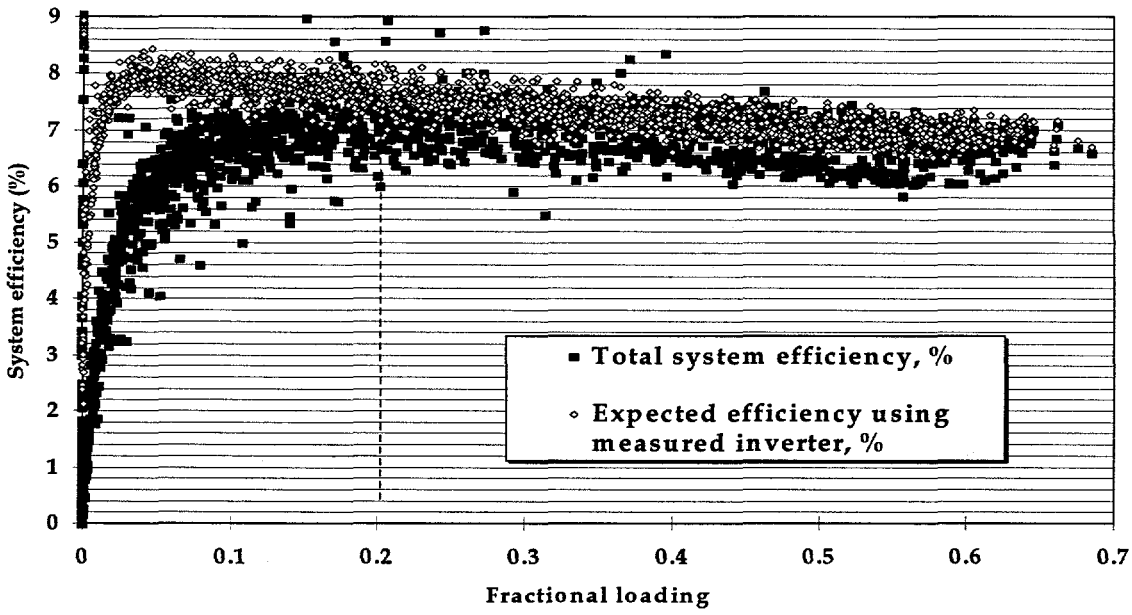


**Figure 4. Aquatic Center PV system total efficiency measurement compared with expected system efficiency value calculated using the measured inverter efficiency, September 1996.**

Using the measured inverter efficiency, expected and measured system efficiencies agree fairly well, with the given mismatch parameter value. If the modeled inverter efficiency is used, the measured system efficiency is slightly lower ($\approx$ 0.5-0.75%) than the expected system efficiency.

Figure 5 shows a comparison between the modeled and measured inverter efficiency curves. There is some discrepancy between measured and modeled efficiencies for the inverter at higher fractional loading. This is most likely due to sensor drift or miscalibration, and is the cause of the aforementioned difference between measured and calculated efficiencies when the inverter model is used.

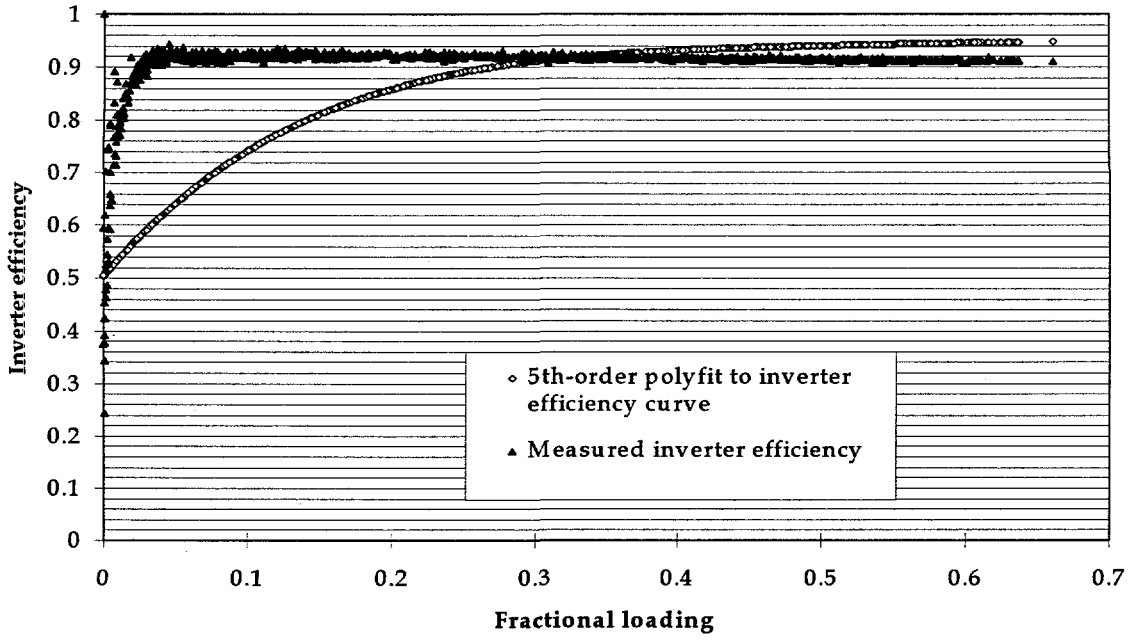


**Figure 5. Comparison between modeled and measured efficiency curves.**

## *REPORT ON THE PERFORMANCE OF THE GEORGIA TECH AQUATIC CENTER PV ARRAY: OCTOBER, 1996*

**Table 1. Summary of the performance of the Georgia Tech Aquatic Center PV Array, October 1996.**

| | |
|---|---|
| Typical PV array DC voltage: | 360-390V |
| Energy produced (AC): | 17.4 MWh |
| Maximum module temperature recorded: | 65.3°C = 156.7 °F |
| Maximum AC power recorded: | 203.3 kW |
| System operational hours: | 218.2 |
| System down time (hours)[a]: | ≈70 |

[a] The system down time includes all hours during which the PV system was turned off. Hours during which the PV system was not producing power due to darkness are not included.

The PV system was inoperative from October 10 to October 17 due to a water main break in the Aquatic Center which flooded the electrical room and required the system to be shut off. This event is reflected in the low number of operational system hours, only 218.2 for the month (for a typical October in which the system operated 9 hours per day, we would have approximately 279 operational hours during the month).

The accompanying figures illustrate the performance of the PV system for October, 1996. The histogram of plane of array insolation for the month shown in Figure 1 indicates that the insolation over the course of the month is slightly lower than average, with maximum values of just under 1 kW/m$^2$. However, although the peak AC power output is fairly good (203.3 kW; see Figure 2), the system's total energy output falls far short of the 33.23 MWh predicted by our modeling for a typical October in Atlanta, and

we must note that if the system had operated for 279 hours at the same energy production rate it would only have produced 22.2 MWh, still far short of expectations.

Whether a possible problem with the system is indicated by this data can be ascertained by examining the system efficiency. We have plotted the system's measured total efficiency and compared it with two different theoretically-predicted efficiencies, one using a fifth-order polynomial model of the inverter's efficiency curve (Figure 3), the other using an inverter efficiency calculated from measured AC and DC power data from the system (Figure 4). In both plots, a vertical dashed line is drawn at a fractional loading value of 20% because neither the measured data nor the model is accurate for $F < 0.20$.

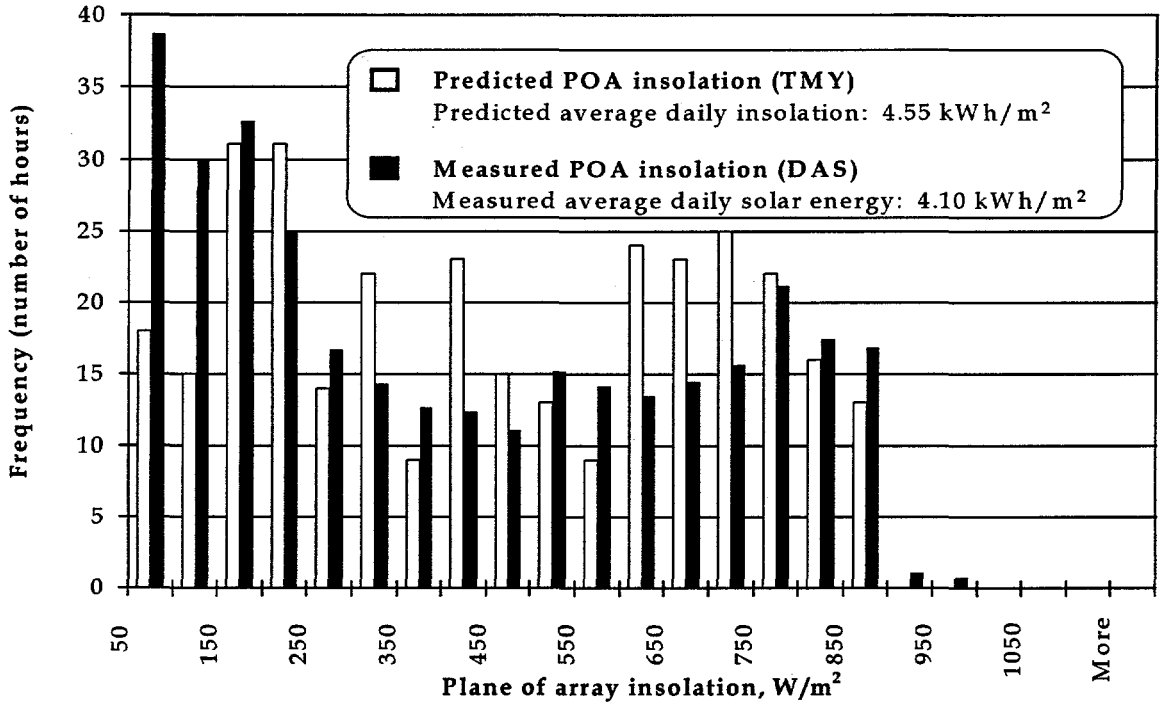


**Figure 1. Histogram of the plane of array insolation on the Aquatic Center PV array, October 1996.**

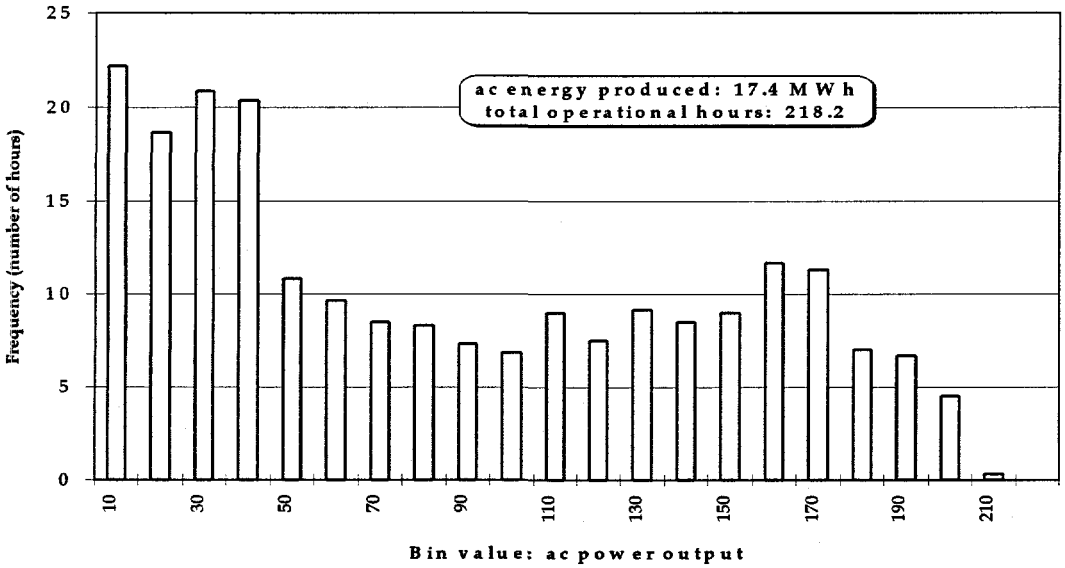


**Figure 2. Histogram of the AC power output of the Aquatic Center PV system, October 1996. Total energy for the month is given also.**

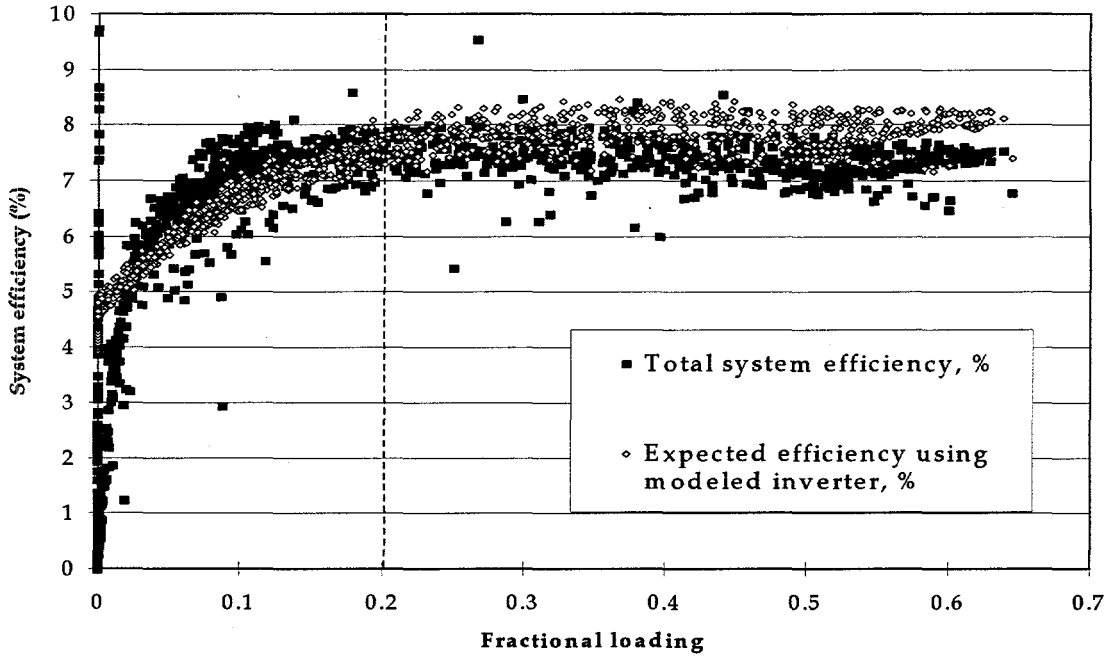


**Figure 3. Aquatic Center PV system total efficiency measurement compared with expected system efficiency value calculated using the modeled inverter efficiency, October 1996.**

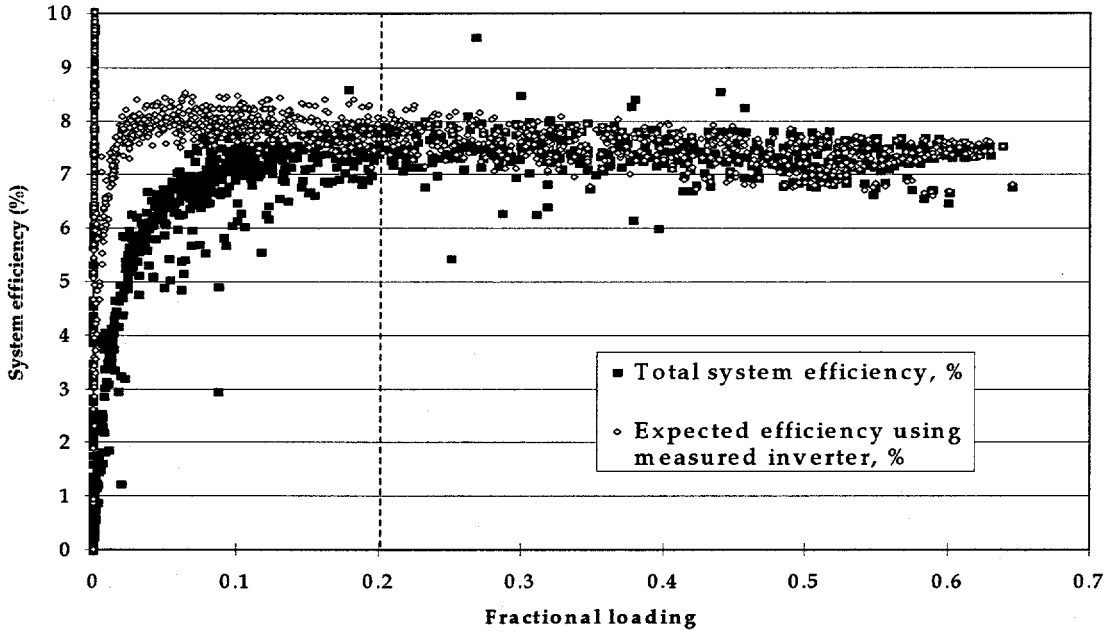


**Figure 4. Aquatic Center PV system total efficiency measurement compared with expected system efficiency value calculated using the measured inverter efficiency, October 1996.**

For the modeled system efficiency, the following model was employed:

$$\eta_{PV,AC} = \eta_{rated}\eta_{inv}\left(1-K_{dust}\right)\left(1-K_{curv}\right)\left(1-K_{mismatch}\right)\left(1-K_{dcloss}\right)\left[1-K_T\left(T_{PV}-T_{STC}\right)\right]$$

where

$\eta_{rated}$ = the rated efficiency of the PV modules = 10.77%

$\eta_{inv}$ = either the measured value (AC power out ÷ DC power out) or the modeled value (from a fifth-order polyfit to the manufacturer's power-efficiency curve) of the inverter's efficiency

$K_{dust}$ = the percentage of power loss due to dust/soiling on modules = 10%

$K_{curv}$ = the power loss due to the roof curvature = 4.2%

$K_{mismatch}$ = the power loss due to module parameter mismatch = 2%

$K_{DCloss}$ = the power loss due to DC-side $I^2R$-type losses = 2%

$K_T$ = the modules' thermal derating coefficient = 0.0037 %/°C

$T_{PV}$ = the module temperature (measured)

$T_{STC}$ = the Standard Test Condition temperature = 25°C

Using the measured inverter efficiency, expected and measured system efficiencies agree fairly well, with the given mismatch parameter value. If the modeled inverter efficiency is used, the measured system efficiency is slightly lower (about 0.5-0.75%) than the expected system efficiency, but still within experimental error. Based on these calculations, we conclude that the system is functioning properly, and the low energy production is due to low insolation.

## *REPORT ON THE PERFORMANCE OF THE GEORGIA TECH AQUATIC CENTER PV ARRAY: NOVEMBER, 1996*

**Table 1. Summary of the performance of the Georgia Tech Aquatic Center PV Array, November 1996.**

| | |
|---|---|
| Typical PV array DC voltage: | 360-415V |
| Energy produced (AC): | 18.1 MWh |
| Maximum module temperature recorded: | 44.9°C = 112.8 °F |
| Maximum AC power recorded: | 194.4 kW |
| System operational hours: | 275.5 |
| System down time (hours)[a]: | 1 |

[a] The system down time includes all hours during which the PV system was turned off. Hours during which the PV system was not producing power due to darkness are not included.

The accompanying figures illustrate the performance of the Aquatic Center PV array for November, 1996. The histogram of plane of array insolation for the month (Figure 1) shows that the insolation over the course of the month is slightly lower than average, never exceeding 850 W/m$^2$. This low insolation and its distribution are reflected in the histogram of the system's AC power output, which is very "left-heavy" for the month with many hours spent below 100 kW of power production. The AC energy production is thus somewhat lower than predicted by our modeling (23.9 MWh).

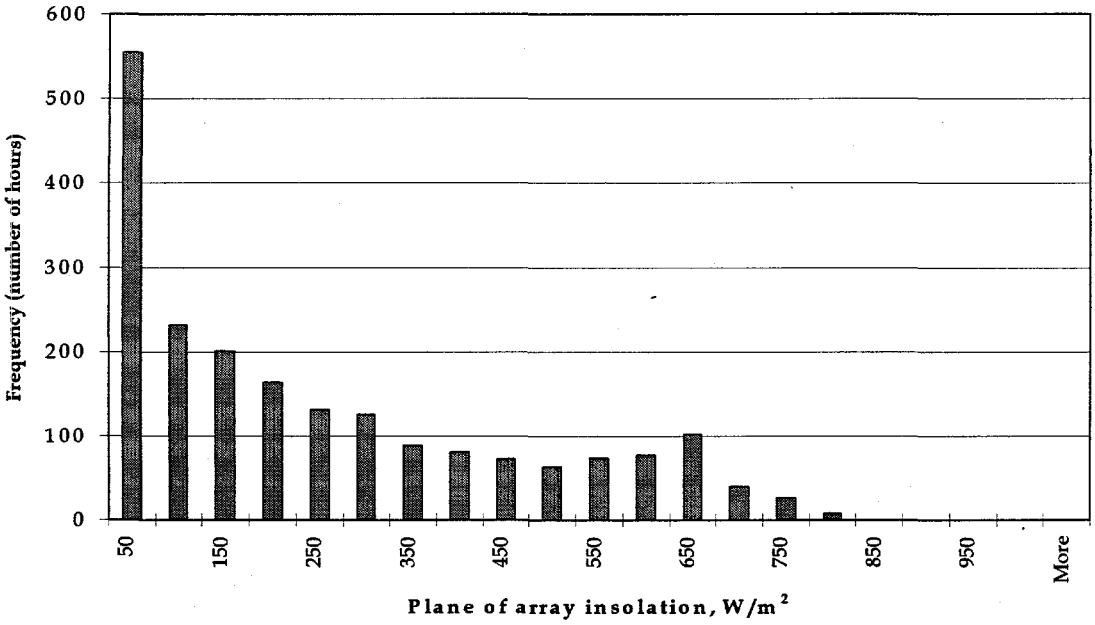


**Figure 1. Histogram of the plane of array insolation on the Aquatic Center PV array, November 1996.**

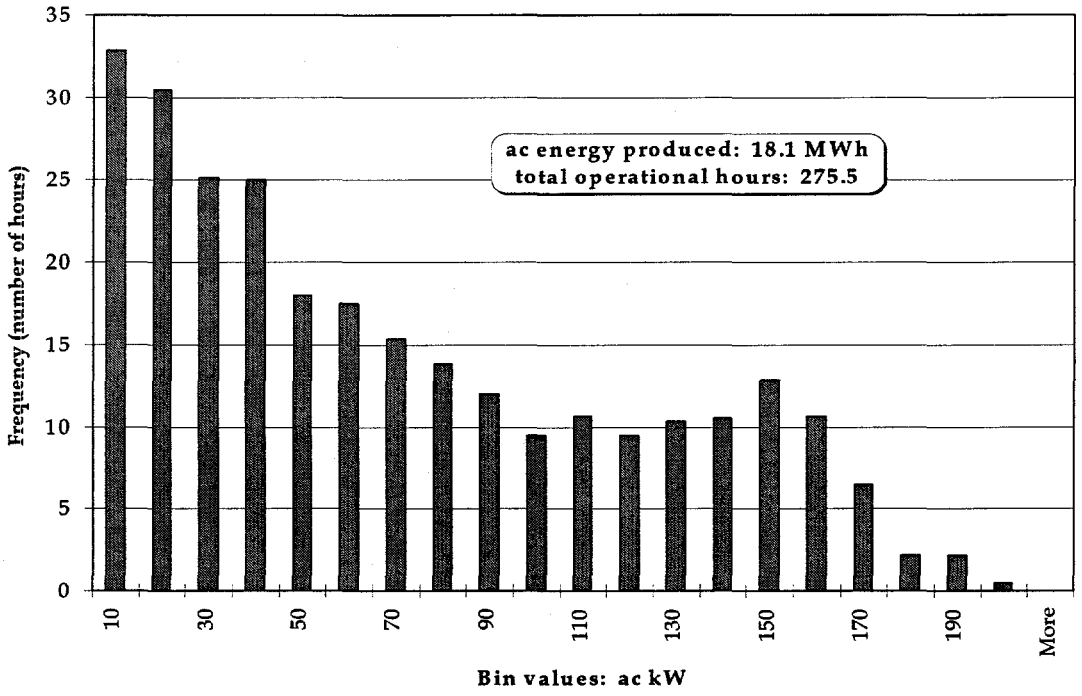


**Figure 2. Histogram of the AC power output of the Aquatic Center PV system, November 1996. Total energy for the month is given also.**

We have also plotted the system's measured total efficiency and compared it with two different theoretically-predicted efficiencies, one using a fifth-order polynomial model of the inverter's efficiency curve (Figure 3), the other using an inverter efficiency calculated from measured AC and DC power data from the system (Figure 4). In both plots, a vertical dashed line is drawn at a fractional loading value of 20% because neither the measured data nor the model is accurate for F < 0.20.

For the modeled system efficiency, the following model was employed:

$$\eta_{PV,AC} = \eta_{rated}\eta_{inv}\left(1-K_{dust}\right)\left(1-K_{curv}\right)\left(1-K_{mismatch}\right)\left(1-K_{dcloss}\right)\left[1-K_T\left(T_{PV}-T_{STC}\right)\right]$$

where

$\eta_{rated}$ = the rated efficiency of the PV modules = 10.77%

$\eta_{inv}$ = either the measured value (AC power out ÷ DC power out) or the modeled value (from a fifth-order polyfit to the manufacturer's power-efficiency curve) of the inverter's efficiency

$K_{dust}$ = the percentage of power loss due to dust/soiling on modules = 10%

$K_{curv}$ = the power loss due to the roof curvature = 4.2%

$K_{mismatch}$ = the power loss due to module parameter mismatch =10%

$K_{DCloss}$ = the power loss due to DC-side $I^2R$-type losses = 2%

$K_T$ = the modules' thermal derating coefficient = 0.0037 %/°C

$T_{PV}$ = the module temperature (measured)

$T_{STC}$ = the Standard Test Condition temperature = 25°C

A plot of the two inverter efficiency curves is also included. Using the measured inverter efficiency, expected and measured system efficiencies agree fairly well, with the given mismatch parameter value. If the modeled inverter efficiency is used, the measured system efficiency is slightly lower (≈0.5 - 0.75%) than the expected system efficiency.

One should note from the plot of the measured inverter efficiency curve that the efficiency of the inverter for F > 0.5 seems to be lower than it was when similar calculations were done in July ($\eta_{inverter}$ hovered around 94.5-95% at that time for similar values of F). This is probably indicative of sensor drift, pointing out a probable need to recalibrate the DAS sensors. It could also indicate some drift in the values of parameters of circuit elements in the inverter circuit, but this is believed to be less likely as this sort of drift should probably occur in much smaller increments and over much longer periods of time than the four months that have passed.

## *REPORT ON THE PERFORMANCE OF THE GEORGIA TECH AQUATIC CENTER PV ARRAY: DECEMBER, 1996*

**Table 1. Summary of the performance of the Georgia Tech Aquatic Center PV Array, December 1996.**

| | |
|---|---|
| Typical PV array DC voltage: | 360-390V |
| Energy produced (AC): | 15.2 MWh |
| Maximum module temperature recorded: | 42.3°C = 108.07°F |
| Maximum AC power recorded: | 199.6 kW |
| System operational hours: | 268.7 |
| System down time (hours)[a]: | 3.2 |

[a] The system down time includes all hours during which the PV system was turned off. Hours during which the PV system was not producing power due to darkness are not included.

During the month of December, an experiment was being conducted on the Aquatic Center PV system for the purpose of determining experimental values for some of the parameters in the model of the system. This experiment involved disconnection of just under 18% of the array; hence, the power and energy production of the system are somewhat depressed from their usual values.

Figures 1 and 2 give the distributions of the insolation on the array and the AC power produced by the system. Figure 1 also shows the insolation distribution predicted by our modeling and the measured and predicted average daily insolations. Note that the average daily insolation values differ only by about 5%. Figure 2 shows that the distribution of power production is "left-heavy", which is to be expected in December and is exaggerated by the disconnection of part of the array for our experiment. The total

operational hours represent nearly 100% of available sun hours for the month, a figure which indicates that the system's automatic controls are working well.

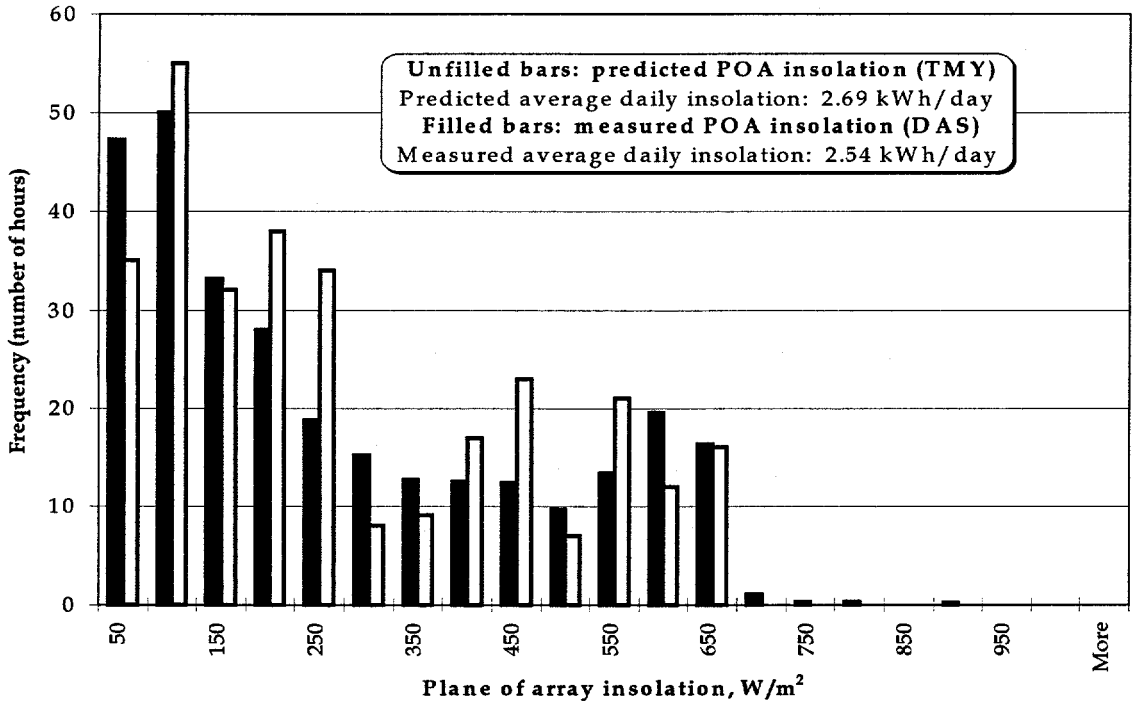


**Figure 1. Histogram of the plane of array insolation on the Aquatic Center PV array, December 1996. The insolation distribution predicted by the TMY and PVFORM is included for comparison.**

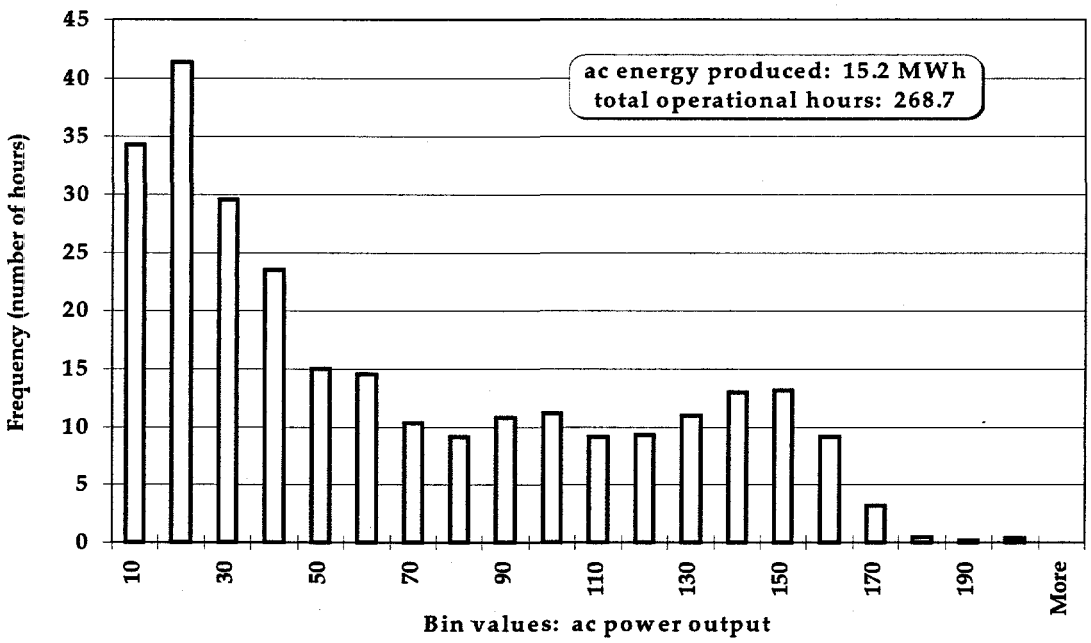


**Figure 2. Histogram of the AC power output of the Aquatic Center PV system, December 1996. Total energy for the month is given also.**

## *REPORT ON THE PERFORMANCE OF THE GEORGIA TECH AQUATIC CENTER PV ARRAY: JANUARY, 1997*

**Table 1. Summary of the performance of the Georgia Tech Aquatic Center PV Array, January 1997.**

| | |
|---|---|
| Typical PV array DC voltage: | 390-440V |
| Energy produced (AC): | 18.3 MWh |
| Maximum module temperature recorded: | 48.0°C = 118.4 °F |
| Maximum AC power recorded: | 189.1 kW |
| System operational hours: | 277.2 |
| System down time (hours)[a]: | 2.5 |

[a] The system down time includes all hours during which the PV system was turned off. Hours during which the PV system was not producing power due to darkness are not included.

The accompanying figures illustrate the performance of the Aquatic Center PV array for January, 1997. The average daily solar energy flux on the array was actually higher this month than what TMY/PVFORM modeling had predicted, as shown in Figure 1. The system's AC power output is shown in Figure 2. As expected, the shape of the AC power histogram closely matches that of the plane of array insolation.

The predicted AC energy production by TMY/PVFORM for January is 19.3 MWh. The measured value of 18.3 MWh compares very favorably with this value. The reason that the energy production of the system is lower than expected while the insolation was higher than predicted is that from January 1-January 16 the system was still undergoing an experiment which involved disconnecting approximately 18% of the array (see the report for December). This experiment, which has now been completed, was intended to aid in determining accurate values for parameters in the model for this

system. During the next few months, the system will undergo a number of such experiments.

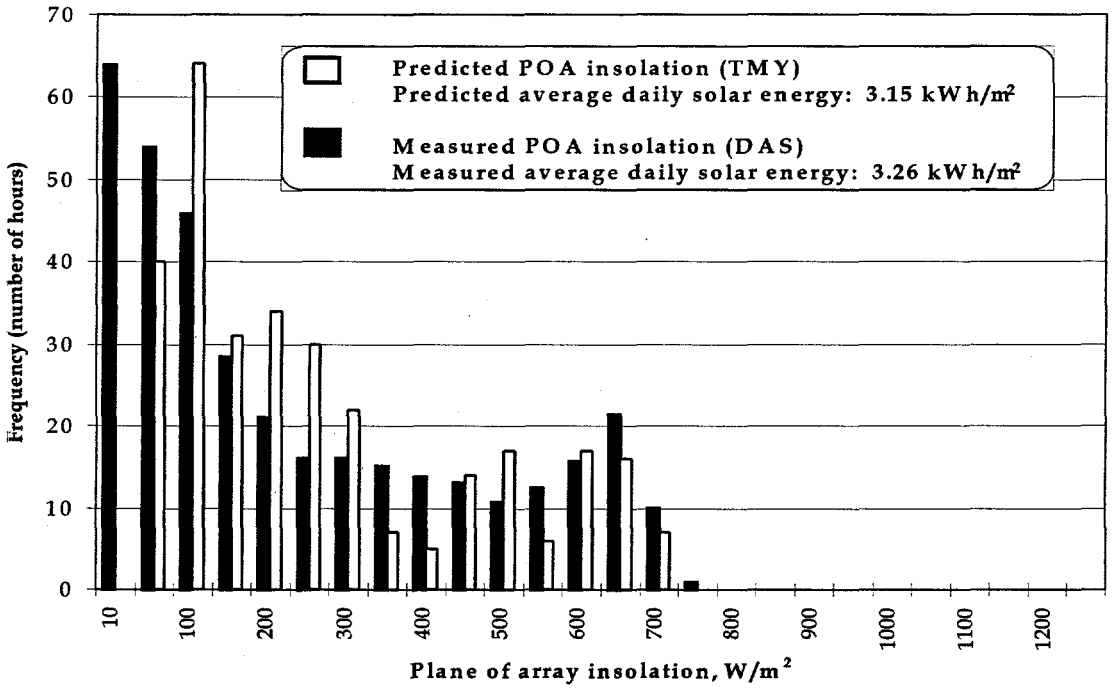


**Figure 1. Histogram of the plane of array insolation on the Aquatic Center PV array, January 1997.**

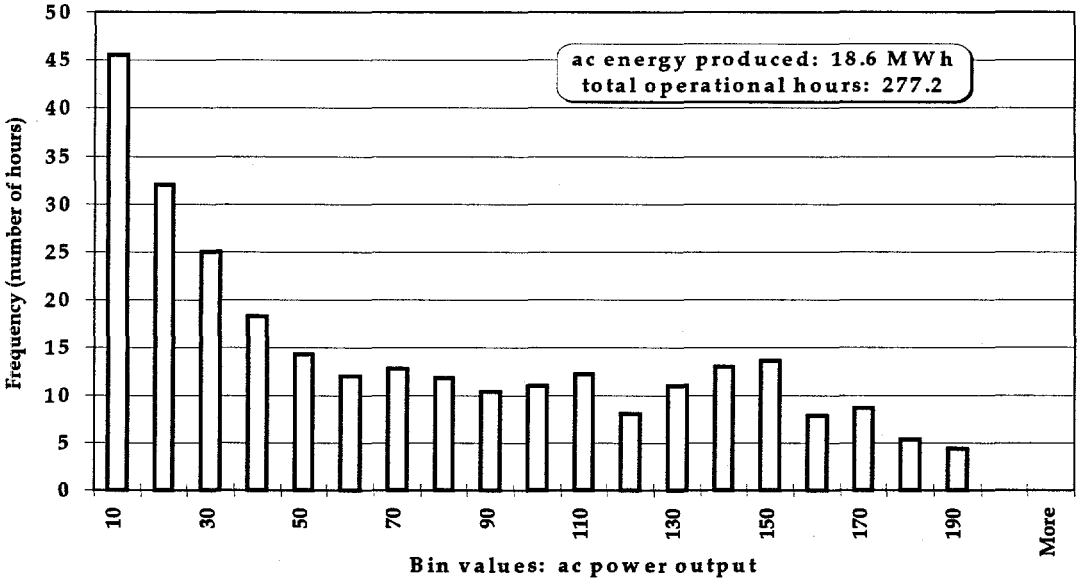


**Figure 2. Histogram of the AC power output of the Aquatic Center PV system, January 1997. Total energy for the month is given also.**

# *REPORT ON THE PERFORMANCE OF THE GEORGIA TECH AQUATIC CENTER PV ARRAY: FEBRUARY, 1997*

**Table 1 Summary of the performance of the Georgia Tech Aquatic Center PV Array, February 1997.**

| | |
|---|---|
| Typical PV array DC voltage: | 350-415V |
| Energy produced (AC): | 19.6 MWh |
| Maximum module temperature recorded: | 52.1°C = 125.8 °F |
| Maximum AC power recorded: | 221.8 kW |
| System operational hours: | ??? |
| System down time (hours)[a]: | ~ 0 |

[a] The system down time includes all hours during which the PV system was turned off. Hours during which the PV system was not producing power due to darkness are not included.

During the month of February, the electrical sensors built into our inverter went out of calibration for as-yet-unknown reasons, and the external data acquisition system was not calibrated until March. For this reason, our data for the month of February is unreliable. The AC energy given above represents our best estimate based on the external sensors' measurements. The system down time hours reflects the fact that, to our knowledge, the system was never deactivated during February 1997.

Figure 1 shows the measured and predicted plane of array irradiances for the month. It can be clearly seen that the sunlight for February was weaker than predicted, the result of an unusually high number of cloudy and stormy days. Figure 2 shows the measured and modeled total system efficiencies. The disagreement between the model and the measurements is primarily due to the sensor miscalibration.

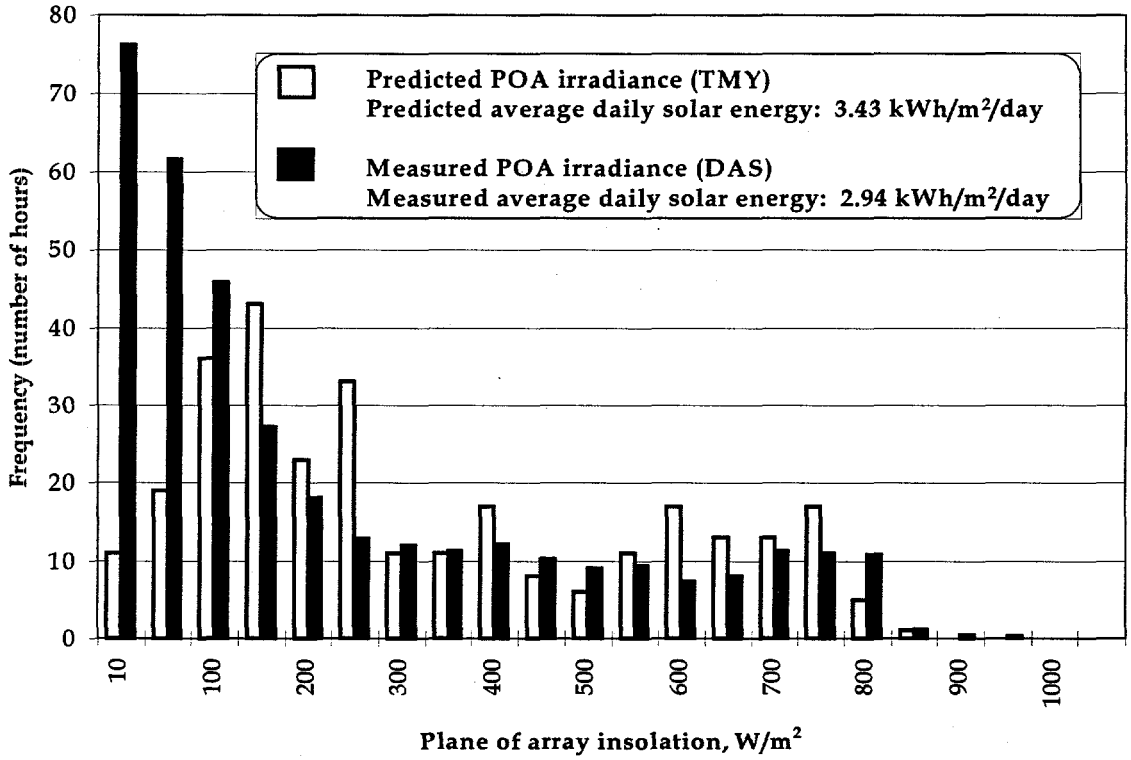


**Figure 1. Measured and predicted plane of array irradiances on the Aquatic Center PV array.**

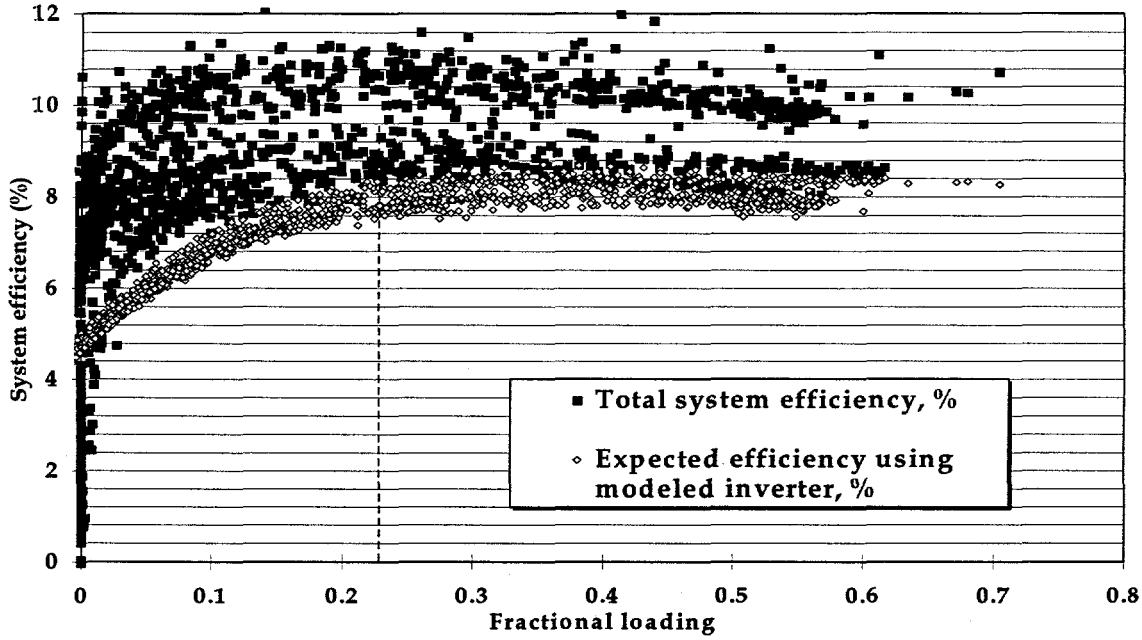


**Figure 2. GTAC PV system total efficiency (sunlight to AC) compared with the expected total system efficiency predicted using the fifth-order inverter efficiency curve.**

## *REPORT ON THE PERFORMANCE OF THE GEORGIA TECH AQUATIC CENTER PV ARRAY: MARCH, 1997*

**Table 1. Summary of the performance of the Georgia Tech Aquatic Center PV Array, March 1997.**

| | |
|---|---|
| Typical PV array DC voltage: | 345-420V |
| Energy produced (AC): | 39.2 MWh |
| Maximum module temperature recorded: | 62.8°C = 145.0 °F |
| Maximum AC power recorded: | 262.6 kW |
| System operational hours: | 350.4 |
| System down time (hours)[a]: | 7.77 |

[a] The system down time includes all hours during which the PV system was turned off. Hours during which the PV system was not producing power due to darkness are not included.

The table above and the accompanying figures illustrate the performance of the Aquatic Center PV array for the month of March, 1997. One important note must be made: the data acquisition system was recalibrated on March 16, meaning that we have reliable data only for the last 16 days of March. The monthly totals have been extrapolated from these sixteen days' worth of data.

The histogram of plane of array insolation for the month (Figure 1) shows that the average daily energy flux for this month is considerably greater than that predicted by PVFORM/TMY modeling. As a result of this and moderate temperatures, the AC power production is quite strong, as shown in Figure 2, with peak values exceeding 260 kW, and the 39.2 MWh of AC energy production for March exceeds the predicted value of 35.0 MWh.

We have also plotted the system's measured total efficiency and compared it with the theoretically-predicted efficiencies using a fifth-order polynomial model of the inverter's efficiency curve (Figure 3) and an inverter efficiency calculated from measured AC and DC power data from the system (Figure 4). The models and measurements are valid for fractional loading $F \geq 0.20$. For the modeled system efficiency, the following model was employed:

$$\eta_{PV,AC} = \eta_{rated}\eta_{inv}\left(1 - K_{dust}\right)\left(1 - K_{curv}\right)\left(1 - K_{mismatch}\right)\left(1 - K_{dcloss}\right)\left[1 - K_T\left(T_{PV} - T_{STC}\right)\right]$$

where

$\eta_{rated}$ = the rated efficiency of the PV modules = 10.77%

$\eta_{inv}$ = either the measured value (AC power out ÷ DC power out) or the modeled value (from a fifth-order polyfit to the manufacturer's power-efficiency curve) of the inverter's efficiency

$K_{dust}$ = the percentage of power loss due to dust/soiling on modules = 10%

$K_{curv}$ = the power loss due to the roof curvature = 1.7%

$K_{mismatch}$ = the power loss due to module parameter mismatch = 4.2%

$K_{DCloss}$ = the power loss due to DC-side $I^2R$-type losses = 2%

$K_T$ = the modules' thermal derating coefficient = 0.0037 %/°C

$T_{PV}$ = the module temperature (measured)

$T_{STC}$ = the Standard Test Condition temperature = 25°C

Using the modeled inverter efficiency, expected and measured system efficiencies agree extremely well, with the given mismatch parameter value. Strangely, if the measured inverter efficiency is used, the measured system efficiency is slightly lower than the expected system efficiency. Recent experiments have indicated that $K_{dust}$ = 10% may be too high; measured values have averaged between 3 and 4%. If we use $K_{dust}$ = 3.5%, the match is better for the measured inverter but worse for the modeled inverter. We are continuing to experiment on the system to "tune" the parameter values in our model.

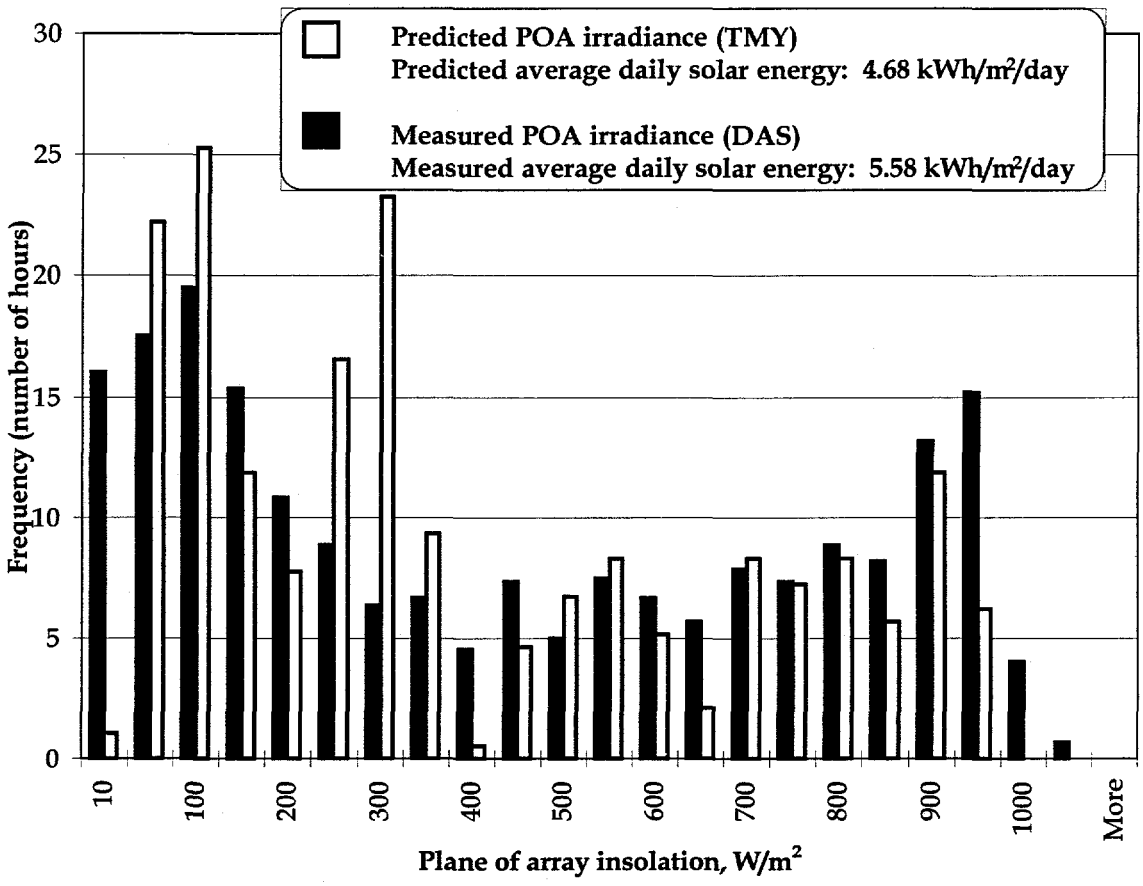


**Figure 1. Histogram of the plane of array insolation on the Aquatic Center PV array, March 1997.**

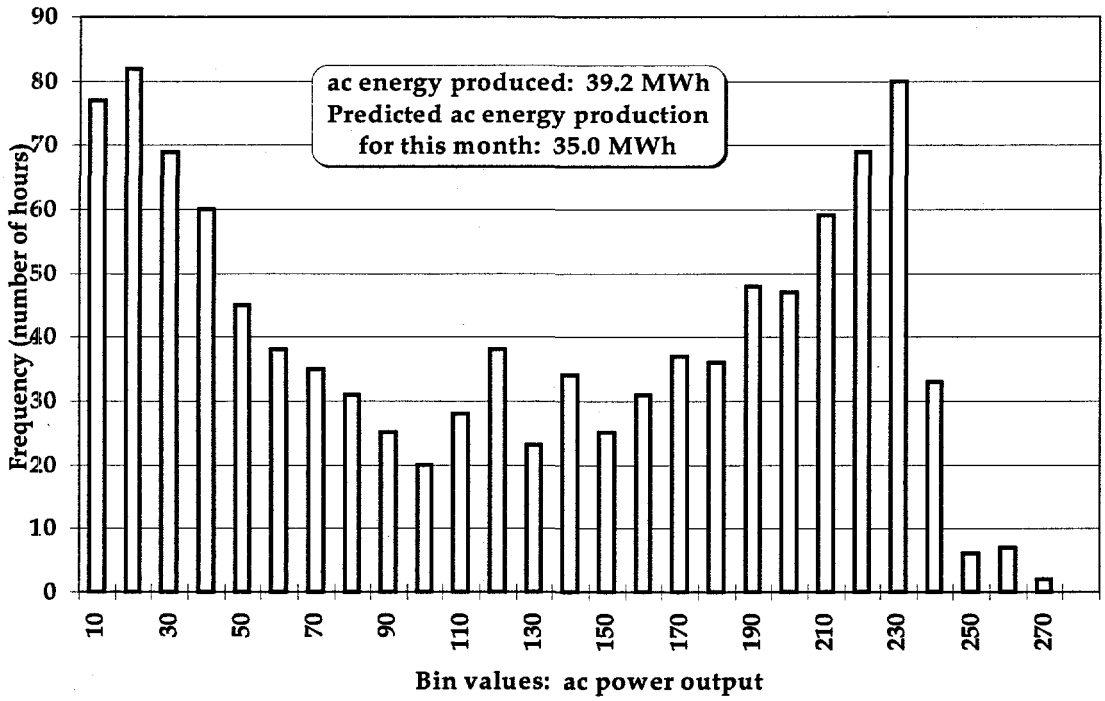


**Figure 2. Histogram of the AC power output of the Aquatic Center PV system, March 1997. Total energy for the month is given also.**

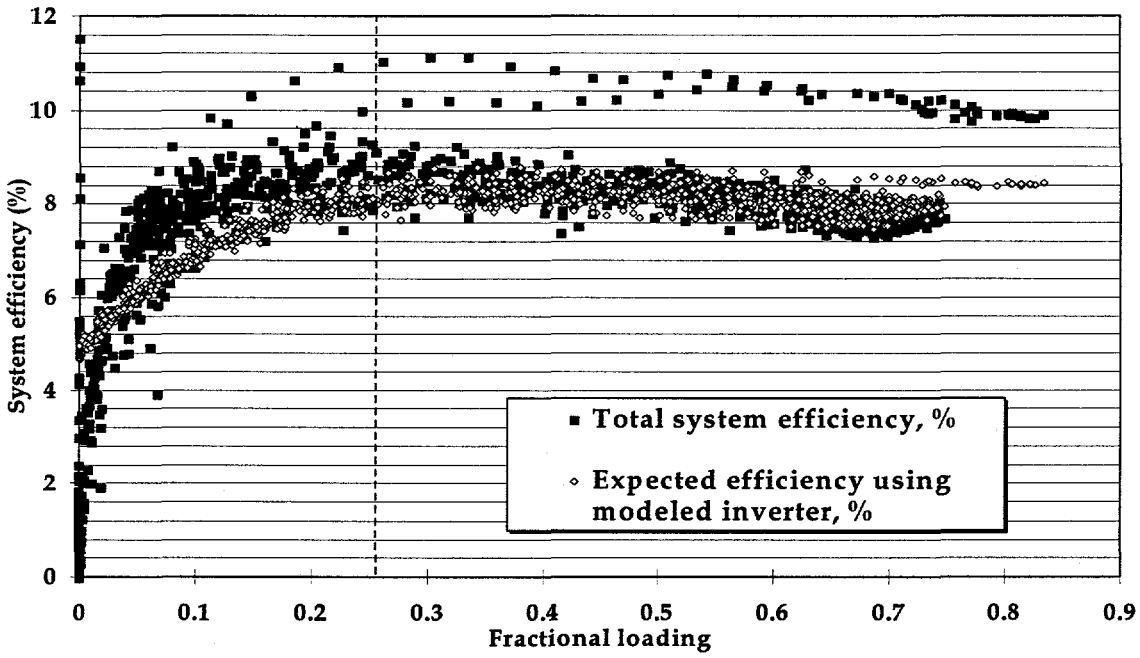


**Figure 3. Aquatic Center PV system total efficiency measurement compared with expected system efficiency value calculated using the modeled inverter efficiency, March 1997.**

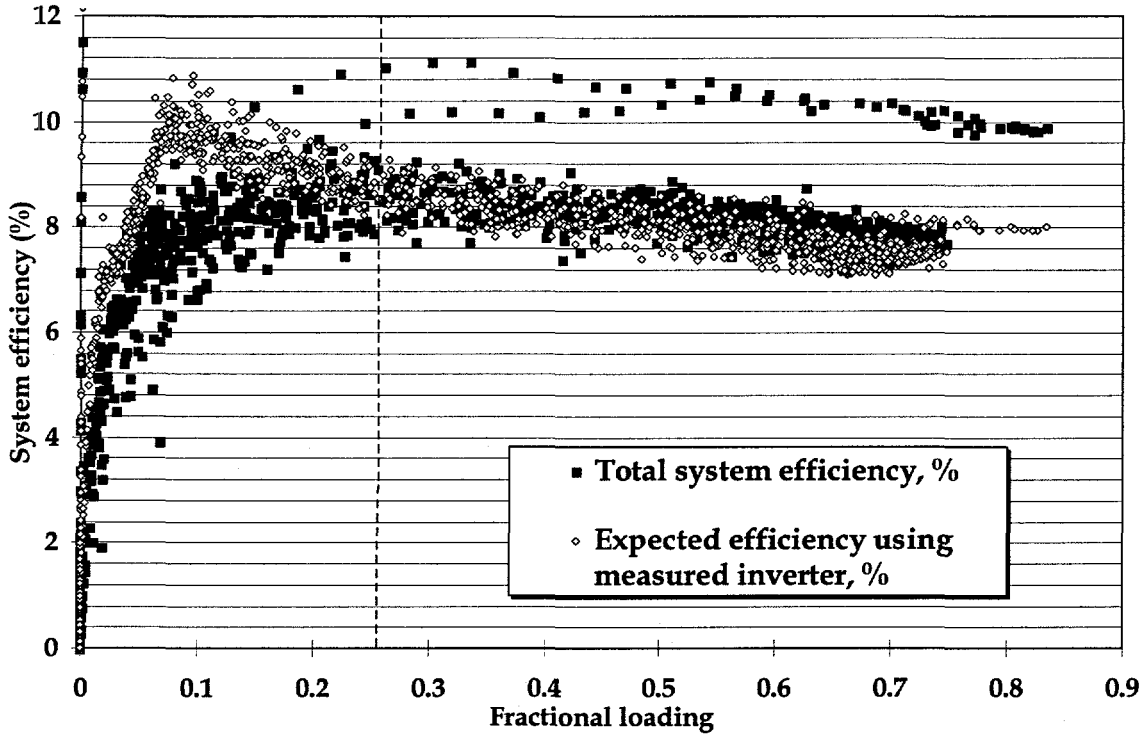


**Figure 4. Aquatic Center PV system total efficiency measurement compared with expected system efficiency value calculated using the measured inverter efficiency, March 1997.**

# *REPORT ON THE PERFORMANCE OF THE GEORGIA TECH AQUATIC CENTER PV ARRAY: APRIL, 1997*

**Table 1. Summary of the performance of the Georgia Tech Aquatic Center PV Array, April 1997.**

| | |
|---|---|
| Typical PV array DC voltage: | 340-420V |
| Energy produced (AC): | 42.3 MWh |
| Maximum module temperature recorded: | 65.3°C = 149.6 °F |
| Maximum AC power recorded: | 264.4 kW |
| System operational hours: | ~347 |
| System down time (hours)[a]: | ??? |

[a] The system down time includes all hours during which the PV system was turned off. Hours during which the PV system was not producing power due to darkness are not included.

The table above and the accompanying figures illustrate the performance of the Aquatic Center PV array for the month of April, 1997.

The histogram of plane of array insolation for the month (Figure 1) shows that the average daily energy flux for April was very strong, and higher than predicted by the PVFORM/TMY modeling. Array temperatures were not exceedingly high, and the combination of strong sunlight and moderate temperatures resulted in strong AC power production, as shown in Figure 2, with peak values exceeding 260 kW. 42.3 MWh of AC energy were produced during April; the predicted AC energy production was 40.8 MWh.

We have also plotted the system's measured total efficiency and compared it with the theoretically-predicted efficiencies using a fifth-order polynomial model of the inverter's efficiency curve (Figure 3) and an inverter efficiency calculated from measured

AC and DC power data from the system (Figure 4). The models and measurements are valid for fractional loading F ≥ 0.20. For the modeled system efficiency, the following model was employed:

$$\eta_{PV,AC} = \eta_{rated}\eta_{inv}\left(1-K_{dust}\right)\left(1-K_{curv}\right)\left(1-K_{mismatch}\right)\left(1-K_{dcloss}\right)\left[1-K_T\left(T_{PV}-T_{STC}\right)\right]$$

where

$\eta_{rated}$ = the rated efficiency of the PV modules = 10.77%

$\eta_{inv}$ = either the measured value (AC power out ÷ DC power out) or the modeled value (from a fifth-order polyfit to the manufacturer's power-efficiency curve) of the inverter's efficiency

$K_{dust}$ = the percentage of power loss due to dust/soiling on modules = 4%

$K_{curv}$ = the power loss due to the roof curvature = 1.0%

$K_{mismatch}$ = the power loss due to module parameter mismatch = 2%

$K_{DCloss}$ = the power loss due to DC-side $I^2R$-type losses = 2%

$K_T$ = the modules' thermal derating coefficient = 0.0037 %/°C

$T_{PV}$ = the module temperature (measured)

$T_{STC}$ = the Standard Test Condition temperature = 25°C

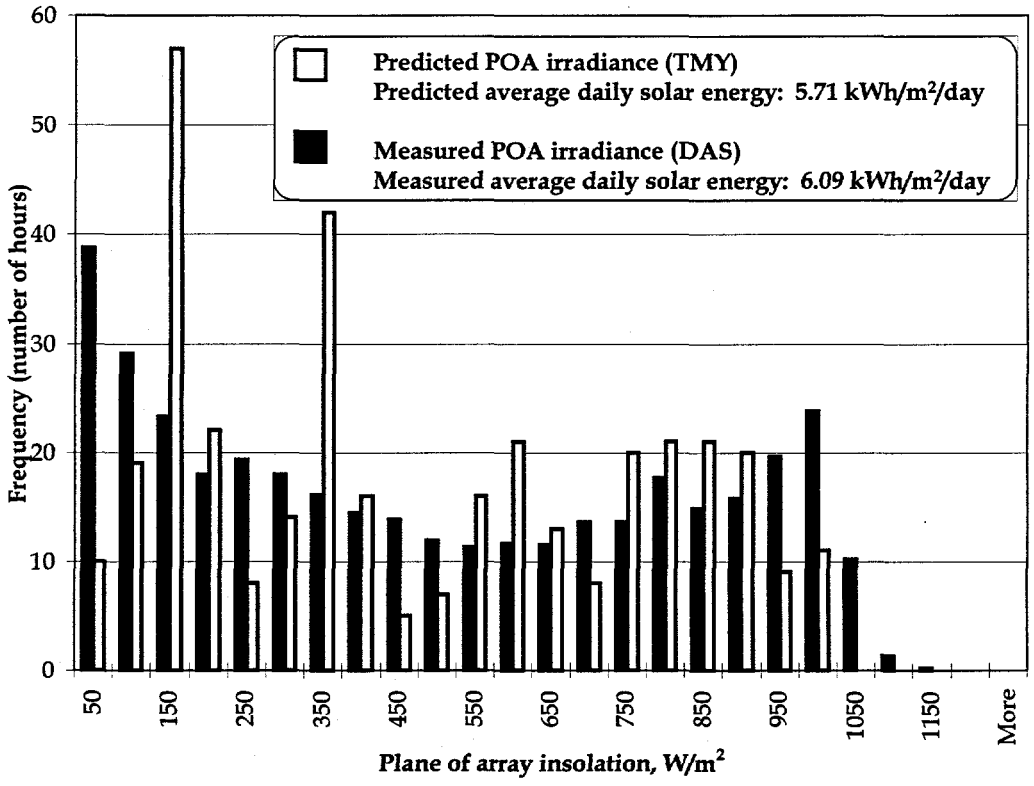


**Figure 1. Histogram of the plane of array insolation on the Aquatic Center PV array, April 1997.**

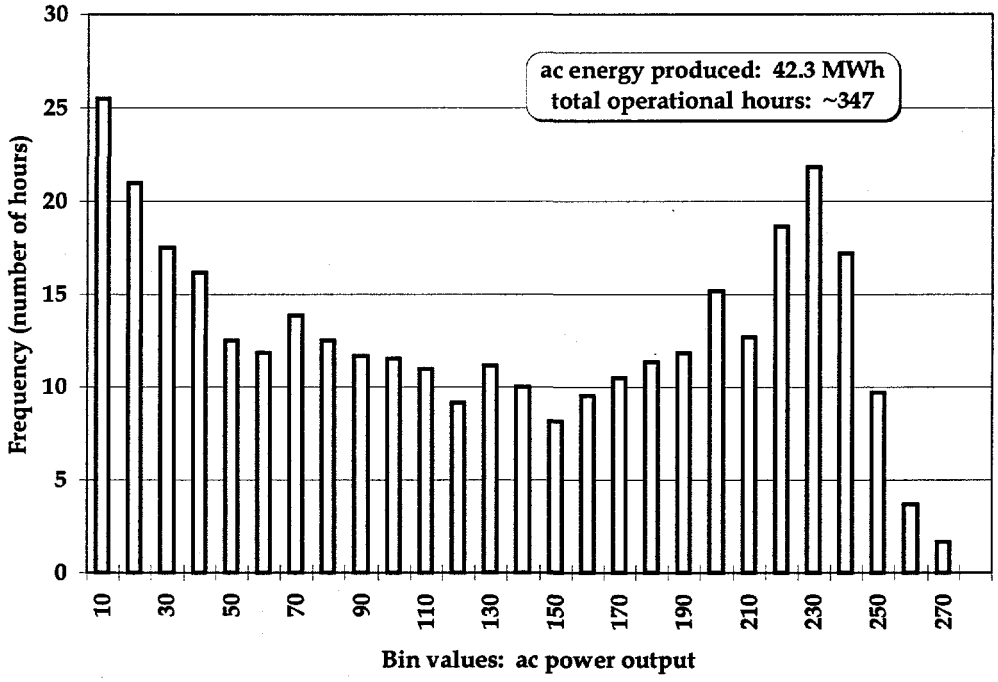


**Figure 2. Histogram of the AC power output of the Aquatic Center PV system, April 1997. Total energy for the month is given also.**

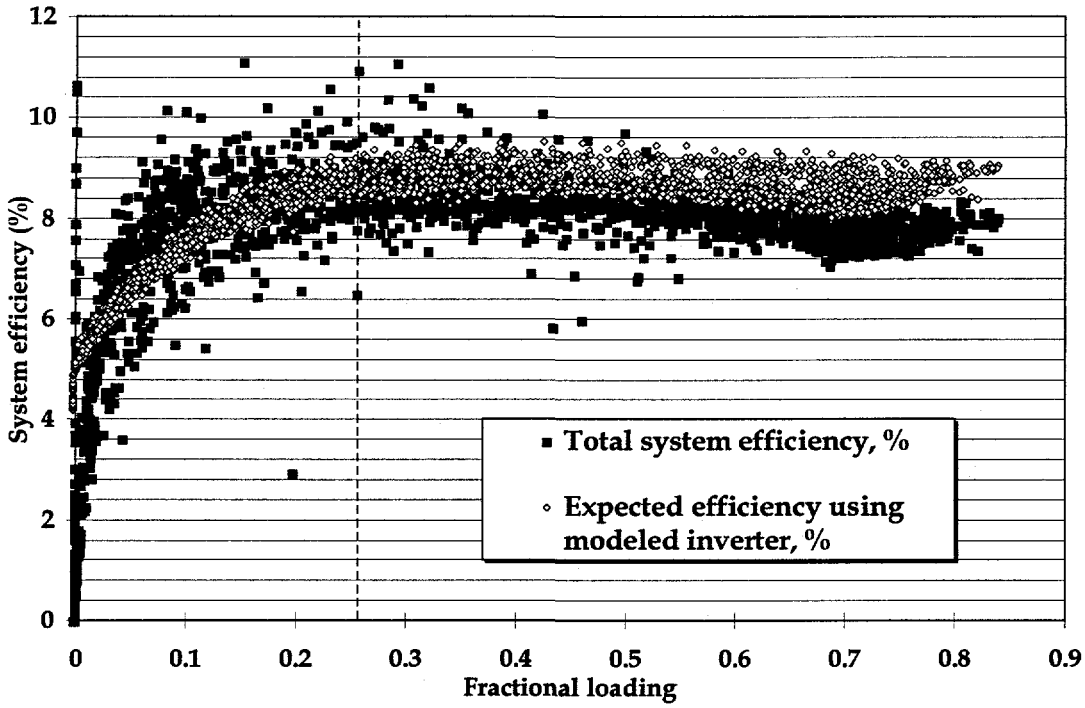


**Figure 3. Aquatic Center PV system total efficiency measurement compared with expected system efficiency value calculated using the modeled inverter efficiency, April 1997.**

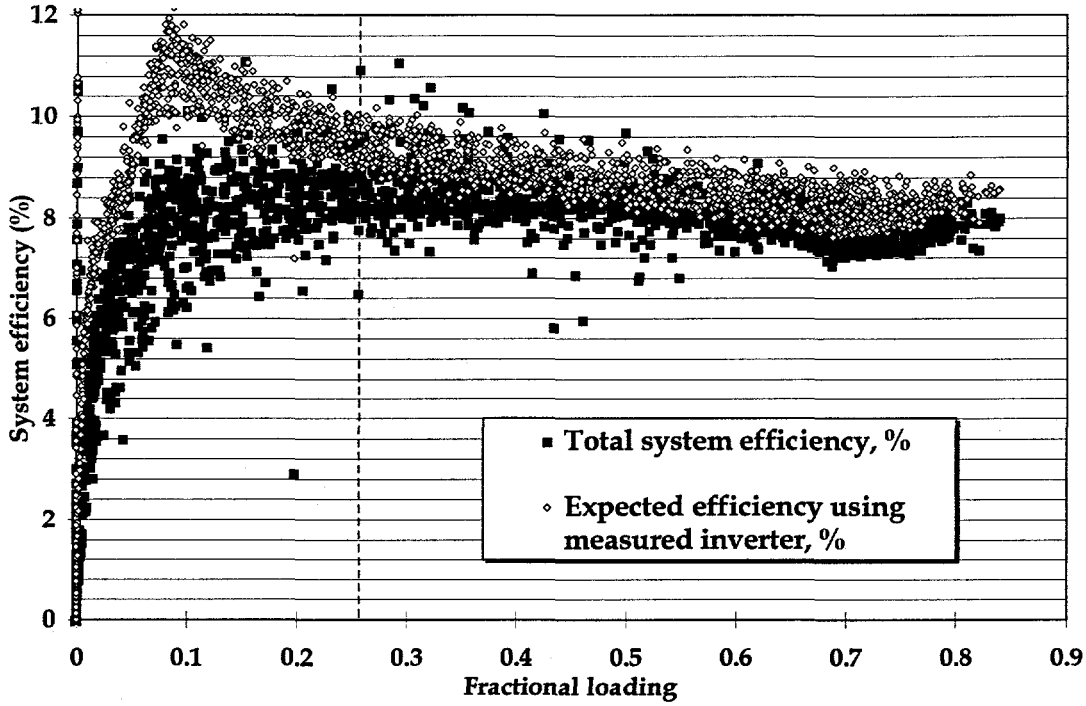


**Figure 4. Aquatic Center PV system total efficiency measurement compared with expected system efficiency value calculated using the measured inverter efficiency, April 1997.**

Note that we are now using values for the model parameters that have been adjusted based on our experiments on the system. In both cases, with the improved parameter values, the expected efficiency is slightly higher than the measured efficiency. This could signify that some source circuit protector box fuses are blown (a possibility corroborated by third-party analysis of the data collected by the SWTDI DAS calibration team in March), or possibly that the inverter is experiencing some difficulty (this latter possibility has been suggested by the inverter's on-board sensors). A factory service representative has been summoned to inspect the inverter, and our team of students will inspect the array.

# *REPORT ON THE PERFORMANCE OF THE GEORGIA TECH AQUATIC CENTER PV ARRAY: MAY, 1997*

**Table 1. Summary of the performance of the Georgia Tech Aquatic Center PV Array, May 1997.**

| | |
|---|---|
| Typical PV array DC voltage: | 335-420V |
| Energy produced (AC): | 38.6 MWh |
| Maximum module temperature recorded: | 67.1°C = 152.8 °F |
| Maximum AC power recorded: | 261.8 kW |
| System operational hours: | ≈347 |
| System down time (hours)[a]: | ≈44 |

[a] The system down time includes all hours during which the PV system was turned off. Hours during which the PV system was not producing power due to darkness are not included.

The table above and the accompanying figures illustrate the performance of the Aquatic Center PV array for the month of May, 1997.

The AC energy production of the system is considerably lower than the 48.3 MWh predicted by PVFORM/TMY modeling. This can be partially explained by the histogram of plane of array insolation for the month (Figure 1) , which shows that the average daily energy flux for May was slightly lower than expected. Also, the system was off-line for four days, as indicated by the number of downtime hours. The AC power production histogram in Figure 2 appears to be normal, with peak values in excess of 260 kW. However, Figures 3 and 4 reveal some interesting behavior. These plots compare the system's measured total efficiency with the theoretically-predicted efficiencies using a fifth-order polynomial model of the inverter's efficiency curve (Figure 3) and an inverter efficiency calculated from measured AC and DC power data from the system (Figure 4).

The models and measurements are valid for fractional loading $F \geq 0.20$. For the modeled system efficiency, the following model was employed:

$$\eta_{PV,AC} = \eta_{rated}\eta_{inv}\left(1 - K_{dust}\right)\left(1 - K_{curv}\right)\left(1 - K_{mismatch}\right)\left(1 - K_{dcloss}\right)\left[1 - K_T\left(T_{PV} - T_{STC}\right)\right]$$

where

$\eta_{rated}$ = the rated efficiency of the PV modules = 10.77%

$\eta_{inv}$ = either the measured value (AC power out ÷ DC power out) or the modeled value (from a fifth-order polyfit to the manufacturer's power-efficiency curve) of the inverter's efficiency

$K_{dust}$ = the percentage of power loss due to dust/soiling on modules = 4%

$K_{curv}$ = the power loss due to the roof curvature = 0.3%

$K_{mismatch}$ = the power loss due to module parameter mismatch = 2%

$K_{DCloss}$ = the power loss due to DC-side $I^2R$-type losses = 2%

$K_T$ = the modules' thermal derating coefficient = 0.0037 %/°C

$T_{PV}$ = the module temperature (measured)

$T_{STC}$ = the Standard Test Condition temperature = 25°C

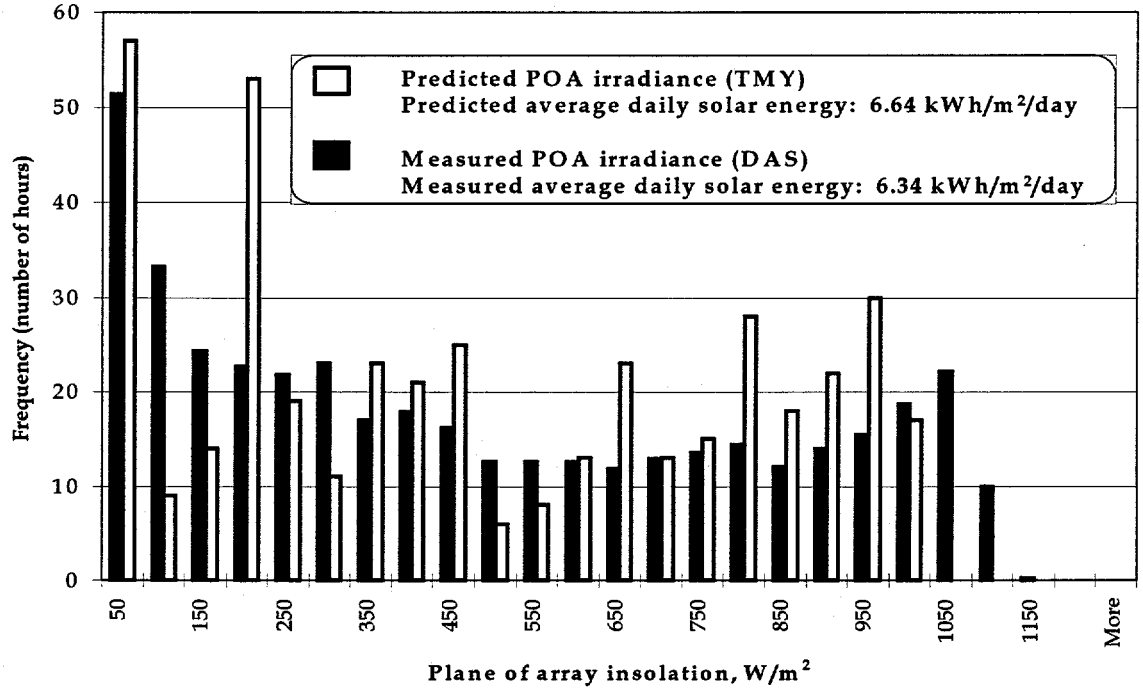


**Figure 1. Histogram of the plane of array insolation on the Aquatic Center PV array, May 1997.**

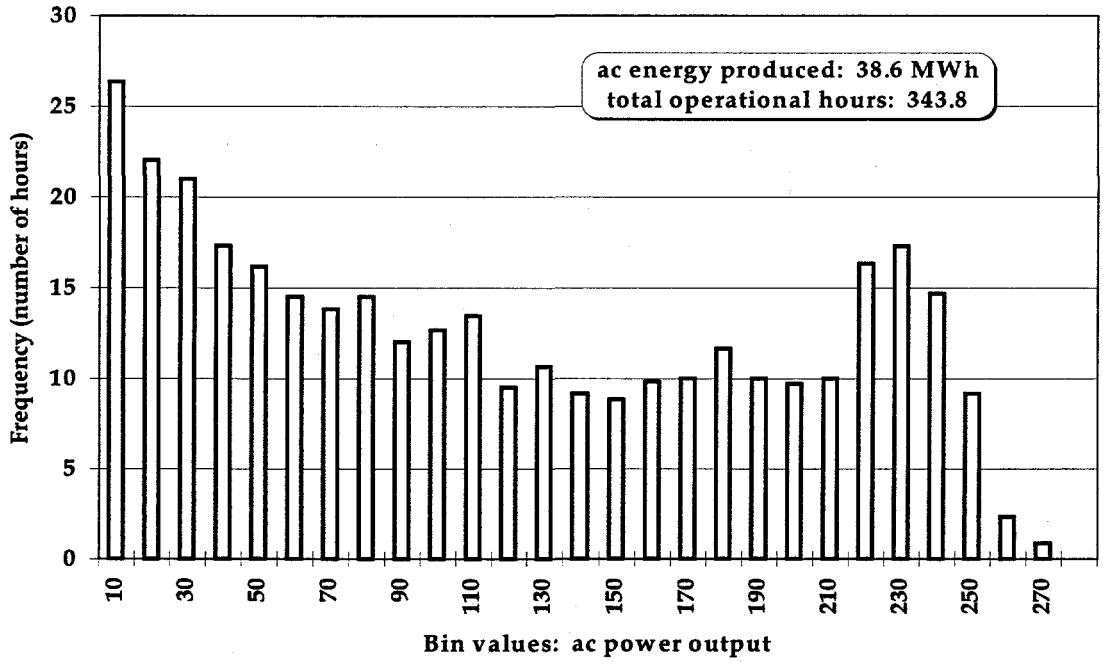


**Figure 2. Histogram of the AC power output of the Aquatic Center PV system, May 1997. Total energy for the month is given also.**

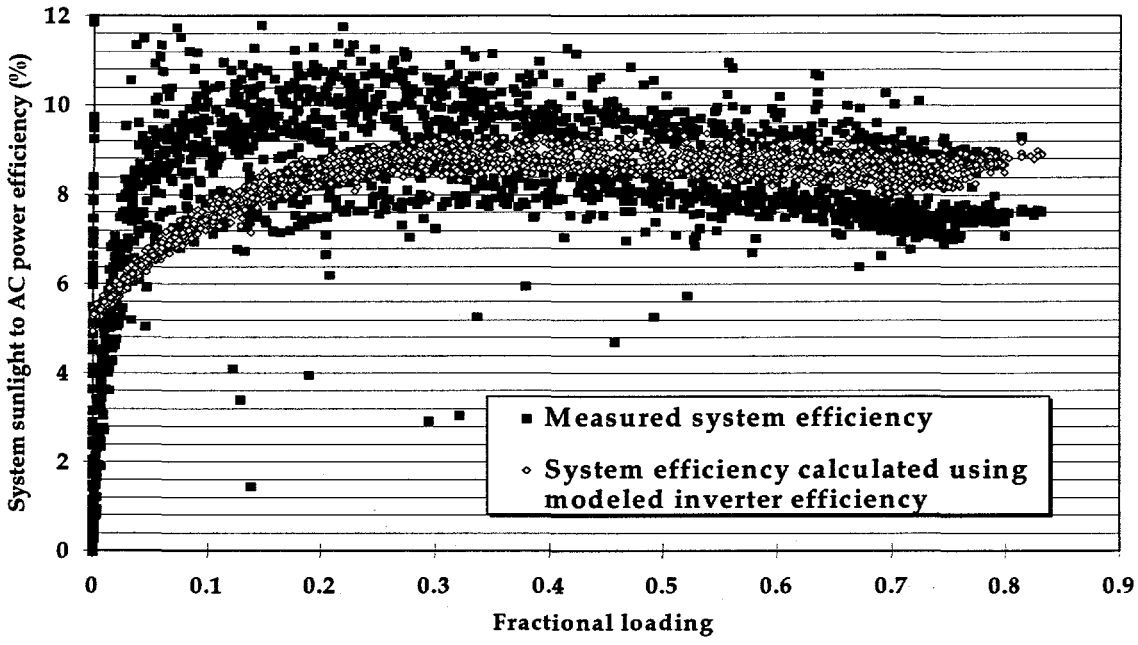


**Figure 3. Aquatic Center PV system total efficiency measurement compared with expected system efficiency value calculated using the modeled inverter efficiency, May 1997.**

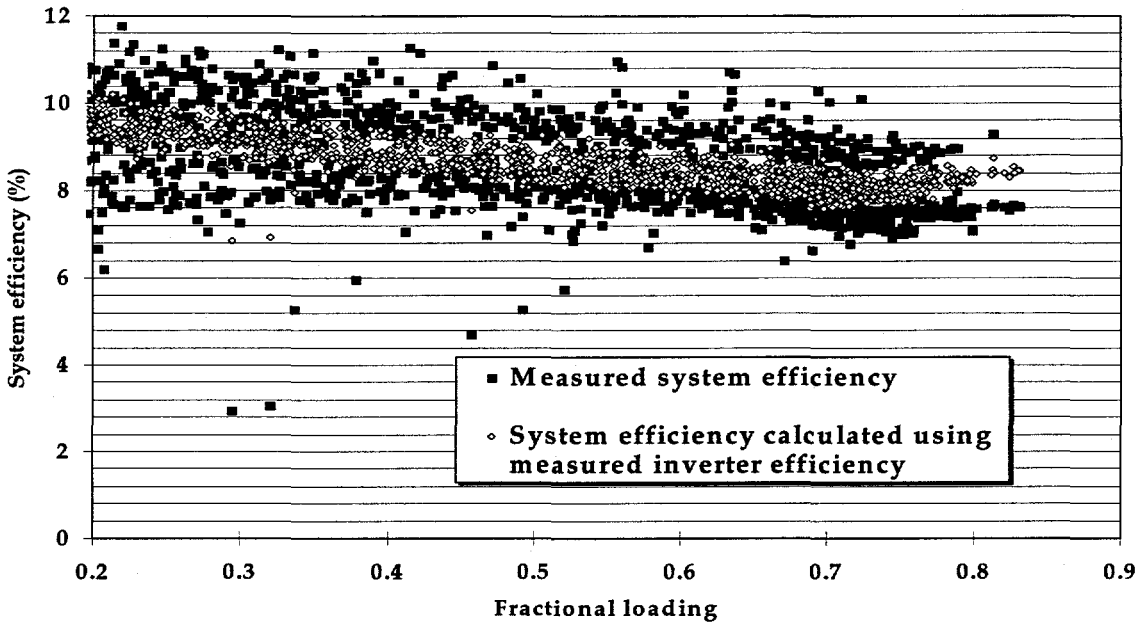


**Figure 4. Aquatic Center PV system total efficiency measurement compared with expected system efficiency value calculated using the measured inverter efficiency, May 1997.**

Note that we are now using values for the model parameters that have been adjusted based on our experiments on the system.

Note the two distinct limbs of the system's measured efficiency curve in Figures 3 and 4. One of the "limbs" agrees fairly well with the expected efficiency curve, but the other is consistently low, particularly if the modeled inverter is used. This behavior is curious and indicates that part of the PV array may have been inoperative for part of the month, and probably also explains the system's low power production. This type of curve has been seen with this system previously—during the months of December 1996 and January 1997, when the entire north-facing part of the PV array was shut off for half of each month. The UCEP was running no such experiment during May 1997. In addition, spot checks of the array's series strings revealed only two which were not functioning, not a large enough number to cause the difference seen here. Therefore, the problem One possibility is that, during the system's down time, the seven source circuit DC switches in the electrical room were turned off, as per system shutdown procedure, and during startup one of these switches was not turned on until considerably later. However, an inspection of the system indicates that all is well and functioning correctly. We must be certain to watch the June data for similar behavior.

## *REPORT ON THE PERFORMANCE OF THE GEORGIA TECH AQUATIC CENTER PV ARRAY: JUNE, 1997*

**Table 1. Summary of the performance of the Georgia Tech Aquatic Center PV Array, June 1997.**

| | |
|---|---|
| Typical PV array DC voltage: | 350-410V |
| Energy produced (AC): | 34.4 MWh |
| Maximum module temperature recorded: | 74.1°C = 165.4 °F |
| Maximum AC power recorded: | 259.0 kW |
| System operational hours: | 374.7 |
| System down time (hours)[a]: | ~0 |

[a] The system down time includes all hours during which the PV system was turned off. Hours during which the PV system was not producing power due to darkness are not included.

The table above and the accompanying figures illustrate the performance of the Aquatic Center PV array for the month of June, 1997.

The AC energy production of the system is considerably lower than the 44.1 MWh predicted by PVFORM/TMY modeling. As in previous months, the plane of array irradiance chart shown in Figure 1 indicates that the average daily energy flux for May was slightly lower than predicted. This is easily understood, since the month of June was unusually cloudy for Atlanta. Accounting for this, we could have expected on the order of 40.1 MWh of energy production, still higher than actually obtained. The system's AC power production, shown in Figure 2, appears to be normal. Figures 3 and 4 compare the system's measured efficiency with that expected based on the following model:

$$\eta_{PV,AC} = \eta_{rated}\eta_{inv}\left(1-K_{dust}\right)\left(1-K_{curv}\right)\left(1-K_{mismatch}\right)\left(1-K_{dcloss}\right)\left[1-K_T\left(T_{PV}-T_{STC}\right)\right]$$

where

$\eta_{rated}$ = the rated efficiency of the PV modules = 10.77%

$\eta_{inv}$ = either the measured value (AC power out ÷ DC power out) or the modeled value (from a fifth-order polyfit to the manufacturer's power-efficiency curve) of the inverter's efficiency

$K_{dust}$ = the percentage of power loss due to dust/soiling on modules = 4%

$K_{curv}$ = the power loss due to the roof curvature = 0.1%

$K_{mismatch}$ = the power loss due to module parameter mismatch = 2%

$K_{DCloss}$ = the power loss due to DC-side $I^2R$-type losses = 2%

$K_T$ = the modules' thermal derating coefficient = 0.0037 %/°C

$T_{PV}$ = the module temperature (measured)

$T_{STC}$ = the Standard Test Condition temperature = 25°C

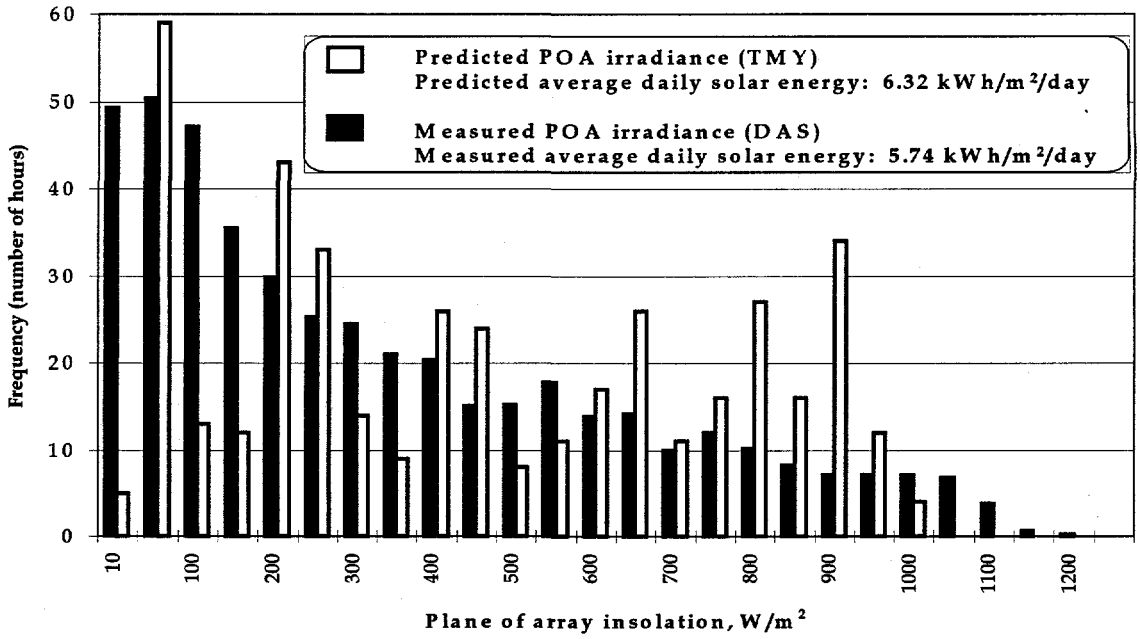


**Figure 1. Histogram of the plane of array insolation on the Aquatic Center PV array, June 1997.**

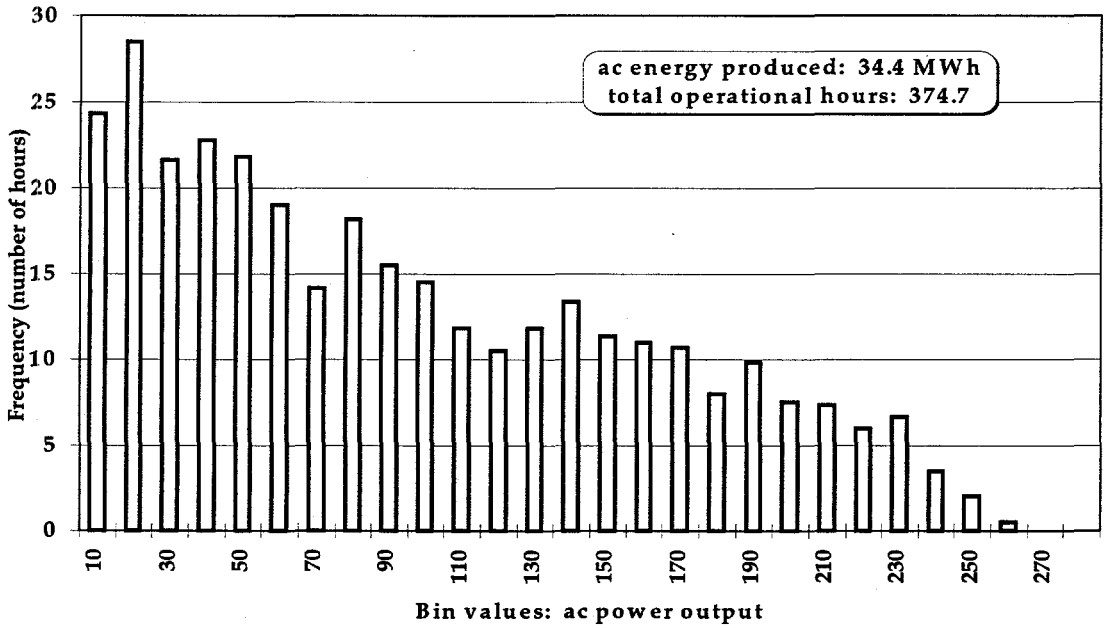


**Figure 2. Histogram of the AC power output of the Aquatic Center PV system, June 1997. Total energy for the month is given also.**

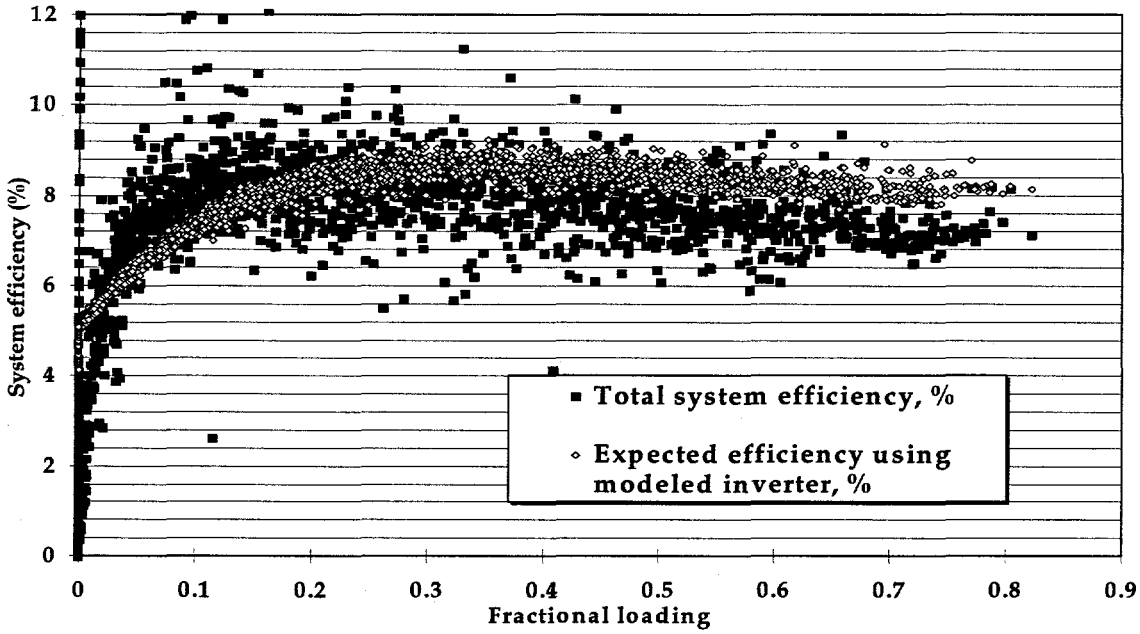


**Figure 3. Aquatic Center PV system total efficiency measurement compared with expected system efficiency value calculated using the modeled inverter efficiency, June 1997.**

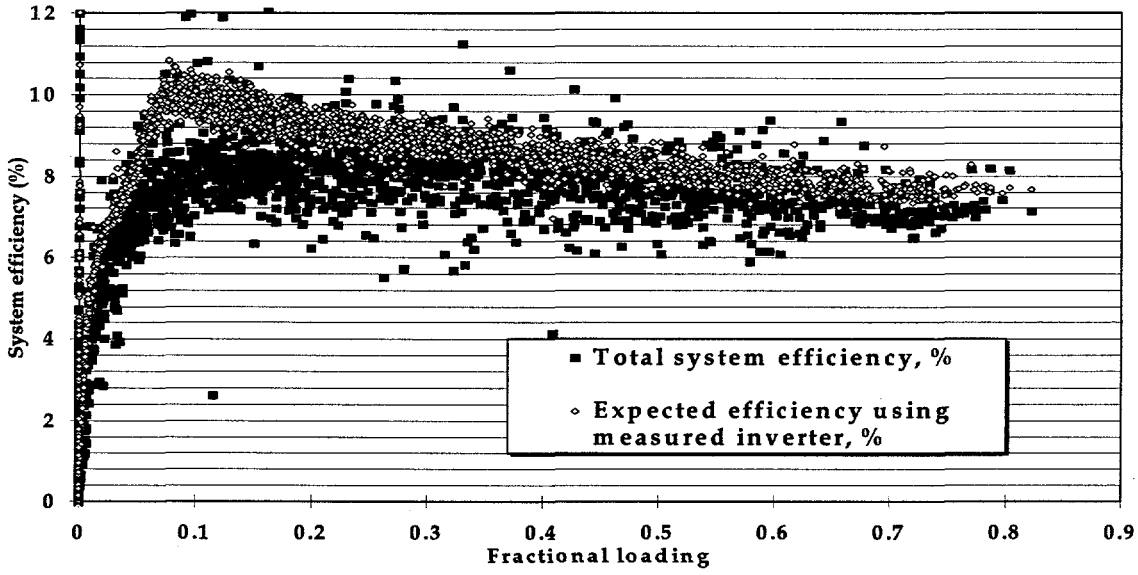


**Figure 4. Aquatic Center PV system total efficiency measurement compared with expected system efficiency value calculated using the measured inverter efficiency, June 1997.**

Note that we are now using values for the model parameters that have been adjusted based on our experiments on the system.

The reader may recall that, during the previous month of May, 1997, two distinct "limbs" appeared in the system's measured efficiency curve, and it was postulated that this was due to an accidental disconnection of part of the system by on-site maintenance personnel. We do not see the two "limbs" in the system's measured efficiency during June, and we therefore assume that our supposition was correct and that the problem has been corrected as was previously reported. Note also that the two curves actually agree quite well in Figure 4 (recall that data corresponding to fractional loading values of less than 0.2 is ignored), but at high fractional loading values the system efficiency predicted using the modeled inverter efficiency is slightly higher than the measured system efficiency. This seems to indicate that the inverter's actual full-load efficiency (measured to be about 90%) is slightly lower than that specified by the manufacturer. Reasons for this are being investigated. Accounting for this factor, we would expect the PV system's AC energy production to be about 38 MWh for this month, which is still greater than actually measured. The remaining difference cannot be explained by thermal effects. Since we have consistently seen lower than expected AC energy production from the system, even after accounting for all of these effects, we will again check the entire array for blown series string fuses in the source circuit combiner boxes.

*Appendix B*

# DESIGN CONSIDERATIONS FOR LARGE ROOF-INTEGRATED PHOTOVOLTAIC ARRAYS

# DESIGN CONSIDERATIONS FOR LARGE ROOF-INTEGRATED PHOTOVOLTAIC ARRAYS

Michael E. Ropp[1], Miroslav Begovic[1], Ajeet Rohatgi[1], Richard Long[2]

[1]College of Electrical and Computer Engineering
Georgia Institute of Technology
Atlanta, GA 30332-0250

[2]Office of Facilities
Georgia Institute of Technology
Atlanta, GA 30332

**Summary**

This paper describes calculations and modeling used in the design of the photovoltaic (PV) array built on the roof of the Georgia Tech Aquatic Center, the aquatic sports venue for the 1996 Olympic and Paralympic Games. The software package PVFORM v. 3.3 was extensively utilized; because of its importance to this work, it is thoroughly reviewed here. Procedures required to adapt PVFORM to this particular installation are described. The expected behavior and performance of the system, including maximum power output, annual energy output, and maximum expected temperature, are then presented, and the use of this information in making informed design decisions is described. Finally, since the orientation of the PV array is not optimal, the effect of the unoptimized array orientation on the system's performance is quantified.

***Keywords:*** *photovoltaic systems, computer modeling, design.*

**Introduction**

PV systems offer an environmentally-friendly way to meet growing electricity demand. They also offer several other advantages that could make them attractive for many applications, such as modularity, peak-shaving compatibility and point-of-load generation capability. However, the widespread use of PV has been impeded by its cost. PV-generated electric energy presently costs about $0.25-$0.35/kWh installed, compared to a national average of about $0.08/kWh for generation by fossil fuels. Although the PV devices themselves contribute much of the cost, other system components and installation costs are also of great importance and will continue to increase in importance as PV cells become less expensive. Therefore, demonstration projects offering experience with PV system components and design practices are very important in order to continue the downward trend in PV electricity costs. Demonstration projects can also be important in increasing the public's awareness of PV as a viable electric power generation technology.

This paper discusses one such project--a grid-connected PV system on the roof of the Georgia Tech Aquatic Center which was used as the swimming venue for the 1996 Olympic and Paralympic Games in Atlanta. The sponsors for this project are the owner of the pool (Georgia Tech), the local utility (Georgia Power Company) and the U.S. Department of Energy (DOE). Each benefits from the project in different ways: the owners will substantially reduce their electricity bill, the local utility will have needed peak-shaving support due to the match

between PV generation and the utility's demand profile, and the DOE gained an excellent opportunity to showcase PV technology in front of a worldwide audience of Olympic spectators.

The design of such a large, roof-integrated PV system is greatly facilitated by the use of modeling programs which can accurately describe the PV systems' performance as well as the conditions which will be experienced by the system under actual conditions. The use of such models in the design of the Georgia Tech Aquatic Center PV system is the topic of this paper.

**Description of the System**

Figure 1 shows an aerial photograph of the Georgia Tech Aquatic Center. The Center houses a 62,000 $ft^2$ enclosed competitive swimming and diving facility which includes a 25m x 25yd diving tank, a 25m x 50m swimming pool, pool decks, 4000 permanent seats, and about 28,000 $ft^2$ of space for student use. It was used for the swimming events of the 1995 Pan Pacific Games, the 1996 Olympic Games, and the 1996 Paralympic Games.

One of the most impressive features of the structure is its barrel-vaulted roof. The roof itself is built up from a structural aluminum base directly welded to the purlins and trusses. Atop this layer are a vapor/moisture barrier and a 2-inch thick layer of insulation, covered by a standing-seam aluminum "skin" layer. On this roof, the world's largest roof-mounted PV system has been constructed. It is comprised of 2,856 120 W modules, giving a total rated power generating capacity of 342 kW. Each module contains 72 series-connected multicrystalline silicon solar cells. At its maximum power point (MPP) under Standard Test Conditions (STC: 25°C cell temperature, 1 $kW/m^2$ of incident irradiation), the array will produce 833 $A_{dc}$ at 410 $V_{dc}$. The dc power is routed to a three-phase, pulse-width-modulated power conditioning unit (PCU), the ac output of which backfeeds an ac circuit breaker in the Aquatic Center's distribution service entrance. [Note: the terms "PCU" and "inverter" are used interchangeably in this paper.] In this way, the PV array will provide roughly a third of the electric energy required by the Aquatic Center.

**Brief Review of PVFORM**

PVFORM v. 3.3 is a comprehensive photovoltaic system simulation software package prepared by Sandia National Laboratories. This program is generally accepted to be one of the most accurate and powerful PV system computer models available today[1,2]. The primary features of the package which make it such a useful analysis and

design tool for PV systems are its two main submodels, the Perez anisotropic diffuse irradiance model and the Fuentes thermal model[3]. This section reviews these submodels. Although PVFORM has been in existence for over ten years and is relatively well-known among the PV community, this review is included to provide a sound basis for understanding the correct use and interpretation of the results presented in this paper.

Generally, the solar irradiation, or insolation, in the plane of the array must be computed from measured values of the total (global) insolation on a horizontal surface, usually augmented by a measurement of one of the components of the horizontal insolation: the direct insolation ($D_h$), which comes directly from the solar disk, or the diffuse irradiation ($d_h$), which is scattered by various mechanisms before it strikes the horizontal surface. The plane-of-array insolation (S) consists of three components: direct ($D_{poa}$), diffuse ($d_{poa}$), and also a ground-reflected component ($D_{refl}$). The direct component $D_{poa}$ can be determined with very little error, since it depends primarily on the position of the sun in the sky, which is a well-known function of several easily-available variables, and on the array orientation[4]. Cloudiness and other atmospheric factors are accounted for using the measured data. The ground-reflected component is given by[5]

$$D_{refl} = \rho G_h[0.5(1 - \cos(s))]$$

where $\rho$ is the albedo (reflectance) of the surrounding ground, s is the array tilt angle, and $G_h$ is the horizontal global irradiance. Correct determination of $\rho$ has been shown to be important[5], but its importance for the Aquatic Center array is minimal because its tilt angle is very low. Determining the diffuse insolation, $d_{poa}$, is considerably more difficult; in fact, the submodel which calculates the diffuse insolation in the plane of the array is a major limiting factor in the accuracy of PV system performance predictions[1]. The Perez anisotropic diffuse irradiance model addresses this limitation by separating the sky into three components with different brightnesses: the circumsolar disk, a "horizon band", and an isotropic background. In PVFORM, a simplified version of the Perez model is used which assumes the horizon band to have only infinitesimal height. With this assumption, the expression for the diffuse insolation on the array becomes[4]

$$d_{poa} = d_h[0.5(1+\cos(s))(1-F_1') + F_1'\left(\frac{a}{c}\right) + F_2' \sin(s)]$$

where $F_1'$ and $F_2'$ are the "reduced brightness coefficients" for the circumsolar and horizon band regions respectively, and a and c are the solid angular size of the circumsolar region weighted by its average incidences on the tilted array and the horizontal surface respectively[4]. $F_1'$ and $F_2'$ are selected by PVFORM from a set of empirically-determined values. The required inputs to the model are the direct normal irradiance and the global horizontal irradiance.

The Fuentes thermal model uses an equation for the cell temperature derived directly from an energy balance on the PV module[6]:

$$h_c \cdot (T_c - T_a) + \varepsilon\sigma \cdot (T_c^4 - T_s^4) + \varepsilon\sigma \cdot (T_c^4 - T_g^4) + mc \cdot \frac{dT_c}{dt} - \alpha \cdot S = 0$$

where $h_c$ is the convective heat transfer coefficient (calculated by PVFORM), $T_c$ is the cell temperature, $T_a$ is the ambient temperature, $\varepsilon$ is the total emissivity of the module, $\sigma$ is the Stefan-Boltzmann constant, $T_s$ is the "sky temperature" (the effective radiating temperature of the sky, which is different from $T_a$ and is calculated by PVFORM), $T_g$ is the ground temperature (calculated by PVFORM), m is the mass of the module, c is the module's heat capacity, $\alpha = (1-r)(1-\eta)$ (where r is the module reflectance and $\eta$ is the module's conversion efficiency) is the fraction of insolation converted into heat, and $S = D_{poa} + d_{poa} + D_{refl}$ is the global plane-of-array insolation [6]. In order from left to right, the terms represent convection to the air, radiation to the sky, radiation to the ground, the rate of change of thermal energy stored within the module, and absorption of sunlight. Conduction is neglected. After linearization of the fourth-order temperature terms and assuming a linear variation between insolation data points, the energy balance equation is solved for $T_c$, leading to an equation which is solved iteratively to obtain the cell temperature[6]:

$$T_c = \frac{(h_c T_a + h_{rs} T_s + h_{rg} T_g + \alpha S_0 + \alpha \frac{\Delta S}{L}) \times (1 - e^L) + \alpha \cdot \Delta S}{h_c + h_{rs} + h_{rg}} + T_{c0} e^L$$

where

$$h_{rs} = \varepsilon\sigma(T_c^2 + T_s^2)(T_c + T_s)$$
$$h_{rg} = \varepsilon\sigma(T_c^2 + T_g^2)(T_c + T_g)$$
$$S = S_0 + \Delta S \frac{t}{\Delta t}$$
$$L = -(h_c + h_{rs} + h_{rg}) \cdot \frac{\Delta t}{mc}$$
$$T_{c0} = \text{cell temperature at start of } \Delta t$$

As inputs, the submodel requires the ambient temperature, the insolation, and the wind speed which is important in calculating $h_c$.

Once the cell temperature is known, PVFORM can calculate the efficiency of the cells using given temperature derating coefficients, and then the plane-of-array insolation can be used to calculate the array's dc power output. A derating factor of 14%, which includes a 10% "dust factor" and 2% each for interconnect and mismatch losses, is also included in our calculations. Implicit in this calculation is the assumption that the array is always operating at its MPP, an assumption which leads to consistent overestimation of the array's power output[2].

To obtain ac results for grid-interactive applications such as ours, PVFORM also includes a power conditioning unit (PCU) submodel which uses a piecewise-defined function of the unit's efficiency as a function of the fractional loading, or the ratio of the array's dc power output to the unit's rated (full-load) power capacity[7]:

$$\eta_{PCU} = \eta_{PCU,rel}\left(\frac{\eta_{PCU,rated}}{0.91}\right)$$

where

$$\eta_{PCU,rated} = \text{PCU efficiency at rated capacity}$$

$$\eta_{PCU,rel} = \begin{cases} 8.46F - 0.15, & 0 \le F < 0.1; \\ 0.774 + 0.663F - 0.952F^2 \\ +0.426F^3, & F \ge 0.1 \end{cases}$$

$$F = \frac{\text{PV array output power}}{\text{PCU rated capacity}}$$

The parameter F is referred to as the "fractional loading" of the PCU. The PCU in the Aquatic Center PV system has a full-load rated efficiency of $\eta_{PCU,rated}$ = 95% and a maximum power rating of 315 kW of continuous power. Figure 2 shows a comparison of the results of this model with actual fractional load efficiency curves for the PCU. The figure shows some disagreement between the PVFORM model and the actual curve. Our original approach to improving on this was to replace the above-described PCU model by a fifth-order polynomial fit to the actual PCU efficiency curve:

$$\eta_{inv} = 3.3089F^5 - 11.1375F^4 + 14.7141F^3 - 9.6373F^2 + 3.1981F + 0.5037$$

where F again is the PCU fractional loading. The plot of this polynomial corresponds almost exactly with the actual curve over the range $0.18 < F < 1$. However, as will be seen shortly, we were unable to use PVFORM's internal PCU model at all due to the non-coplanar nature of our PV array.

**Determination of an Appropriate PCU Power Capacity**

For economic reasons, it is desirable to use the smallest-capacity PCU possible which can still handle the full power output of the array. The best candidate PCU for this system was rated at 315 kW, but it was already known that the rated array output power would be 342 kW. The PCU's maximum power point (MPP) tracking circuitry incorporates a self-protection mechanism against PCU damage due to overload: if PV power production exceeds the PCU's power-handling ability, the MPP tracker moves the array off of its MPP, reducing the array output power. For this reason, damage to the PCU is not a concern. However, if this condition could occur frequently under actual operating conditions, the result would be a waste of significant amounts of PV power. It is

well known that the 342-kW nameplate rating of the array is determined under conditions which will never be duplicated in the field, so the array will probably never produce that much power, and therefore an exact knowledge of the maximum power which the array will produce under "real" conditions would facilitate PCU selection. PVFORM was used to obtain this information. However, before this could be done, a problem had to be circumvented. The Aquatic Center array is flush-mounted to the roof of the Center, which is curved, and a portion of the array is actually on the north-facing slope of the roof. Obviously, there would be considerable mismatch in the plane-of-array insolation across the array, but PVFORM contains no provisions for dealing with this case, and furthermore we have found no software package which integrates capabilities for handling noncoplanar arrays with those for determining the insolation on each section of the array. Certainly, such a package could be created by integrating PVFORM with a model such as that presented by Bishop[8], but the computation time involved in simulating an array like the one on the Aquatic Center would be extreme. To avoid these difficulties, we adopted a simpler approach.

On the south-facing side of the roof, the tilt angles of the modules vary from about 13° up from horizontal to 0° , with an average tilt of 6.4°; on the north-facing side, the variation is from about 2° to about 10° , with an average tilt of 5.9°. All series strings are coplanar; there is no insolation mismatch between series-connected modules. Since the sections of the array which are under differential illumination are connected in parallel, their operating voltages will be affected. However, it is well-known that the voltage of a PV module or array is only logarithmically dependent on the insolation, and therefore a relatively large difference in insolation is required to produce an appreciable change in voltage. Considering the north-facing and south-facing sides of the roof separately, we noted that the variations from the average tilt on each side are small, and thus, with the above-mentioned consideration about the relative insensitivity of voltage to insolation variations taken into account, the insolation over each side of the roof could be considered to be roughly uniform. Each side of the roof could then be modeled as a separate array with tilt equal to the average tilt on that side. However, a suitable method for combining the two subarrays was required. PVFORM will assume that each subarray operates at its maximum power point, thus ignoring their interaction (effectively "decoupling" them). Due to their parallel interconnection and voltage interaction this will not be strictly true; each subarray will slightly pull the other off of its MPP. If it could be shown that the insolation difference between the two parallel-connected subarrays is sufficiently small, the

power output of the subarrays computed independently by PVFORM and that actually produced under parallel interconnection would be almost the same, and the total array power output could then be computed by simply summing the power and energy outputs of the two subarrays. First, PVFORM was employed to quantify the difference in insolation between the two subarrays. It was found that the maximum insolation mismatch occurred during a time at which there was 645 W/m$^2$ of insolation on the south-facing side. If the mismatch was defined as

$$G_{mismatch} = G_{South} - G_{North}$$

then $G_{mismatch}$ at the time described above was 165 W/m$^2$. Then, a software package called IVCURVE was employed to determine the amount of voltage mismatch between the two subarrays while operating at their maximum power points. IVCURVE computes the array I-V curve given the insolation, module temperature, and the module electrical parameters. It also can calculate the current and power produced by the array if given the operating voltage, so the maximum power point can be located by iteration, substituting in voltage values until the maximum in power is located. Under the conditions described above, it was found that $V_{MP}$ for the south-facing side was about 363V and that for the north side was 10V lower. This represents just under a 3% difference in voltage. To predict what the "real" operating voltage would be under this condition, we note that the south-facing subarray accounts for 82% of the total array area and should therefore operate closer to its decoupled voltage than the north-facing side will. Thus, we linearly scale the difference between the two operating voltages and predict that the real, coupled operating voltage will be about 361V. Plugging this operating voltage into IVCURVE and computing the PV power produced by the two subarrays, we find that the difference in the predicted power output between the decoupled subarrays and the parallel-interconnected subarrays would be only about -0.1%. This is a negligible error, particularly when compared with other known errors such as that introduced by the assumption of 100% efficient maximum power point tracking, which can be nearly 5%[2]. Therefore, the approach of modeling the Aquatic Center array as two independent subarrays and then adding their power outputs is justified and will result in negligible error.

Using this approach, the array's power output over the course of a year was calculated. Figure 3 shows a histogram of the array dc power output based on the Typical Meteorological Year (TMY) for Atlanta. [Note: the National Renewable Energy Laboratory (NREL) has recently produced a new set of TMYs called TMY2s which are more accurate than the TMY. However, some difficulty has been experienced in using this data with PVFORM.

Large spikes have been observed in the plane-of-array insolation calculated from TMY2 raw data. For this reason, the TMY has been retained in this study, and work is under way to resolve the problem encountered in using the TMY2.] Note that the maximum array power output, which occurs on April 1 of the TMY, is 279.7 kW, which is well below the PCU's rated capacity. Therefore, we can conclude that the 315 kW PCU is sufficient for this installation and that its self-protection against overload will not result in a significant loss of power.

Using the dc power histogram, we also calculated an "effective PCU efficiency" using the expression

$$\eta_{inv,eff} = \frac{\sum_{j=1}^{N_b} \{N(F_j) \cdot P_j \cdot \eta_{inv,j}(F_j)\}}{\sum_{j=1}^{N_b} N(F_j) \cdot P_j}$$

where $\eta_{inv,j}(F_j)$ is the PCU efficiency at fractional load $F_j$ (determined from the actual curve), $N(F_j)$ is the number of hours during the year that the PV power production results in fractional loading $F_j$, $P_j$ is the power production corresponding to bin j, and $N_b$ is the number of bins (discrete values of F considered), as demonstrated in Figure 4. An important feature of this expression which should be noted is that the effective PCU efficiency depends not only on the PCU efficiency itself but also on the power production of the array, and therefore this parameter can also be used as a measure of how well the PCU is matched to the PV array by comparing the effective PCU efficiency to the full-load PCU efficiency. Using this expression and the information in Figure 4, the PCU's effective efficiency for this installation is found to be approximately 90.5%. This compares favorably with the PCU's full-load efficiency of 95%, supporting the choice of this PCU for this PV array. The effective PCU efficiency also provides an easy way to determine the system's ac output. Note that, as mentioned previously, our modeling procedure renders PVFORM's internal PCU submodel unusable, because it is the sum of the subarray powers which needs to be fed into the PCU submodel. This effective PCU efficiency can be used in lieu of writing software to compute the solution of the fifth-order polynomial given above for each dc output data point given by PVFORM. Using the 90.5% effective PCU efficiency, PVFORM predicts that the annual energy production of the PV system will be almost 409 MWh.

**Maximum Voltage vs. PCU dc Input Rated Voltage**

The 315kW PCU has a maximum dc open-circuit input voltage of 600V, as do the dc-side conductors and switchgear. Therefore, care must be taken to ensure that the series-parallel configuration of the array is such that the array voltage will not exceed 600 V. Since the array has a negative voltage temperature coefficient, and temperatures lower than the STC-specified 25°C could be encountered in the field, PVFORM was used to model the temperature of the cells for an entire year, using the TMY as input. The output was then scanned for the lowest cell temperature which occurred during daylight hours. This temperature was -7.3°C. The maximum voltage produced by the array was calculated using the equation

$$V_{\max} = \left[V_{OC} + (K_{Voc})(\Delta T_{\max})\right] \times N$$

where N is the number of series modules (12), $\Delta T_{max}$= ($T_{min}$ - 25°C), $V_{OC}$ is the open-circuit voltage (42.6V), and $K_{Voc}$ is the voltage derating coefficient per module given by the manufacturer (-0.146 V/°C). Substituting the values for this system, $V_{max}$ is found to be 568 V. It is important to note that when this low temperature occurs there will be very little usable sunlight, so the actual voltage will be lower than 568 V. Therefore, based on PVFORM modeling, we conclude that the array design is acceptable and will not produce voltages in excess of the 600 $V_{dc}$ rating of the dc-side equipment.

It should also be noted that Underwriters' Laboratories (UL) standards dictate that the lowest expected ambient temperature at the site should be used in determining the maximum array voltage[9]. In order to determine this temperature, all 30 years of the NSRDB-SAMSON database on CD-ROM were scanned for the minimum temperature during that time period in Atlanta, which was -22.2°C (occurring on January 21, 1985). Substituting this value into the above equation gave

$$\Delta T = -47.2^{\circ} C$$
$$V_{\max} = 594V$$

This is still below the 600 $V_{dc}$ limit, again supporting the suitability of the array design.

**Investigation of the Effects of Standoff Height**

One of the novel features of this PV installation is that the array will be mounted to the roof directly using clamps connected to the standing seams (Figure 5). The standing seam height is about 2.5 inches, and the mounting clamps hold the modules about 1 inch above the standing seams, resulting in an array-roof standoff height of about 3.5 inches. From a photovoltaic standpoint, the standoff height is important because it strongly affects the ventilation behind the array and thus the array temperature. PVFORM was utilized to quantify this effect. In the program, the standoff height is reflected in the choice of INOCT, where INOCT is the Installed NOCT (Nominal Operating Cell Temperature) and is calculated using the manufacturer's specified NOCT and a set of empirically-determined rules [3,6]. We used INOCT values of 56°C, 50°C, and 48°C, which correspond to standoff heights of 2", 4" and 6" respectively. We also assessed an additional "penalty" of $+4^{o}C$[3,6] because the underlying standing-seam roof is "channelized", meaning that the standing seams will partially restrict airflow behind the array and increase INOCT. To investigate the importance of the standoff height, we examined the array annual ac energy production and the maximum temperature attained by the array as a function of standoff height (Figure 6). As expected, the model calculations reveal that as the array-roof standoff height increases, the maximum cell temperature attained during the year decreases and as a result the annual energy production of the array increases. Notice that the maximum temperatures attained by the cells in the array are quite high, approaching 77°C for the 3.5" array-roof distance. Note also that the array annual ac energy production at the 3.5-inch standoff height is about 427 MWh/year, and that the ac energy production continues to increase with decreasing INOCT. Figure 6 quantifies the effect of the array-roof standoff height on the PV array's energy output. In addition, this calculation is justified because it allows for design within tighter tolerances, since the maximum temperature which will be attained by the array will be known. Cable temperature ratings (90°C for this system) and other factors affected by operating temperatures beneath the array, which will always be below the array temperature (assuming that ampacities are properly selected), can be adjusted for greater economy without jeopardizing reliability.

**Investigation of the Optimum Orientation of the PV Array**

The orientation of the Aquatic Center PV array is not optimized. The tilt and azimuth of the array were determined by the shape of the roof, which in turn was selected according to architectural and aesthetic

considerations. We undertook the task of quantifying the performance penalty incurred by this unoptimized orientation using PVFORM. For this exercise, the array was modeled as being coplanar because the computational intensity involved in accounting for the variable tilt in such a large number of PVFORM simulations would have become extreme. The baseline for these comparisons was thus a coplanar array at the average tilt of the south-facing side (6.4°), whose annual ac energy production as computed by PVFORM is about 427 MWh. A matrix of 84 PVFORM simulations covering tilt angles from 0° (horizontal) to 60° up from horizontal and azimuth angles of 20° east of south to 90° west of south at 10° increments was constructed. From this matrix, two sets of data were extracted and plotted: the total annual ac energy production as a function of array orientation, and the array's ac energy production during the peak hours of 12-7 pm, June through September, as a function of array orientation ("peak-shaving energy production"). Figure 7, which is a contour plot of the array's annual energy production as a function of array orientation, shows that the optimum array orientation for maximum annual energy production is a tilt of about 30° with a due-south azimuth. To increase the accuracy of this figure, we ran further simulations at increments of 2° and found that 30° is the optimum to within 2°. Notice that the optimum tilt is slightly less than the site latitude (33.7°N). This is to be expected, since the optimum tilt for maximum annual energy production is roughly equal to the site latitude, but high-humidity locations can have slightly lower optimum tilts because high humidity will increase the diffuse component[10], and this component decreases with increasing tilt because more diffuse light hits the back of the array at higher tilts[4]. However, Figure 7 also demonstrates that the sensitivity of the system performance to such small deviations is fairly small (performance penalties of only about 1% or less). The model calculations show that the annual energy output could be increased from about 427 MWh/year to about 462 MWh/year (an 8% increase) by changing the tilt angle to 30° from its installed orientation (6.4°). Recall that the 427 MWh/year baseline figure was computed for a coplanar array. If the comparison is instead made to the curved array as represented by our two-subarray model, thus adding the effect of the roof curvature, we find that the output could have been increased by almost 14%, from 407 MWh to 462 MWh, by placing the entire array at the same (optimized) tilt.

Since peak shaving is an important potential application of PV systems, we also investigated the "peak-shaving effectiveness" of our system. To optimize the array for peak shaving, conventional wisdom would state that the array should be oriented by the position of the sun at the peak demand time on the local utility's system. For

the Georgia Power Company, the peak demand occurs at about 3-4pm during the four summer months of June-September. According to the simple set of equations for determining solar position found in References 10 and 11 or the solar geometry charts found in Reference 10, the "rule of thumb" optimum array orientation should be approximately 43° tilt and about 82° azimuth west of south to achieve maximum peak shaving at the peak demand time (3-4pm). To look for the peak shaving optimum, we examined the array's energy production during "peak hours", defined by Georgia Power as noon-7pm during the four summer months, as a function of array orientation. The results of our simulations are shown in Figure 8, which shows that the peak shaving optimum is approximately 30° tilt and 70° W of S azimuth. As before, we increased the resolution of our matrix near this point and found that the optimum is actually 35° tilt and 75° W of S azimuth. These results demonstrate that applying the rule of thumb in Atlanta yields values that are slightly high, although again the sensitivity of the system performance to small deviations from the optimum orientation is small. The small discrepancy between predicted optimum tilts can be explained as before: as the tilt angle is increased, more and more diffuse irradiation is lost because it strikes the back of the array. In the case of the azimuth, the disagreement arises because the peak demand time falls relatively late in the day, at a time when less solar energy is available, and orienting the array for maximum production at that time sacrifices energy production at earlier times in the window, when more insolation is available. Too great an azimuth results in an excessive loss of this midday solar energy and an eventual reduction of peak shaving capability, with the peak window as defined here (noon-7pm).. The model calculations (Figure 8) show that the annual electricity generation of the Aquatic Center array during the peak window could be increased from about 109.1 MWh/year to 123.6 MWh/year, an increase of 13%, by moving the orientation to 35° tilt and 75° azimuth west of south.

**Use of modeling in system monitoring**

The Aquatic Center PV system is equipped with an extensive monitoring and data acquisition system (DAS) which allows researchers to closely observe the performance of the system and compare this performance with expected values. The DAS also collects meteorological data for comparison purposes. In early July, 1996, just before the start of the Summer Olympics, observers at Georgia Tech's University Center of Excellence in Photovoltaics noted that the power output of the system recorded by the DAS was much lower than had been

predicted by the modeling described here. Where power outputs of 220-240 kW were expected, only 180-190 kW of PV electric power was actually being produced. The meteorological measurements and readings of the module temperatures were used to calculate the expected system output according to the simple system model

$$P_{dc} = G_{poa} A_{array} \eta_{PV}$$

where

$$\eta_{PV} = \eta_{rated} \cdot (1 - K_{dust})(1 - K_{mismatch})(1 - K_{dcloss})[1 - (T_{\mathrm{mod}\,ule} - T_{STC})K_{\eta}]$$

with $\eta_{rated}$ = the modules' rated efficiency (10.77%), $K_{dust}$ = 10% is the derating factor due to soiling, $K_{mismatch}$ = 2% is the derating factor due to module-module intrinsic parameter mismatch, $K_{dcloss}$ = 2% is the derating factor due to losses in dc-side conductors and equipment, $T_{module}$ is the measured module temperature, $T_{STC}$ is the standard test condition temperature (25°C), and $K_{\eta}$ is the modules' efficiency temperature coefficient. The expected dc-side system efficiencies were around 7.5%; actual dc-side system efficiencies were as low as 5%. This made it clear that there was a problem with the system, and subsequent on-site investigation revealed the nature of the problem: one-seventh of the array was producing no power. It turned out that the roof had received a direct lightning strike in early July, and this strike blew fuses and surge arrestors in one entire section of the array. Fortunately, the problem was detected in time to allow for repairs before the Olympics. However, without the forewarning provided by the lack of consistency with performance expectations obtained from both simple and detailed models, the situation might have been very different, and the opportunity to showcase the system before a worldwide audience could have been lost.

**Conclusions**

The use of modeling in design considerations for the PV array on the Georgia Tech Aquatic Center has been described. The primary model used, PVFORM v. 3.3, was thoroughly reviewed. Calculations of the predicted PV array power output showed that it could be expected to remain below 315 kW, and thus the 315 kW PCU was adequate. PVFORM's cell temperature submodel was used to obtain the lowest cell temperature attained by the array, with which it was shown that the maximum array voltage would not exceed the 600 V dc-side limit and thus the array design was acceptable. The effects of varying the array standoff height on array energy output were

quantified and shown to be consistent with expectations. Finally, the effect of the array's non-optimal orientation, which was fixed by aesthetic considerations, was examined. We have demonstrated that the array's annual energy production is reduced by 8% and that its peak shaving capability is reduced by 13% due to the unoptimized orientation, when compared with a coplanar array. If the effect of the roof curvature is taken into account, the reduction in annual energy production becomes almost 14%, and the reduction in peak-shaving capability would similarly increase.

Further work is underway to improve this modeling procedure using measured data from the installed system. In Reference 6, a FORTRAN program is provided which solves the Fuentes thermal model for an improved INOCT value based on measured installed temperatures and insolation values; this will be run after several months' worth of data have been collected. We are also closely scrutinizing the effects of the non-coplanar array using IVCURVE, a program from Photovoltaic Resources International, and theoretical calculations versus measured system performance. Finally, the performance of the data acquisition system is being optimized using an error-minimization technique to be described in a future paper.

**Acknowledgments**

The authors wish to thank Mark Seiderman at the National Climatic Data Center for his invaluable assistance in this work, and also Jose Mejia and Keith Tate of Georgia Tech's University Center of Excellence in Photovoltaics for many helpful discussions and suggestions.

This project was co-sponsored by the U.S. Department of Energy, Georgia Power Company, and the Georgia Institute of Technology.

**References**

1. S. Rahman and B. H. Chowdhury, "Simulation of Photovoltaic Power Systems and Their Performance Prediction", *IEEE Transactions on Energy Conversion* **3**(3), p. 440-446 (1988).
2. R. Perez, J. Doty, B. Bailey, and R. Stewart, "Experimental Evaluation of a Photovoltaic Simulation Program", *Solar Energy* **52**(4), p. 359-365 (April 1994).
3. D. F. Menicucci and J. P. Fernandez, *User's Manual for PVFORM: Photovoltaic System Simulation Program for Stand-Alone and Grid-Interactive Applications*, Sandia National Laboratories publication SAND85-0376 (October 1989).

4. R. Perez, R. Seals, P. Ineichen, R. Stewart, and D. Menicucci, "A New Simplified Version of the Perez Diffuse Irradiance Model for Tilted Surfaces", *Solar Energy* **39**(3), p. 221-231 (1987).

5. P. Ineichen, R. Perez, and R. Seals, "The Importance of Correct Albedo Determination for Adequately Modeling Energy Received by Tilted Surfaces", *Solar Energy* **39**(4), p. 301-305 (1987).

6. M. K. Fuentes, "A Simplifies Thermal Model for Flat-Plate Photovoltaic Arrays", Sandia National Laboratories publication SAND85-0330 (May 1987).

7. D. F. Menicucci, "Photovoltaic Array Performance Simulation Models", *Solar Cells* **18**, p. 383-392 (1986).

8. J. W. Bishop, "Computer Simulation of the Effects of Electrical mismatch in Photovoltaic Interconnection Circuits", *Solar Cells* **25**(1), p. 73-89 (October 1988).

9. J. C. Wiles, *Photovoltaic Power Systems and the National Electric Code: Suggested Practices*, Photovoltaic Design Assistance Center, Sandia National Laboratories (March 1995).

10. M. Buresch, *Photovoltaic Power Systems*, by McGraw-Hill, 1981.

11. S. R. Wenham, M. A. Green, and M. E. Watt, *Applied Photovoltaics*, Centre for Photovoltaic Devices and Systems, University of New South Wales, Australia, 1994.

12. R. Hulstrom (ed.), *Solar Resources*, MIT Press, 1989.

## Biographies

**Miroslav Begovic** (S'87, M'89, SM'92) is an Associate Professor in the College of Electrical and Computer Engineering, Georgia Institute of Technology, Atlanta, GA. He is a member of Sigma Xi, Eta Kappa Nu, Tau Beta Pi, and Phi Kappa Phi. Dr. Begovic's research interests include photovoltaic systems and computer applications in power systems.

**Richard Long** is the architect and Manager of Project Support in the Office of Facilities, Georgia Institute of Technology, Atlanta, GA. Mr. Long is the Director and Coordinator and a Co-principal investigator for the project discussed in this paper.

**Ajeet Rohatgi** (F'91) is a Regents Professor and the Director of the University Center of Excellence for Photovoltaic Research and Education in the College of Electrical and Computer Engineering, Georgia Institute of Technology, Atlanta, GA. Dr. Rohatgi is a Georgia Power Distinguished Professor and is a Co-principal investigator for the project discussed in this paper. His research interests include high-efficiency photovoltaic devices, semiconductor processing, and photovoltaic systems.

**Michael Ropp** (S'95) is a Ph.D. candidate in the College of Electrical and Computer Engineering, Georgia Institute of Technology, Atlanta, GA. His research interests include photovoltaic systems, power electronics and electric power systems.

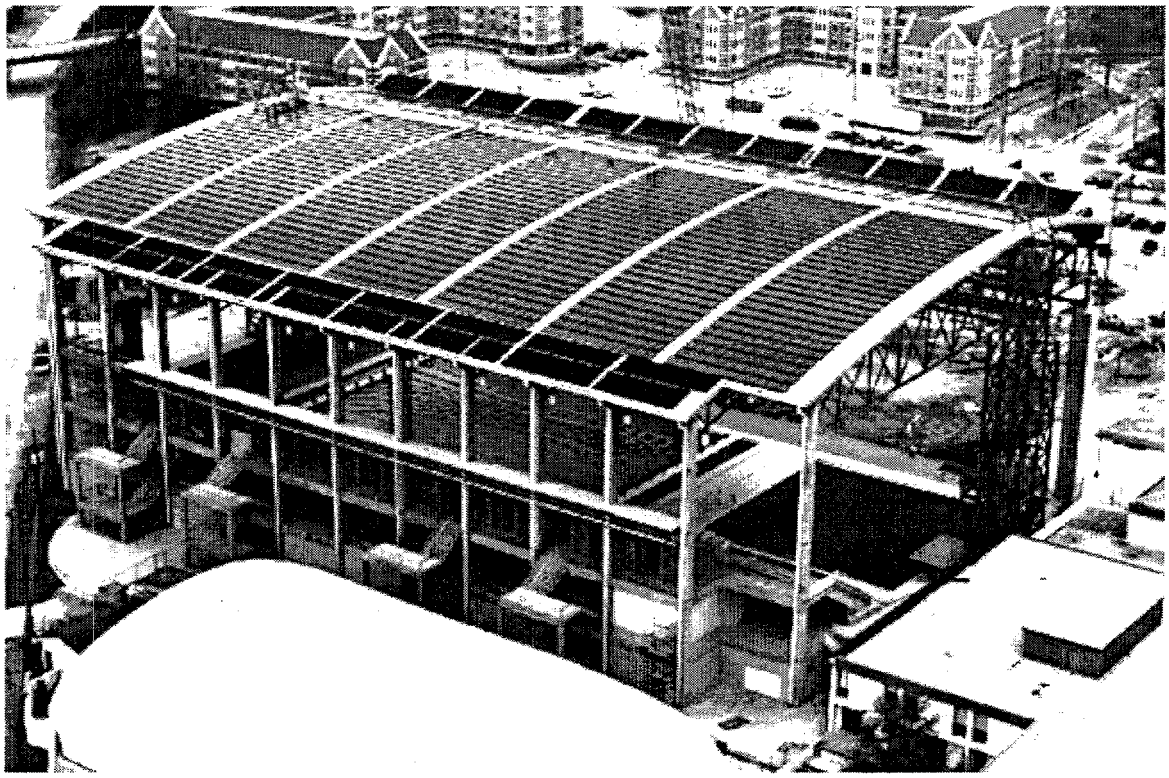

**Figure 1.** An aerial view of the Georgia Tech Aquatic Center. The black panels along the roof edges are the collectors of a solar thermal system which maintains the pool water temperature at 78°F for Olympic competition. The remainder of the roof is covered by 2856 PV modules.

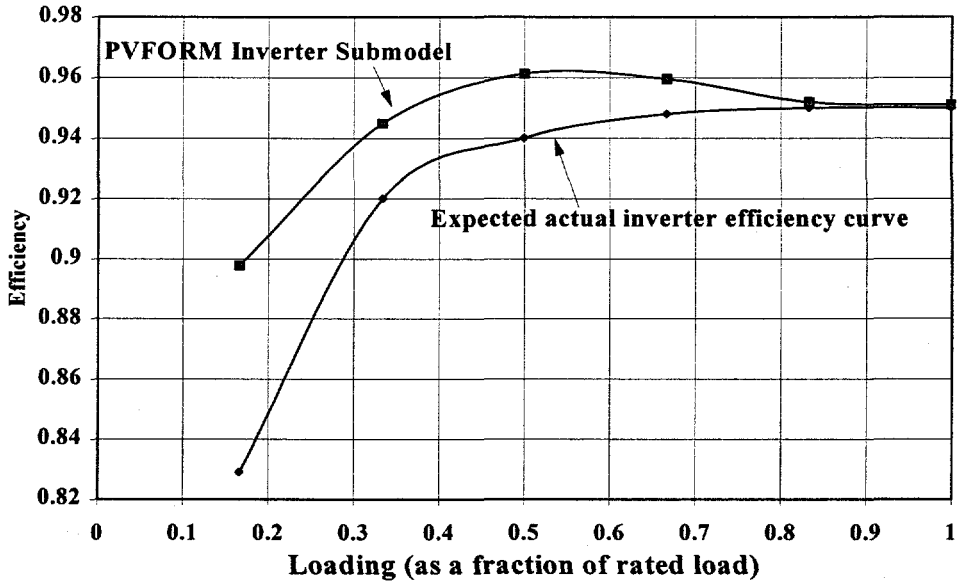


**Figure 2.** PCU efficiency curve compared with PVFORM model.

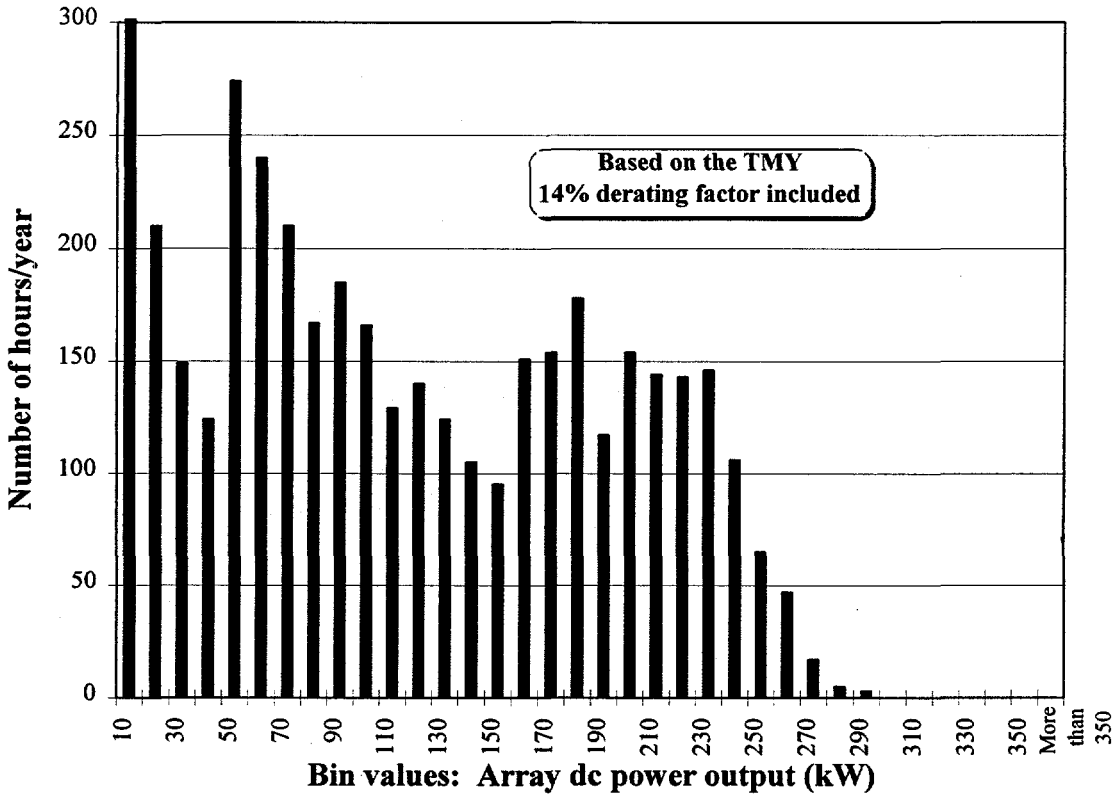


**Figure 3.** Histogram of the Aquatic Center array's dc power output. The y-axis shows the number of hours that the array produced an amount of power between the x-axis bin value and the next-lowest bin value.

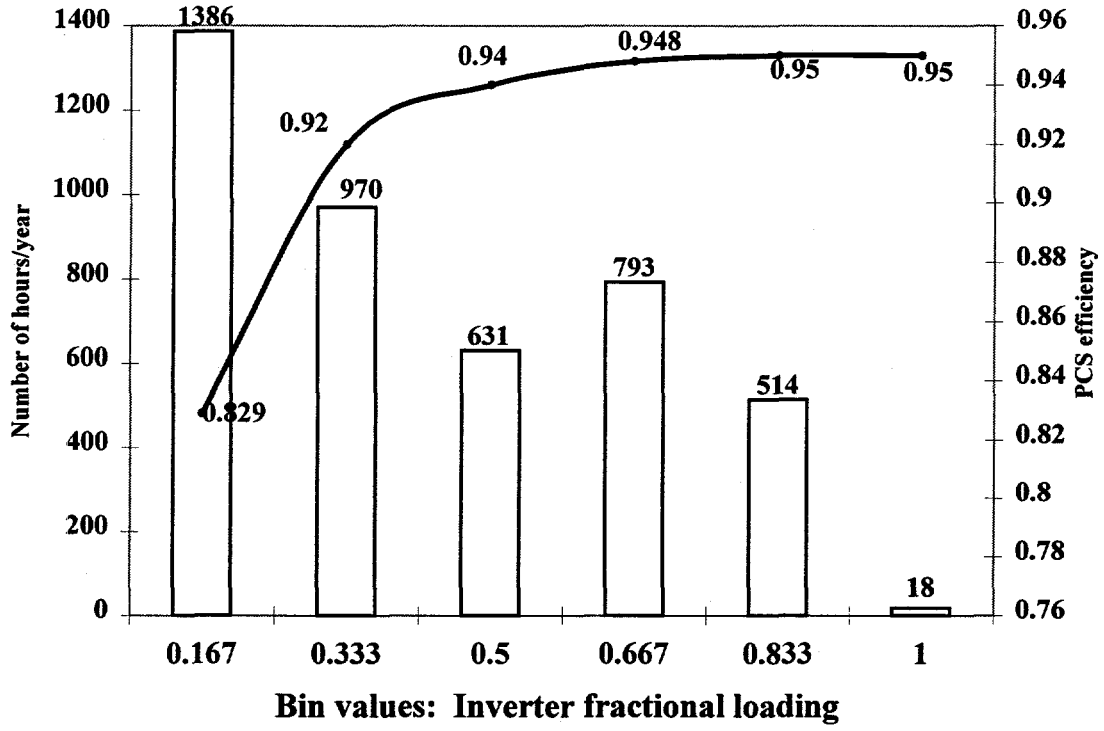


**Figure 4.** Comparison between the array dc power output histogram and the PCU's efficiency curve. The right-side axis is for the bar chart, showing the number of hours/year that the PV array's power output falls into the given bin value. The left-side axis is for the PCU efficiency curve.

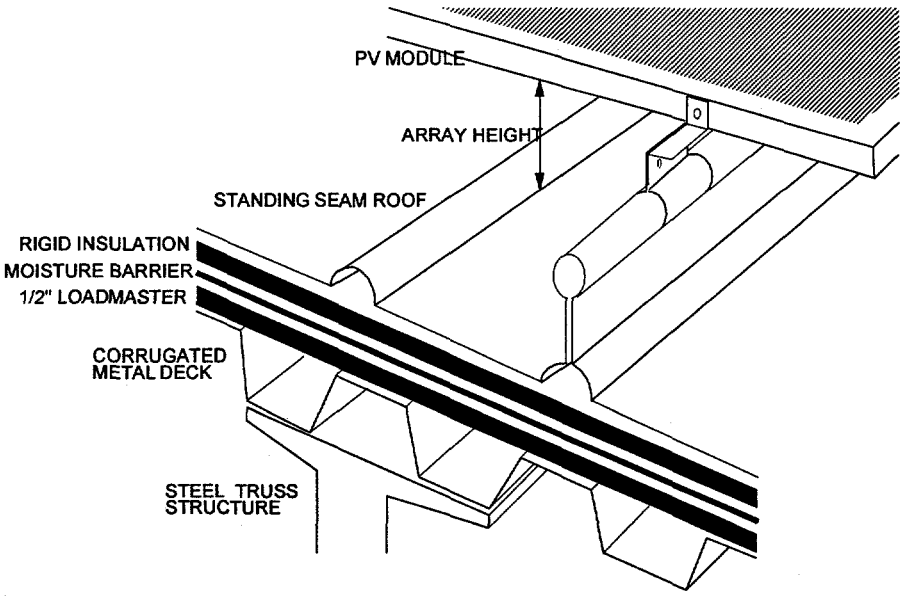


**Figure 5.** Schematic representation of the array mounting scheme.

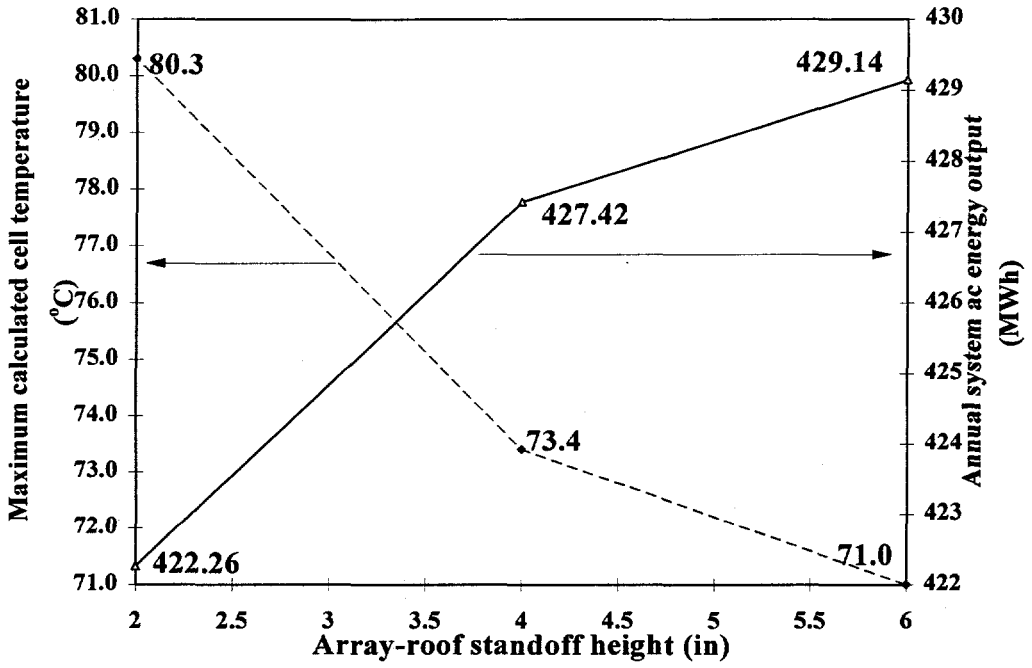


**Figure 6.** Maximum cell temperature attained during a typical year in Atlanta vs. array-roof standoff height, compared with the annual PV energy production vs. array-roof standoff height.

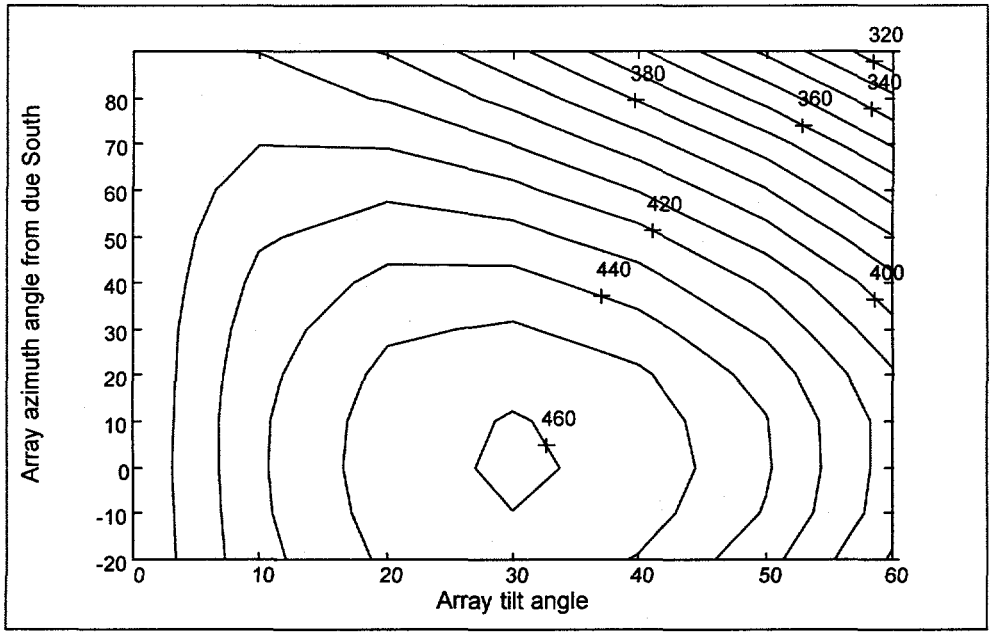


**Figure 7.** Contour plot of the Aquatic Center PV array's annual energy production as a function of array orientation. The contour line values are in units of MWh/year. Azimuth angles are measured from due south = 0°, with angles west of south being positive.

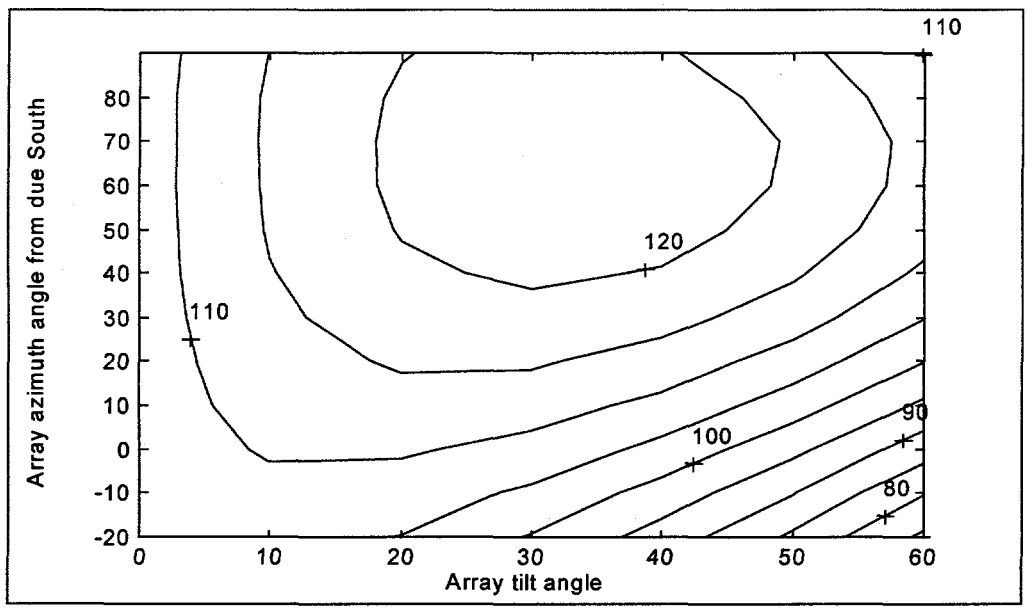


**Figure 8.** Contour plot of the Aquatic Center PV array's annual energy output during the peak-shaving window (noon-7pm. June-September) as a function of array orientation. The contour line values are in units of MWh/year. Azimuth angles are measured from due south = 0°, with angles west of south being positive.

*Appendix C*

# PERFORMANCE EVALUATION OF THE GEORGIA TECH AQUATIC CENTER PHOTOVOLTAIC ARRAY

# PERFORMANCE EVALUATION OF THE GEORGIA TECH AQUATIC CENTER PHOTOVOLTAIC ARRAY

**M. Begovic[1] , M. E. Ropp, A. Rohatgi, R. Long**
[1]Corresponding author
School of Electrical and Computer Engineering
Georgia Institute of Technology
Atlanta, GA 30332-0250
Phone: (404) 894-4834
FAX: (404) 894-4832
E-mail: miroslav@power.ee.gatech.edu

**ABSTRACT:** The Georgia Tech Aquatic Center photovoltaic (PV) array, one of the world's largest roof-mounted PV arrays, has been in operation since late June, 1996. This paper describes the system's performance during this inaugural year. Also, computer modeling used in the design and monitoring of the system is described, and comparisons between measured and expected system performances are made. Based on this information, the performance of the system and of the PV system computer models are judged, and future research directions are indicated.
**Keywords:** PV Array - 1: Performance - 2: Simulation - 3

## 1. INTRODUCTION

The PV array on the roof of the Georgia Tech Aquatic Center (GTAC) was the world's largest roof-mounted PV array at the time of its construction, and it remains one of the world's largest with 342 kW of rated PV generation capacity and an area of 3175 $m^2$. The array consists of 2856 multicrystalline Si modules arranged in 238 series strings of 12 modules each, giving a nominal DC operating voltage of approximately 410 V and a nominal DC operating current of about 830 A. The PV array is mounted directly to the aluminum standing-seam roof of the GTAC using clamps which provide an approximately 9 cm standoff height from the roof. Power from this array is fed down from the roof into a 315 kW (DC) power conditioning unit (PCU) which performs maximum power point tracking, inversion, and protection functions. The 480 V AC power is then fed through a $\Delta$-Y isolation transformer into the GTAC's main electrical service entrance, thus establishing grid connection.

The PV system is equipped with two data acquisition systems (DASs). One of these, located on the roof, monitors and records meteorological conditions including plane-of-array and horizontal irradiance, ambient temperature, wind speed, and six module temperatures. The other is located in the building's electrical room and monitors the electrical parameters of the system, including DC and AC power outputs, DC and AC voltages and currents, the power factor of the system's power conditioning unit (PCU), and system status information.

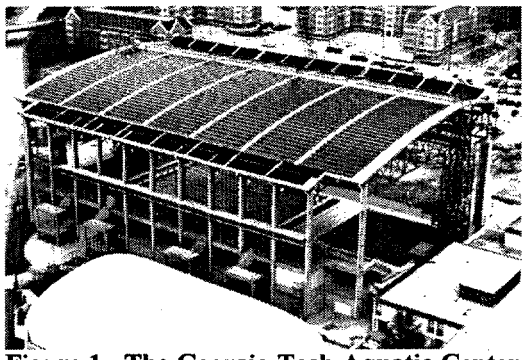

**Figure 1. The Georgia Tech Aquatic Center from the air, showing the 342 kW PV array on the roof. The black "mesh" at the top and bottom of the roof is part of the solar thermal water heating system.**

The photovoltaic systems modeling program PVFORM v. 3.3 was extensively used throughout our work on this system. This computer model was chosen because its primary submodels, namely the plane-of-array irradiance and cell temperature models, are rigorously based, published in the literature, and have experimentally been shown to be

highly accurate [1-4]. However, in the case of the GTAC PV system, a unique opportunity exists because the PV array does not have a constant tilt angle. It is flush-mounted to the curved roof of the Aquatic Center, as seen in Figure 1. This results in PV array tilts ranging from about 13° facing south to about 10° facing north. This situation will be encountered with increasing frequency as more PV systems are retrofitted to building structures, and it is therefore important to be able to accurately model and predict the performance of such a system.

PVFORM was used in the early system design stages to verify that the 12-module series strings would not produce DC voltages in excess of 600 V under the temperatures expected in Atlanta, to demonstrate the match between the PCU's 315-kW DC power rating and the 342-kW DC rating of the PV array, and to show that a 90°C temperature rating for cables to be used under the array was sufficient. (We consider the PV array and inverter to be "matched" well when the PV array's DC power output is consistently in the highest efficiency range of the inverter. This was quantified using the "effective inverter efficiency" described in [5].) In the modeling, the roof curvature was taken into account by modeling the PV array as two parallel-connected subarrays, one at the average tilt of the south-facing side (6.4°) and one at the average tilt of the north-facing side (5.9°) as described previously [5]. This was necessary because currently no computer model for PV systems has the ability to compute irradiances on multiple "facets" of a curved PV array from a meteorological database *and* predict the system's electrical performance. In monitoring of the system, monthly energy production predictions made by PVFORM have been useful in determining whether the system was performing as expected.

Due to its importance not only for our work on this system but for PV systems design and performance assessment in general, we have used the data collected from the GTAC system to examine the performance of both the PV system and the computer model during this inaugural year of operation.

## 2. ASSESSMENT OF SYSTEM PERFORMANCE

We have primarily used four criteria to assess the system's electrical performance during its first year of operation. These criteria are:

1.) The monthly energy production of the system, evaluated by comparison with results predicted by computer models;
2.) The system's power production as compared with the expected power production of the system as calculated using the measured plane-or-array irradiance and an efficiency from Equation [1];
3.) The sunlight to AC power efficiency of the PV system, as compared with the efficiency calculated using Equation [1];
4.) The total number of system operational hours, as compared with the total number of daylight hours.

Using the TMY and the two-subarray model of the GTAC system, PVFORM was used to predict the monthly energy output of the system. We define the "total number of operational hours" as the total number of daylight hours (measured irradiance of greater than 10 W/m$^2$) during which the system was functioning. Theoretically-predicted efficiencies are calculated using the following model:

$$\eta_{PV,k} = \eta_{rated} \cdot (1 - K_{dust})(1 - K_{curv}) \cdot (1 - K_{mismatch}) \cdot (1 - K_{dcloss}) \cdot [1 + (T_{module,k} - T_{STC}) K_{\eta}] \quad [1]$$

where $\eta_{rated}$ is the rated efficiency of the PV modules (10.77%), $K_{dust}$ is the fractional power loss due to dust and debris on the PV array (10% for July 1996-March 1997; 4% for April and May 1997), $K_{curv}$ accounts for the power loss due to the roof curvature (obtained from Figure 2), $K_{mismatch}$ is the fractional power loss due to module parameter mismatch (2%), $K_{dcloss}$ represents the dc-side $I^2R$ losses (2%), $T_{module,k}$ is the module temperature at time step k (measured), $T_{STC}$ is the Standard Test Condition temperature (25°C), and $K_{\eta}$ is the manufacturer-specified thermal derating coefficient for these modules (-0.0037 %/°C). (Work is currently in progress which will experimentally refine these parameter values.)

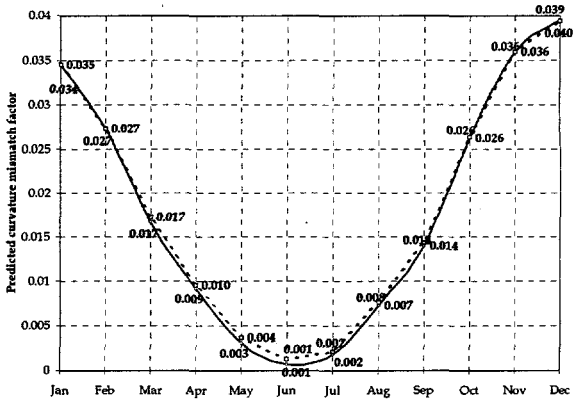


**Figure 2. Chart showing the curvature mismatch factor $K_{curv}$ as a function of month for use in Equation [1]. These results were obtained using PVFORM and the TMY as described in [5].**

Figure 3 shows the predicted and measured AC energy production of the GTAC PV system for the period July 1996-May 1997. The discrepancies seen in several of the months can be explained by events not related to the system performance. During July and August 1996, there was extensive system down time required to correct start-up difficulties and to repair the array after a lightning strike (detected because the expected DC power production of the system, calculated as described in Criterion #2, was higher than the measured power by nearly 20% under full sunlight). The system was operational for only 218 hours (out of a possible ~279 daylight hours) during the month of October 1996 due to a major plumbing failure in the Aquatic Center which flooded the PV electrical room. For half of each of the months of December 1996 and January 1997, the entire north-facing portion of the system, roughly 18% of the total array area, was deactivated as part of an experiment to examine the effect of the roof curvature on the system's performance (this experiment and its results will be described in a future publication). Finally, in May of 1997, the system was shut down for several days so that the building's transformer could be moved. To explain the discrepancies during the other months, we examined the predicted and measured amounts of available solar energy, represented by the average daily solar energy flux (Figure 4), and the differences in module temperature, quantified by the mean module temperatures (Figure 5) during this period. We can crudely "correct" the predictions for the system's AC energy production by first multiplying by the ratio of the measured to predicted average daily solar energy flux, and then multiplying by a temperature derating term defined by

$$E_{corrected} = \frac{S_{measured}}{S_{predicted}} \cdot T_{derating} \cdot E_{predicted} \qquad [2]$$

$$T_{derating} = 1 - K_{\eta}(T_{meas} - T_{pred})$$

where $S$ is the average daily solar energy flux on the south side of the array and $E_{predicted}$ is the monthly energy production of the system originally predicted using the TMY in PVFORM. $T_{meas}$ and $T_{pred}$ are the measured and predicted daylight-hours mean module temperatures averaged over both sides of the array and over all daylight hours.

We applied this correction procedure to the monthly energy production predictions made by PVFORM/TMY, modifying them to reflect the measured meteorological conditions. Then, we calculated a percentage difference between the corrected predicted AC energy production and the measured value. The results of this computation are shown in Figure 6. We assume an error of about 5% or less to signify good agreement between predictions and measurements because the assumption that the system's maximum power point tracker is 100% efficient, which is made in PVFORM, has been shown to be able to introduce that level of error [1]

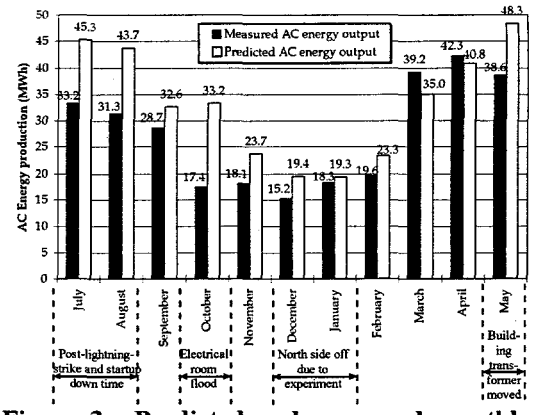


**Figure 3. Predicted and measured monthly AC energy production for July 1996-April 1997.**

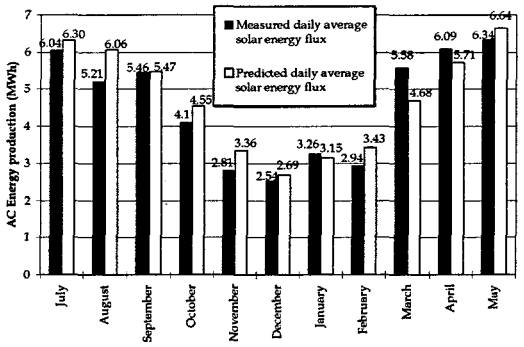


**Figure 4. Measured and predicted daily average solar energy flux on the GTAC PV array for July 1996-April 1997.**

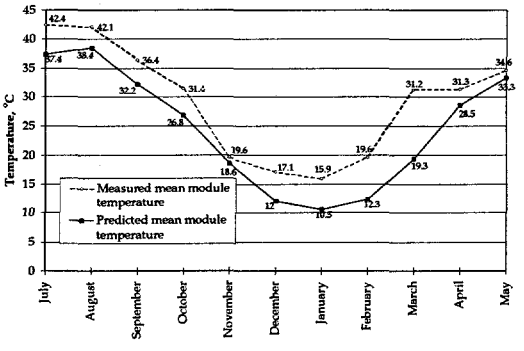


**Figure 5. Plot of the measured and predicted mean daylight-hours module temperature during July 1996-April 1997.**

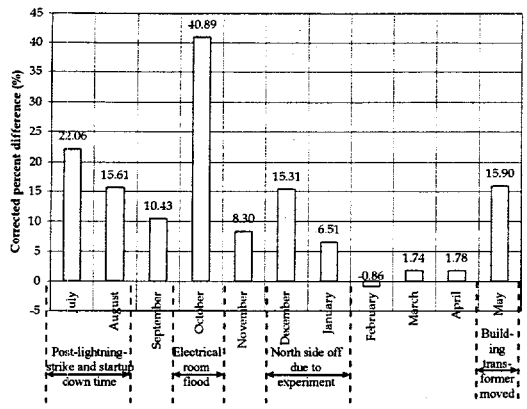


**Figure 6. Plot of the percent difference between predicted and measured AC energy production of the GTAC PV system as a function of month, calculated *after* the predicted value has been corrected for insolation and temperature factors.**

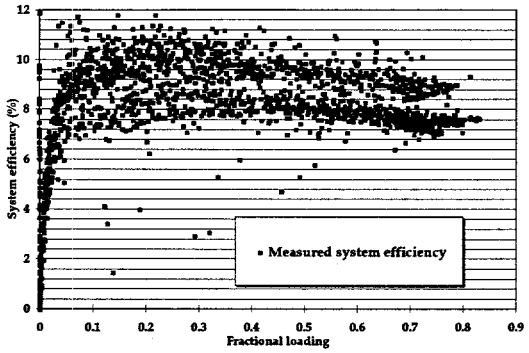


**Figure 7. The measured sunlight to AC power efficiency of the GTAC PV system.**

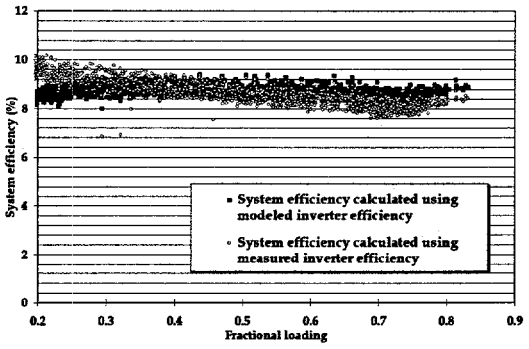


**Figure 8. The theoretically-predicted sunlight to AC power efficiency of the GTAC PV system, using the measured inverter efficiency and also a fifth-order polynomial fit to the inverter manufacturer's efficiency curve.**

With this in mind, we note that the predicted and measured AC energy production for November 1996 and February-April 1997 are actually in very good agreement, and therefore the system is performing very well. The final piece of evidence of this good performance is found in the system's irradiance to AC power efficiency. Measured values for the month of May, 1997, are plotted in Figure 7, and theoretically-calculated values using Equation [1] are plotted in Figure 8, both against the "fractional loading" of the inverter which is the array's DC power output normalized to the PCU's DC power rating (315 kW). Calculations and measurements are seen to be in very good agreement.

At first glance, it appears that the model's performance may not have been as good as the system's. Figure 5 indicates that, regardless of whether the available sunlight is greater or less than predicted, PVFORM consistently underpredicted the module temperatures, although they are in general fairly close (within about 4°C). We assume this to signify good agreement since it is about the same error as that found by Fuentes himself while verifying his model on actual modules [3]. However, an examination of mean daylight-hours ambient air temperatures during this time shows that the measured mean daylight-hours ambient air temperature for each month is higher than the predicted (TMY) mean daylight-hours ambient air temperature by nearly the amount of the difference between measured and predicted mean daylight-hours module temperatures. Differences in measured and predicted wind speeds do not appear to be a factor; in fact, the maximum predicted wind speed over the Aquatic Center PV array is 1.5 m/sec, but daylight-hours measured wind speeds frequently reach and exceed 3-4 m/sec, which should reduce the measured temperatures relative to those predicted, but because the wind speeds are low and the differences are not large, the Fuentes model shows that the temperature difference due to this factor would not be large [3]. Future work will include implementing the Fuentes model in MATLAB to enable us to run the model with measured data and to quantify the error in its predictions, but from the data currently available it appears that the error between predicted and measured mean daylight-hours module temperatures is due to the error in the ambient air temperature used as the input to the model.

There is another factor which appears to have caused much of the error during September and November 1996. The DAS which records the system's electrical parameters incorporates a doubly-redundant set of current, power and voltage sensors in order to improve accuracy. However, due to time constraints, one set of sensors (Set #2) was not calibrated during the installation of the system, and therefore these measurements were not used, and until March 1997 we relied upon the other, supposedly calibrated set (Set #1) for monitoring of the system. In early March, 1997, Set #2 was calibrated, and at that time comparisons between the

calibration standard and Set #1 revealed that Set #1 consistently gave system electrical parameter values which were too low. It is difficult to quantify exactly how much difference this made in the results, but we estimate from measurements made in March and April 1997 that the offset in the AC power reading was about 20 kW when the system was producing about 250 kW. This leads us to conclude that the difference in power, and thus energy, produced is on the order of -8%. If we then multiply the measured energy production in September and November 1996 by 1.08, the amount of error between the measurements and predictions drops to 3.3% in September and 1.0% in November, showing very good agreement with the adjusted predictions.

## 3. CONCLUSIONS

In its inaugural year, the GTAC PV system has performed well, producing 263.3 MWh of AC energy during the period July 1, 1996-May 1, 1997. Based on efficiency measurements and comparisons with theoretical calculations and computer models, problems with the system have been quickly detected and resolved, and the system has been shown to be performing as expected. This demonstrates the importance of such modeling for PV systems. Furthermore, the computer model PVFORM v. 3.3 and the two-array model of the GTAC PV array have been shown to yield very reasonable performance predictions for this system, thus establishing their usefulness and accuracy as design and performance assessment aids.

## 4. ACKNOWLEDGMENTS

This work was supported by grants from the United States Department of Energy, Georgia Power Company, Sandia National Laboratories, Amoco/Enron, and the National Electric Energy Testing, Research, and Applications Center (NEETRAC) at Georgia Tech.

## 5. REFERENCES

[1] R. Perez, J. Doty, B. Bailey, and R. Stewart, "Experimental Evaluation of a Photovoltaic Simulation Program", *Solar Energy* **52**(4), April 1994, p. 359-365.

[2] D. F. Menicucci, "Photovoltaic Array Performance Simulation Models", *Solar Cells* **18** (1986), p. 383-392.

[3] M. K. Fuentes, "A Simplified Thermal Model for Flat-Plate Photovoltaic Arrays", Sandia National Laboratories report SAND85-0330, May 1987.

[4] R. Perez, R. Seals, P. Ineichen, R. Stewart, D. Menicucci, "A New Simplified Version of the Perez Diffuse Irradiance Model for Tilted Surfaces", *Solar Energy* **39**(3), 1987, p. 221-231.

[5] M. Ropp, M. Begovic, A. Rohatgi, R. Long, "Design Considerations for Large Roof-Integrated Photovoltaic Arrays", *Progress in Photovoltaics* **5**(1), Jan-Feb 1997, p. 55-67

*Appendix D*

# MONITORING AND DATA ACQUISITION FOR A LARGE ROOF-MOUNTED PHOTOVOLTAIC ARRAY

# MONITORING AND DATA ACQUISITION FOR A LARGE ROOF-MOUNTED PHOTOVOLTAIC ARRAY

**M. Begovic[1], M. Ropp[1], A. Rohatgi[1], S. Durand[2], A. Rosenthal[2]**
[1]School of Electrical and Computer Engineering
Georgia Institute of Technology
Atlanta, GA 30332-0250
[2]Southwest Technology Development Institute
Las Cruces, NM 88003-0001

*Abstract* - **This paper describes a data acquisition system (DAS) used to monitor the large photovoltaic system mounted on the roof of the Georgia Tech Aquatic Center. An example of the data collected from the DAS is given in an example monthly report of the system's performance. This report also describes a diagnostic application of this data.**

## *INTRODUCTION: THE GEORGIA TECH AQUATIC CENTER PV SYSTEM*

The Aquatic Center photovoltaic (PV) system is a 342 kW dc solar electric generation plant. The PV array, mounted on the Aquatic Center roof, is comprised of 2,856 solar modules. PV-generated dc power is routed down from the roof to the system's power conditioning unit (PCU), which converts the dc electricity to ac, controls the operating state of the system, and performs vital safety functions. The system is interfaced through an isolation transformer to the main building electrical service entrance by backfeeding an ac circuit breaker. The PV system is described in detail in [1].

## *THE DATA ACQUISITION SYSTEM MONITORING THE AQUATIC CENTER PV SYSTEM*

The PV system is monitored by two independent data acquisition systems (DASs) linked by a local area (MD-9) network. The Inverter Room DAS monitors system electrical parameters such as real and reactive ac power, dc power, voltage and current, and PCU status. The Rooftop DAS monitors relevant meteorological parameters such as solar irradiation, ambient and module temperatures, and wind speed. Both DASs sample all input channels every 10 seconds and record 10 minute averages of these data. Daily data files are collected and stored by the Data Server Computer which makes them accessible to remote users via telephone modem.

### *Monitoring of the PV system*

Researchers at Georgia Tech have been collecting the data each month and generating monthly reports on the status and performance of the PV system. These reports are available on the World Wide Web at http://www.ece.gatech.edu/users/gt3960b/natatorium.html.

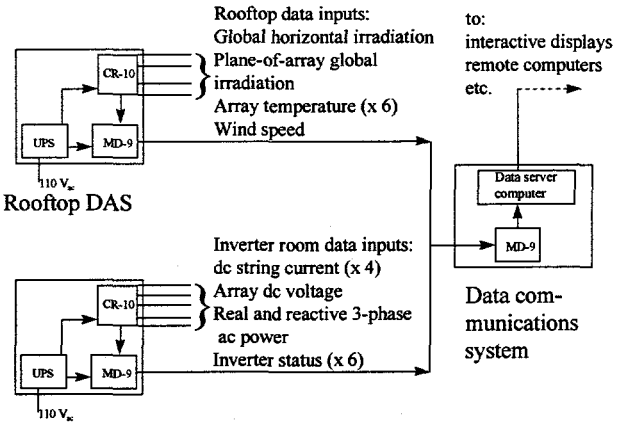


Figure 1. The Aquatic Center array data acquisition system.

A sample of such a report, based on data for July 1996, is included below.

---

***Summary***

| | |
|---|---|
| Typical PV array dc voltage: | 340-370V |
| Energy produced (ac): | 33.2 MWh |
| Maximum module temperature recorded: | 75.3°C = 167.5 °F |
| Maximum ac power recorded: | 221.3 kW |
| System operational hours: | 379.5 |
| System down time (hours)[a]: | 23.8 |

[a]*The system down time includes all hours during which the PV system was turned off. Hours during which the PV system was not producing power due to darkness are not included.*

Figures 2 and 3 give the distributions of the insolation on the array and the ac power produced by the system during July, 1996. Figure 2 also shows the insolation distribution predicted by the software package PVFORM and the measured and predicted average daily insolation.

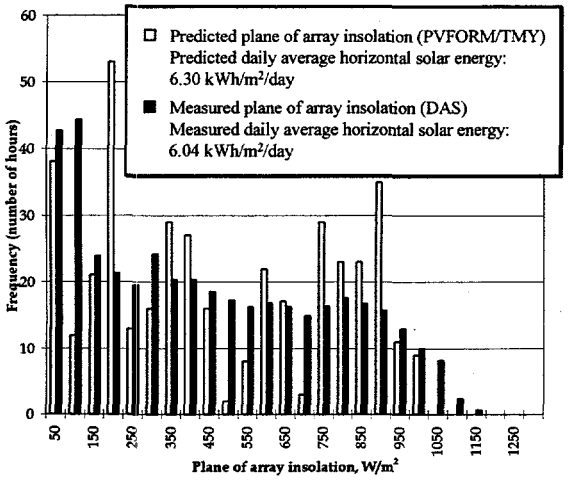


Figure 2. Histogram of the plane of array insolation on the Aquatic Center PV array, July 1996. The insolation distribution predicted by PVFORM using the TMY is included for comparison.

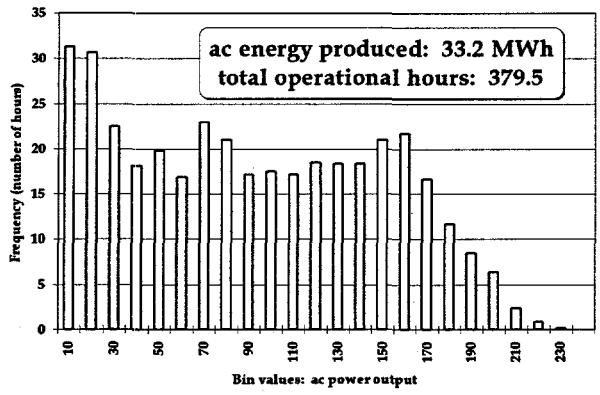


Figure 3. Histogram of the ac power output of the Aquatic Center PV system, July 1996. Total energy for the month is also given.

Figure 4 presents the system's measured and theoretically-predicted energy conversion efficiencies during July, 1996. Note that there are two distinct curves for the measured data. During the first part of July, it was noted by Georgia Tech researchers that the system's apparent efficiency was following the lower measured curve, exhibiting a significant reduction from the expected apparent efficiency. Investigation of the PV array revealed that blown fuses, probably the result of a direct lightning strike, had isolated one of the seven PV source circuits. Replacement of the fuses resulted in the higher measured efficiency data recorded for the remainder of the month, which more closely matched the theoretical expected apparent efficiency.

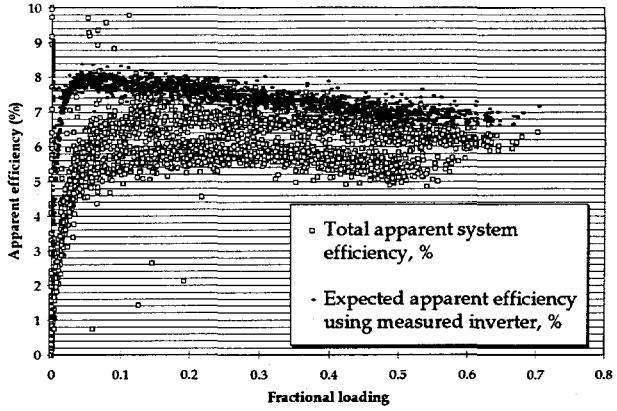


Figure 4. The apparent efficiency of the Aquatic Center PV system. The dashes are the apparent efficiencies predicted theoretically, and the hollow squares are the measured values.

The system's expected apparent dc efficiency is calculated using the expression

$$\eta_{app} = \eta_{rated}(1-K_{dust})(1-K_{curv})(1-K_{mismatch})(1-K_{dcloss})[1-K_{\eta}(T_m - T_{STC})]$$

where $\eta_{rated}$ = 10.77% is the rated efficiency of the PV modules; $K_{dust}$ = 10% accounts for dust and debris on the array; $K_{curv}$ = 4.2% accounts for power loss due to the roof curvature, the value being derived from PVFORM modeling; $K_{dcloss}$ = 2% accounts for $I^2R$ losses on the dc side; $K_{mismatch}$ = 2% represents loss due to inherent module-module parameter mismatch; $K_{\eta}$ = 0.0037 %/°C is the thermal derating coefficient of the modules used; and $T_{STC}$ = 25°C is the Standard Test Condition temperature.

### *A NOTE ABOUT "APPARENT EFFICIENCY"*

The efficiency we calculate using the measured power in and power out from our PV system is not the true system efficiency because of the curvature of the roof. The power in is measured by a single pyranometer tilted at the average tilt of the south-facing portion of the PV array. However, since a portion of the array is actually facing north, not all of the measured irradiation is received by the PV array. Hence, when calculating a system efficiency as (power out) ÷ (power in), the (power in) term is artificially high, meaning that the system efficiency is artificially low. In our calculations, we have introduced the curvature mismatch parameter $K_{curv}$ to compensate for this effect. We have defined $K_{curv}$ as

$$K_{curv} = 1 - \frac{E_{curv}}{E_{cop}}$$

where $E_{curv}$ and $E_{cop}$ are, respectively, the energy produced by our curved array and that produced by an imaginary array which is coplanar at the tilt of the south-facing side of the curved array. These energies were determined using PVFORM as described in [2].

## *CONCLUSIONS*

The DAS which monitors the Georgia Tech Aquatic Center PV system has been described. Examples of the collected data have been presented, and the value of monitoring the system has been clearly demonstrated by the diagnostic use of the data during the month of July, 1996.

## *REFERENCES*


[1] M. Ropp, M. Begovic, A. Rohatgi, R. Long, "Roof-Installed PV system on the Olympic Swimming Pool at Georgia Tech", Proceedings of the 13th European Photovoltaic Solar Energy Conference, vol. 1, p. 965-968, 1994.

[2] M. Ropp, M. Begovic, A. Rohatgi, "Design Considerations for Large Roof-Integrated Photovoltaic Arrays", accepted for publication in Progress in Photovoltaics.

*Appendix E*

# DETERMINATION OF THE CURVATURE DERATING FACTOR FOR THE GEORGIA TECH AQUATIC CENTER PHOTOVOLTAIC ARRAY

# DETERMINATION OF THE CURVATURE DERATING FACTOR FOR THE GEORGIA TECH AQUATIC CENTER PHOTOVOLTAIC ARRAY

**M.E. Ropp, M. Begovic, A. Rohatgi**
*School of Electrical and Computer Engineering*
*Georgia Institute of Technology*
*Atlanta, GA 30332-0250*

## ABSTRACT

**The photovoltaic (PV) array on the roof of the Georgia Tech Aquatic Center (GTAC) is unique in that it is curved, following the curvature of the roof of the Center. This curvature leads to some power loss in the system due to the difference in irradiance over the area of the array, as well as difficulties in obtaining the system efficiency from measured data. These problems could become increasingly common as more PV arrays are integrated into building structures. This paper describes a simple method of overcoming these difficulties using a "curvature derating factor". First, the parameter is defined. Model calculations are then employed to obtain an estimate of the parameter's value for a particular system. Finally, an experimental estimation of the parameter is described, and its results are compared with the predictions.**

## INTRODUCTION

In the design, analysis, and performance assessment of PV systems, the following equation is used to describe a system's dc efficiency at a time step k:

$$\eta_{PV,k} = \eta_{rated}\eta_{dust}\eta_{mismatch}\eta_{DCloss}\eta_{MPPT}\eta_T \quad [1]$$

where $\eta_{rated}$ is the rated efficiency of the PV modules (10.77%), $\eta_{dust}$ is (1 - the fractional power loss due to dust and debris on the PV array), $\eta_{mismatch}$ is (1- the fractional power loss due to module parameter mismatch), $\eta_{DCloss}$ represents (1 - the DC-side $I^2R$ losses), $\eta_{MPPT}$ is (1 - the power loss due to DC current ripple and "algorithm error" caused by the switching converter which performs the maximum power point tracking function), and

$$\eta_T = 1 + K_T[T_{cell,k} - T_{STC}] \quad [2]$$

where $T_{cell,k}$ is the module temperature at time step k, $T_{STC}$ is the Standard Test Condition temperature (25°C), and $K_T$ is the modules' thermal derating coefficient in %/°C and is negative; $K_T < 0$. The parameter values used in our simulations are given in Table 1. Two of these parameters, $\eta_{dust}$ and $K_T$, have been verified experimentally. For $\eta_{MPPT}$ we use the value suggested by Perez et.al. [1]; the other two values are based on the suggestions of manufacturers and experienced field personnel.

**Table 1. Parameter values for Equation [1].**

| Parameter | Value |
|---|---|
| $\eta_{dust}$ | 0.96 |
| $\eta_{mismatch}$ | 0.95 |
| $\eta_{DCloss}$ | 0.98 |
| $\eta_{MPPT}$ | 0.95 |
| $K_T$ | -0.0037 $(°C)^{-1}$ |

The factor $\eta_{PV,k}$ can then be used to predict the power output of a planar PV array at time step k

$$P_{k,pl} = \eta_{PV,k} G_{poa,k} A_{array} \quad [3]$$

or energy output over n time steps of length $t_k$

$$E_{pl} = \sum_{k=1}^{n} \eta_{PV,k} G_{poa,k} A_{array} t_k \quad [4]$$

where $G_{poa,k}$ is the plane of array irradiance in W/m$^2$ at time step k and $A_{array}$ is the area in m$^2$ of the PV array.

However, in using a single irradiance value, Equations [3] and [4] assume that the entire PV array has the same tilt and azimuth angles, as indicated by the "pl" (planar) subscript on E and P. The Georgia Tech Aquatic Center (GTAC) PV array is curved; the modules are flush-mounted to a roof with pitch varying from about 13° facing south to almost 10° facing north. Figure 1 shows a schematic of the PV array. The dotted line shows the position of a catwalk. All modules above the dotted line in the figure are facing north; the rest are south-facing. When modeling this system, the variable tilt problem could be solved by simply modeling the array as a large number

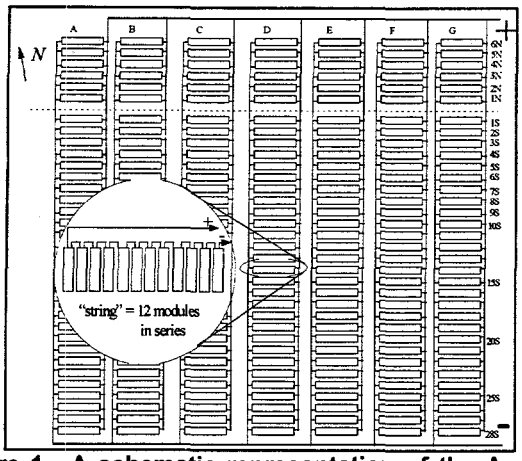


**Figure 1. A schematic representation of the Aquatic Center PV array.**

of interconnected subarrays at different tilts. For a complete solution which takes into account the electrical interactions of the modules, the irradiance on each section of the array at a different tilt must be calculated, and from this and the module parameters the temperatures must be found and then the I-V curves constructed. Next, the common operating point of all modules must be determined, and finally the array power can be calculated by combining the I-V curves according to the series-parallel configuration of the array. However, this solution is computationally intensive, and it does not solve the problem caused by the lack of simultaneous measurements of the irradiance on all the various subarrays, which complicates accurate comparison of measured and modeled results. An example of this latter difficulty is the calculation of the system's efficiency. The DC efficiency of the PV array can be used for many diagnostic purposes, and normally can be easily calculated by comparing the results of Equation [1] with the ratio of measured output (measured $P_{pl,k}$) to measured input ($G_{poa,k} \times A_{array}$). However, for the GTAC system, $G_{poa,k}$ is measured only in the plane of the average tilt of the south-facing side of the array, augmented by a horizontal measurement. This "plane of array" irradiance *measurement is clearly not accurate for the entire array*, and therefore the calculated system efficiency using this value will also be inaccurate.

As a simple solution to these problems, we introduce a "curvature derating factor" into Equations [3] and [4] to cause them to give correct power and energy values. This paper defines this parameter and discusses computer modeling and experiments performed to obtain a value for this factor for the GTAC PV system.

## DEFINITION OF THE CURVATURE DERATING FACTOR

We define the new derating factor, the curvature mismatch factor $K_{curv}$, by comparison with Equations [3] and [4]:

$$E_{curv} = \sum_{k=1}^{n} \eta_{PV,k} G_{poa,k} A_{array} t_k (1 - K_{curv,k}) = \sum_{k=1}^{n} P_{k,curv} t_k$$
$$= (1 - K_{curv}) \sum_{k=1}^{n} \eta_{PV,k} G_{poa,k} A_{array} t_k = (1 - K_{curv}) \sum_{k=1}^{n} P_{k,pl} t_k \quad [5]$$

$E_{curv}$ and $P_{k,curv}$ are the energy and power produced by the curved PV array at time step k under irradiance $G_{poa,k}$ and with efficiency $\eta_{PV,k}$, $P_{k,pl}$ is the power produced by a planar array *under the same irradiance and with the same efficiency (i.e. temperature)*, and $t_k$ is the length of the time step in hours.

## ESTIMATION OF $K_{curv}$ BY COMPUTER MODELING

In a previous paper [2], we described a method for obtaining an estimate of the curvature derating factor using the software package PVFORM v. 3.3 and a "two-subarray model". That method involved separating the PV array into two planar subarrays interconnected in parallel. The "south" subarray was tilted at the average tilt of the south-facing side of the Aquatic Center system (6.4°); the "north" subarray was tilted at the average tilt of the north-facing side (5.9°). These subarrays could be modeled independently and the results summed. In order to do this, two conditions must be met:

1) The range of tilts within a section being replaced by a planar array cannot be too great. This is because irradiance varies nonlinearly with tilt (it varies as a dot product, or cosine), and if the extremes of tilt are too far from the average there will be an asymmetry of the irradiance about the average, which will lead to an offset error when the curved section is replaced by a planar section at the average tilt of the curved section.

2) The difference in tilts between the two sections cannot be too large. This is because when we model the two subarrays separately the modeling program will assume that each subarray operates at its own maximum power point, and thus at its own maximum power voltage. This is not true in the actual system, where the two subarrays are connected in parallel. We must therefore be certain that the tilts do not vary so widely that the maximum power voltages of the individual array sections differ by more than a small amount.

*To test these assumptions, we selected a time point at* which the irradiance difference between the two average tilts was the largest, thus yielding a worst-case scenario, and found the horizontal irradiance at that time. From this, we computed the irradiance on five different tilts and constructed I-V curves of one module string at each tilt (assuming identical modules). Finally, we varied the DC voltage and, using the I-V curve, computed the power-versus-voltage (P-V) curve of each series string as a function of voltage. A plot of the results is shown in

Figure 2. Clearly, the difference in maximum power voltages is negligible, and Assumption 2 is valid. Checking Assumption 1 by comparing powers produced by the various strings, we find that the powers produced by strings on the south side are approximately symmetric about that produced by the string at the average south side tilt. However, this is not quite true on the north side. We performed a detailed analysis using the actual configuration of the GTAC array and discovered that the error incurred in the predicted power is +1.1% under this worst-case condition. This is not a large error, but it should be noted that it will cause the predicted $K_{curv}$ values to be slightly lower than actual.

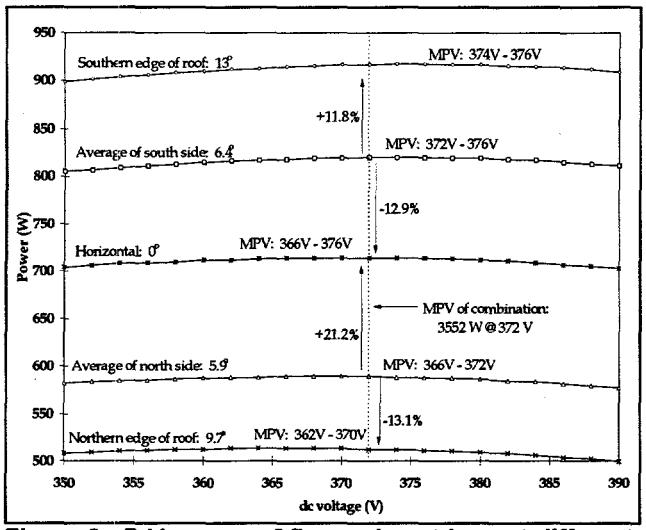


**Figure 2. P-V curves of five series strings at different tilts. The region near the maximum power point is shown.**

$K_{curv}$ is caused by the varying angle of incidence of the direct-beam irradiance. Therefore, it will be a function of solar position, which is in turn a function of time of day and day of the year. We can account for the seasonal variation by finding $K_{curv}$ as a function of month. This was done using the two-subarray modeling method, and the results are plotted in Figure 3. The diurnal variation of $K_{curv}$ was averaged out in our calculations because the array's performance will be evaluated over longer periods than one day.

$K_{curv}$ is also a function of cloud cover, because it is caused by the direct-beam irradiance. Since the tilt angles of all portions of the Aquatic Center array are fairly small, the diffuse irradiance over the entire array will be very nearly constant. Therefore, under cloudy conditions, $K_{curv}$ will be approximately zero. Because of this effect, if a certain month during which measurements were taken were cloudier than the corresponding month in the Typical Meteorological Year (TMY) used in the PVFORM simulations, the computed $K_{curv}$ value would be lower; similarly, if the month were unusually clear, the $K_{curv}$ value would increase. This factor could cause the

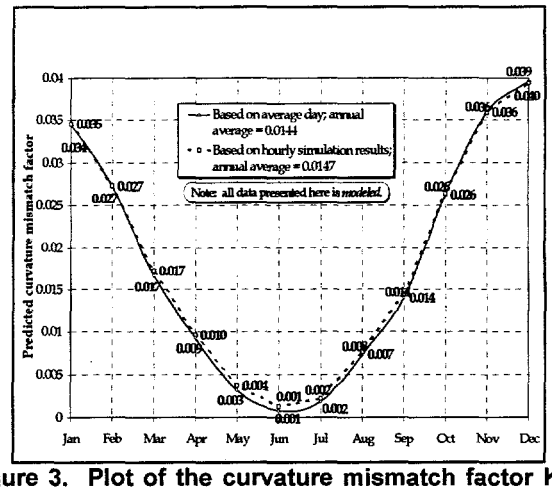


**Figure 3. Plot of the curvature mismatch factor $K_{curv}$ as a function of month.**

measured $K_{curv}$ values for a given month to deviate significantly from the expected values.

## EXPERIMENTAL VERIFICATION OF $K_{curv}$ VALUE

$K_{curv}$ can be calculated from the data being acquired from the GTAC system. The data acquisition system (DAS) which monitors the GTAC PV system measures and records, among other parameters, the irradiance ($G_{poa,k}$) at the average tilt of the south-facing portion of the array (6.4°), the temperatures of six modules scattered throughout the array($T_{mod,k}$), and the system's DC voltage and current, from which we can easily obtain the system's DC power ($P_{k,curv}$). Using Equation [5], we can solve for $K_{curv}$ in terms of the measured quantities:

$$K_{curv} = 1 - \frac{\sum_{k=1}^{n} P_{k,curv}}{\sum_{k=1}^{n} P_{k,pl}} \qquad [6]$$

$$= 1 - \frac{\sum_{k=1}^{n} P_{k,curv}}{\sum_{k=1}^{n} \eta_{PV,k} G_{poa,k} A_{array}}$$

The numerator represents the summation of the measured DC power produced by the GTAC array. In the denominator, $\eta_{PV,k}$ is found using the measured temperatures and Equation [1], and $G_{poa,k}$ is the irradiance measured in the average tilt of the south-facing side. The results of this calculation during April-August 1997 are shown in Figure 4. During this time period, two of the 238 series strings in the array were known to be inoperative. The results in Figure 4 were adjusted to compensate for this factor by altering $A_{array}$ appropriately.

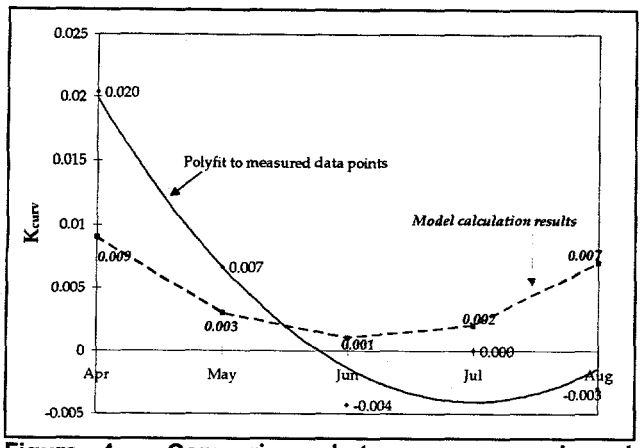


**Figure 4. Comparison between measured and computed $K_{curv}$ values.**

It is difficult to make any solid conclusion based on this data. One reason is that the value of the parameter we are trying to isolate is well within the uncertainties introduced by meteorological and measurement variables. Another is that two of the parameters in Equation [1], $\eta_{mismatch}$ and $\eta_{MPPT}$, are not known with great certainty. The procedure given by Equation [6] will transfer any error in these parameters directly to the calculated $K_{curv}$ value, and again the uncertainty in these parameters is probably larger than the $K_{curv}$ value we are trying to measure. A final potential source of error is the aforementioned affect of cloud cover. As previously mentioned, if during a month of measurements the skies are unusually cloudy compared with the corresponding month in the TMY, the measured $K_{curv}$ would be much lower than the modeled one. This possible error source can be investigated by calculating the clearness indices (CI) for the five months of the measurements and the corresponding five months of the TMY. The clearness index we have used here is given by [3]

$$CI = \frac{H}{H_0} \qquad [7]$$

where $H$ and $H_0$ are the terrestrial and extraterrestrial (outside the atmosphere) total average daily radiant energy fluxes (kWh/m$^2$/day). The values of CI based on the measurements and the model are shown in Table 1.

**Table 1. Clearness index values based on measurements and models.**

| Month | CI based on measurements | CI based on PVFORM/TMY |
|---|---|---|
| April | 0.3949 | 0.3650 |
| May | 0.3841 | 0.4155 |
| June | 0.2998 | 0.3852 |
| July | 0.3819 | 0.3898 |
| August | 0.3679 | 0.3763 |

The $K$ values from the model and the measurements agree fairly well with the exception of June, in which the measured value is lower than expected, which may contribute to the very low value of $K_{curv}$ measured for that month. However, for the other months, a change in cloudiness does not appear to have been a factor.

In spite of the difficulties in interpreting this data, it should be noted that the expected seasonally-varying shape is present, with $K_{curv}$ generally decreasing toward mid-summer. Also, we find that the $K_{curv}$ values are small for this system, which is in line with the model results.

## CONCLUSIONS

We have presented the results of our efforts to introduce a curvature derating factor into Equation [1] which will account for the fact that our PV array is curved. The new parameter has been defined, and values for it for the Georgia Tech Aquatic Center PV system were calculated using computer models and without using extensive electrical modeling of the system. The computer modeling methodology has been shown to be valid for modest curvatures. Furthermore, we have presented the results of experimental attempts to validate the $K_{curv}$ values calculated by modeling. Future work will include repeating the experimental portion of this work several more times, particularly during the winter months when $K_{curv}$ is larger, to help eliminate the error caused by meteorological variables. Also, we are currently devising and performing experiments to help alleviate the uncertainty in $\eta_{mismatch}$ and $\eta_{MPPT}$.

## ACKNOWLEDGMENTS

This work was supported by the United States Department of Energy, the Georgia Power Company, and the National Electric Energy Testing, Research and Applications Center (NEETRAC).

## REFERENCES

[1] R. Perez, J. Doty, B. Bailey, R. Stewart, "Experimental Evaluation of a Photovoltaic Simulation Program", *Solar Energy* v. 5 no. 4, April 1994, p. 359-365.

[2] M. E. Ropp, M. Begovic, A. Rohatgi, R. Long, "Design Considerations for Large Roof-Integrated Photovoltaic Arrays", *Progress in Photovoltaics* Jan/Feb 1997, v. 5, p. 55-67.

[3] Liu, B. Y. H, Jordan, R. C., "The Interrelationship and Characteristic Distribution of Direct, Diffuse and Total Solar Radiation", *Solar Energy* v. 4 no. 3, July 1960, p. 1-19.